UNIVERSITÀ DEGLI STUDI DI PADOVA

DIPARTIMENTO DI SCIENZE CARDIOLOGICHE, TORACICHE E VASCOLARI

**SCUOLA DI DOTTORATO DI RICERCA IN
SCIENZE MEDICHE, CLINICHE E SPERIMENTALI**

Direttore della Scuola: Ch.mo Prof. Gaetano Thiene

INDIRIZZO: SCIENZE CARDIOVASCOLARI

CICLO XXV

TITOLO DELLA TESI DI DOTTORATO

ARRHYTHMOGENIC CARDIOMYOPATHY: ELECTRICAL INSTABILITY AND INTERCALATED DISC ABNORMALITIES IN TRANSGENIC MICE

Coordinatore d'indirizzo: Ch.mo Prof. Gaetano Thiene
Supervisore: Ch.ma Prof.ssa Cristina Basso

Dottorando:
Dr.ssa Stefania Rizzo

INDEX

ABSTRACT

Aims: Mutations in genes encoding desmosomal proteins have been implicated in the pathogenesis of arrhythmogenic right ventricular cardiomyopathy (ARVC). However, the consequences of these mutations in early disease stages are unknown. We investigated whether mutation-induced intercalated disc remodeling impacts on electrophysiological properties before the onset of cell death and replacement fibrosis.

Methods and Results: Transgenic mice with cardiac overexpression of mutant Desmoglein2 (Dsg2) Dsg2-N271S (Tg-NS/L) were studied before and after the onset of cell death and replacement fibrosis. Mice with cardiac overexpression of wild-type Dsg2 and wild-type mice served as controls. Assessment by electron microscopy established that intercellular space widening at the desmosomes/adherens junctions occurred in Tg-NS/L mice before the onset of necrosis and fibrosis. At this stage, epicardial mapping in Langendorff-perfused hearts demonstrated prolonged ventricular activation time, reduced longitudinal and transversal conduction velocities, and increased arrhythmia inducibility. A reduced action potential upstroke velocity due to a lower Na+ current density was also observed at this stage of the disease. Furthermore, co-immunoprecipitation demonstrated an in vivo interaction between Dsg2 and the Na+ channel protein NaV1.5.

Conclusion: Intercellular space widening at the level of the intercalated disc (desmosomes/ fascia adherens junctions) and a concomitant reduction in action potential upstroke velocity, as a consequence of lower Na+ current density, leads to slowed conduction and increased arrhythmia susceptibility at disease stages preceding the onset of necrosis and replacement fibrosis. The demonstration of an in vivo interaction between Dsg2 and NaV1.5 provides a molecular pathway for the observed electrical disturbances during the early ARVC stages.

4

RIASSUNTO

Introduzione: Mutazioni nei geni che codificano per le proteine desmosomali giocano un ruolo fondamentale nella patogenesi della cardiomiopatia aritmogena del ventricolo destro (ARVC). Tuttavia, le conseguenze di tali mutazioni negli stadi precoci della malattia sono sconosciute.

Scopo del nostro studio è stato di indagare se il rimodellamento dei dischi intercalari come conseguenza di mutazioni nelle proteine desmosomali modifichi le proprietà elettrofisiologiche cardiache prima dello sviluppo di morte cellulare e fibrosi sostitutiva.

Metodi e Risultati: Topi transgenici con overespressione cardiaca della proteina Desmogleina2 mutata (Dsg2) -Dsg2-N271S (Tg-NS/L)- sono stati studiati prima e dopo lo sviluppo di morte miocitaria e fibrosi sostitutiva. Come controlli, abbiamo usato topi wild-type e topi con overespressione della Dsg2 normale.

Studi di microscopia elettronica hanno evidenziato la presenza di spazi intercellulari allargati in corrispondenza delle giunzioni meccaniche desmosomi/giunzioni aderenti nei topi Tg-NS/L prima dello sviluppo di necrosi e fibrosi. Contemporaneamente, il mappaggio epicardico in cuori perfusi con soluzione Langendorff ha dimostrato prolungamento del tempo di attivazione ventricolare, riduzione della velocità di conduzione longitudinale e trasversale, ed aumento della inducibilità di aritmie. Inoltre, nello stesso stadio di malattia, si osservava ridotta velocità del potenziale d'azione dovuta a minore densità della corrente del sodio.

Studi di co-immunoprecipitazione, infine, dimostravano un'interazione in vivo tra la Dsg2 e la proteina NaV1.5 dei canali del sodio.

Conclusioni: Un allargamento degli spazi intercellulari a livello dei dischi intercalari e una concomitante riduzione del potenziale d'azione, come conseguenza di una minore corrente del sodio, portano ad un ritardo di conduzione ed ad aumentata suscettibilità aritmica negli

stadi di malattia che precedono la necrosi e la fibrosi sostitutiva. La dimostrazione di

un'interazione

in vivo tra Dsg2 e NaV1.5 suggerisce una spiegazione a livello molecolare dei disturbi elettrici

osservati negli stadi precoci dell'ARVC.

ABBREVIATIONS

AP   Action potential

ARVC   Arrhythmogenic right ventricular cardiomyopathy

Cx43   Connexin 43

DSC2   Desmocollin-2

DSG2   Desmoglein-2

DSP   Desmoplakin

ICDs   Implantable cardioverter defibrillators

iPSC   Induced pluripotent stem cells

LDAC   Left Dominant Arrhythmogenic Cardiomyopathy

LV   Left ventricle

MRI   Magnetic resonance imaging

PG   Plakoglobin

PKP2   Plakophilin-2

RYR2   Ryanodine receptor 2

RV   Right ventricle

SCD   Sudden cardiac death

TGFB3   Transforming growth factor-β3

TMEM43   Transmembrane protein 43

GENERAL PART

Definition

Arrhythmogenic right ventricular cardiomyopathy (ARVC), or just arrhythmogenic cardiomyopathy, is a genetically-determined heart muscle disease, associated with myocardial abnormalities and electrical dysfunction, characterized histopathologically by fibro-fatty replacement of the ventricular myocardium (mainly localized in the right ventricle-RV) and clinically by severe ventricular arrhythmias at risk of cardiac arrest (Marcus et al., 1982; Thiene et al., 1988; Basso et al., 1996; Nava et al., 2000). It is one of the major causes of sudden cardiac death (SCD) in the young (Thiene et al., 1988) and in the athletes (Corrado et al., 1990; Corrado et al., 2003; Corrado et al., 2006). Heart failure is infrequent but may occur due to severe right or biventricular enlargement (Basso et al., 1996).

Initially thought to be a developmental defect of RV myocardium and thus termed "RV dysplasia," more recent advances in pathophysiology led to the recognition of ARVC as a cardiomyopathy (Basso et al., 2010). Since its entry into the classification of cardiomyopathies by the World Health Organization (Richardson et al., 1996), major progress has been achieved in the field of molecular pathophysiology, genetics, diagnosis, risk stratification, and treatment. Our concepts of the disease continue to evolve in parallel with wider recognition and identification of critical genetic, epigenetic and/or environmental factors that interact to determine disease severity and risk of SCD.

Epidemiology

ARVC occurs worldwide, but the incidence varies considerably among different geographic regions (Basso et al., 2009). The prevalence of 1:1,000 to 1:5,000 people has been estimated (Nava et al., 1988; Rampazzo et al., 1994; Norman et al., 1999; Peters et al., 2004; Sen-

Chowdhry et al., 2010), however, it could be higher because of the existence of many misdiagnosed cases.

Historical notes

The first historic mention was in the eighteenth century in the book De Motu Cordis et Aneurismatibus, published in 1736 by Giovanni Maria Lancisi, who reported a family with palpitations, heart failure, aneurysms of the RV, and SCD, recurring in four generations (Lancisi, 1736; quoted by Basso et al., 2009).

Osler was the first to describe a parchment heart with thinned and dilated cardiac chambers (Osler, 1905). In 1952, Uhl reported a case in which the wall of the RV was paper thin and nearly completely devoid of muscle fibers (Uhl, 1952). Until 1979, the term Uhl's anomaly was frequently used for the disease. It was in 1961 that Dalla Volta et al reported cases with "auricularization of the right ventricular pressure" showing a fibrofatty, nonischemic pathology of the RV (Dalla Volta et al., 1961). In 1979, Fontaine described a similar lesion of the RV and coined the term ARVC (Fontaine et al., 1979). In 1982 Marcus and colleagues provided the first clinical description of 24 patients with "right ventricular dysplasia" (Marcus et al., 1982), emphasizing the origin of arrhythmias from the RV and the histopathological substrate consisting of fibro-fatty replacement of the RV free wall. Years later, Nava and colleagues (Nava A. et al., 1988) demonstrated the variable clinical features and the genetic trait of the disorder. Thiene et al observed a case series of SCD in the young (≤35 years) with pathology consisting of ARVC, accounting for 20% of all SCD, mostly occurring during effort, and all characterized by inverted T-waves in the right precordial leads at electrocardiogram (ECG) and ventricular arrhythmias of left bundle branch block morphology. Thiene hypothesized that this disease affected primarily the myocardium with progressive atrophy, unrelated to

9

developmental defects (Thiene et al., 1988).

Pathologic substrates

Gross Pathology

The degree of RV involvement varies from localized infiltration of the RV apex, infundibulum, and the posterior wall (''triangle of dysplasia''), resulting in RV dilatation and aneurysms, to diffuse replacement of the myocardium of the RV and ultimately involvement of the left ventricle (LV), particularly the posterior-inferior wall (Thiene et al., 1988; Basso et al., 1996).

In contrast to common heart diseases in which subendocardial muscle shows the greatest pathological changes (e.g., in ischemic heart disease), degeneration of cardiac myocytes and their replacement by fibro-fatty scar in ARVC occur mostly in subepicardial and midmyocardial muscle, and the subendocardial tissue is relatively spared.

The septum is usually spared in ARVC probably because it is not a subepicardial structure. Recently, it has been recognized that the disease can show a phenotypic spectrum much wider than previously thought, with biventricular and predominantly left ventricular forms (Basso et al., 2009; Tavora et al., 2012; Rizzo et al., 2012). Moreover, some victims of SCD show little or no structural remodeling of ventricles. The coronaries are characteristically normal.

In some cases, plaques of endocardial fibrosis, related or not to dystrophic areas, have been observed, probably resulting from the organization of a mural thrombus.

Fatty infiltration of the RV has not to be considered "per se" a sufficient morphologic hallmark of ARVC. A certain amount of intramyocardial fat is present in the RV antero-lateral and apical region even in the normal heart and increases with age and body size. Moreover, ARVC should be kept distinct from adipositas cordis. Presence of replacement-type fibrosis

and myocyte degenerative changes at histology are essential to provide a certain diagnosis, besides remarkable fat replacement (Basso et al., 2005).

Histopathology

The typical histological pattern of ARVC consists of a progressive loss of RV myocardium with fibro-fatty replacement which starts from subepicardium towards the endocardium (Thiene et al., 1988; Basso et al., 2009), embedding strands or sheets of degenerated cardiomyocytes. Careful examination of the heart in classical ARVC reveals at least some pathological changes (foci of fibro-fatty tissue and/or mononuclear inflammatory infiltrates) in the interventricular septum or LV free wall in up to 75% of cases (Corrado et al., 1997). Affected cardiac myocytes show degenerative features such as myofibrillar loss and hyperchromatic changes in nuclear morphology (Basso et al., 2008). Clusters of myocytes can also be seen to be dying at histology, providing evidence of the acquired nature of myocardial atrophy. The myocardial loss is the consequence of cell death occurring after birth, usually during childhood. James was the first to suggest that apoptosis as the mechanism of cell death in ARVC (James, 1994). Later, the occurrence of apoptotic myocardial cell death in ARVC has been reported, either at post-mortem or in vivo in endomyocardial biopsy specimens (Mallat et al., 1996; Valente et al., 1998; Yamamoto et al., 2000).

These changes are frequently associated with inflammatory infiltrates, presenting as patchy myocarditis (Thiene et al., 1991; Basso et al., 1996).

Nobody knows whether inflammation is a reactive phenomenon to cell death, or whether it is the consequence of an infection or immune mechanism. Cardiotropic viruses have been reported in the myocardium of patients with ARVC, thus supporting an infective pathogenesis,

11

even though viruses might not play a role or the dystrophic myocardium favours viral settlement (superimposed myocarditis) (Bowles et al., 2002; Calabrese et al., 2006). Rather than being a continuous process, disease progression might occur during periodic bursts in an otherwise stable disease. These disease exacerbations can be clinically silent in most patients but sometimes can be characterised by the appearance of life-threatening arrhythmias and chest pain. Environmental factors, such as exercise or inflammation, might facilitate disease progression by worsening cell adhesion.

Troponin-I elevation in the context of ARVC indicates a "hot phase" of the disease, and might be used as a prognostic marker in the course of the disease (Kostis et al., 2008; Lazaros et al., 2009).

Ultrastructural pathology

Electron microscopic studies, performed in cases that underwent heart transplantation, disclosed that most of the surviving myocytes did not exhibit any specific alteration. Within the fibrotic areas, lymphocytic infiltrates around capillary vessels, as well as myocyte debris ascribable to recent death, could be observed (Basso et al., 2006).

Intercalated disc ultrastructural abnormalities consisting of decreased desmosome number and intercellular gap widening have been observed in ARVC biopsy samples (Basso et al., 2006). Moreover, abnormally located and irregularly oriented desmosomes were identified in the majority of cases, often with pale internal plaques. Furthermore, some of the adhering junction-like junctions appeared widened in the intercalated disc (Lahtinen et al, 2008). Recently (Noorman et al., 2012), focal accumulation of electron dense material at the Z-lines was observed in the myocardium of an ARVC patient underwent to heart transplantation, a finding previously reported only in boxer dogs suffering from ARVC (Oxford et al., 2011),

suggesting an involvement of cytoskeletal components in the disease. The presence of

similar electron dense material corresponding to aggregation of alpha-actinin within

sarcomeres, is the hallmark of the nemaline myopathy, a disease due to mutations in genes

encoding for actin filament proteins and affecting both skeletal muscle and heart (Clarkson et

al., 2004). Whether mislocalization of one group of proteins is consequent to the other, or the

events occur independently, is to be determined in future studies.

Genetics

In approximately half of all cases, ARVC is familial (Nava et al., 2010; Basso et al., 2009;

Hamid et al., 2002). Familial forms have been reported since the beginning of the 1980s.'

(Marcus et al., 1982). Different genetic variants of ARVC have been mapped and over 140

disease-causing ARVC mutations have been published, reflecting high genetic heterogeneity.

Most of the mutations encod desmosomal proteins, residing in the intercalated disc that

connects adjacent cardiomyocytes, and are predicted to cause loss of function.

The ARVC Genetics Variants Database (www.arvcdatabase.info) was recently established to

provide a public repository for variants in genes that cause ARVC in order to assist with

genotype–phenotype correlations and help determine pathogenicity.

Studies of individuals from the Greek island of Naxos with an autosomal recessive syndrome

characterized by the triad of ARVC with diffuse non-epidermolytic palmoplantar keratoderma

and woolly hair led to the identification of the first causative gene of an ARVC-associated

disorder. Initial mapping of this disorder pointed to the chromosomal locus 17q21, and

candidate-gene sequencing within this region revealed a homozygous deletion in the

plakoglobin (PG) gene (Coonar et al., 1998; Mckoy et al., 2000). In 2000, homozygosity

mapping led to the discovery of a desmoplakin (DSP) gene mutation in three Ecuadorian

families with Carvajal syndrome (Norgett et al., 2000). These mutational discoveries in the PG and DSP genes prompted attention to be focused on the desmosome in the ARVC pathogenesis.

Finding mutations in genes encoding desmosomal proteins, namely DSP (Rampazzo et al., 2002), Plakophilin-2 (PKP2, Gerull et al., 2004; van der Zwaag et al., 2010), Desmocollin-2 (DSC2, Syrris et al., 2006; Heuser et al., 2006; Beffagna et al., 2007), Desmoglein-2 (DSG2, Pilichou et al., 2006; Awad et al., 2006) and PG (Asimaki et al., 2007) led to current idea that ARVC is due to desmosomal dysfunction (Basso et al., 2011).

Although rare, mutations in some non-desmosomal additional proteins, such as transforming growth factor-β3 (TGFB3), which encodes for a cytokine-stimulating fibrosis and modulating cell adhesion (Beffagna et al., 2005), transmembrane protein 43 (TMEM43), which function as a response element for PPAR gamma (peroxisome proliferator-activated receptor gamma), an adipogenic transcription factor which may explain the fibrofatty replacement of the myocardium (Merner et al., 2008), ryanodine receptor 2 (RYR2), which induces the release of calcium from the myocardial sarcoplasmic reticulum (Tiso et al., 2001), desmin (Klauke et al., 2010), lamins A/C (Quarta et al., 2012), titin (Taylor et al., 2011) and phospholamban (van der Zwaag et al., 2012; Groeneweg et al., 2012) have also been associated with human ARVC. Recently, screening for novel candidates of ARVC causing genes have been extended to typical fascia adhaerens components, leading to the identification of α-T-catenin as a new disease-causing gene (van Hengel et al., 2012).

The disease is usually transmitted as an autosomal dominant trait with reduced penetrance and variable clinical expression, even within members of the same family who carry the same disease-associated mutation. This indicates the presence of genetic and/or epigenetic modifiers that interact with environmental factors such as exercise to determine the risk of

SCD or other adverse events. Single mutations in individual genes may not be sufficient to cause ARVC development; compound heterozygous mutations in the same gene (two or more gene variants) or digenic mutations in desmosomal genes (gene variants in two or more desmosomal genes) may be required for disease development and clinical manifestation. Co-inheritance of multiple desmosomal gene sequence variations has been reported to be associated with a higher risk of developing ARVC (Lahtinen et al., 2008; Bhuiyan et al., 2009; den Haan et al., 2009) and with a more severe cardiac phenotype (Bauce et al., 2010; Xu et al., 2010; Quarta et al., 2011).

The availability of molecular genetic testing allows the identification of gene-positive individuals. However, because of the lack of knowledge about long-term outcome in genetically-affected relatives, lifelong follow-up of these relatives is required for early detection of signs of disease.

Despite the ability to positively identify genotypes in a majority of patients with ARVC, genotype–phenotype correlations are still limited and the pathogenic significance of some mutations remains unclear (Bauce et al., 2005; Norman et al., 2005; Sen-Chowdhry et al., 2005; Syrris et al., 2007; Cox et al., 2011; van der Smagt et al., 2012).

Patients carrying PKP2 mutations present at an earlier age than those without mutations and the arrhythmia-free survival is lower (). DSG2 and DSC2 mutations have been predominantly associated with predominantly LV involvement. Finally, it is hypothesised that DP mutations predispose to early LV involvement from disruption of cytoskeletal integrity.

More in-depth knowledge from functional genotype–phenotype analyses and additional identification of disease-modifying factors (genetic or environmental) could allow a reliable preclinical diagnosis of the disease and may open the way for the target-directed therapeutic interventions to refine individualized treatment strategies, and finally to prevent SCD.

Intercalated disc

The end-to-end connection between cardiomyocytes is maintained by the intercalated disc, an electron-dense structure harbouring the intercellular junctions that provide electrical and mechanical coupling in the heart.

The classical definition of intercalated disc involves three main junctional complexes: gap junctions, adherens junctions, and desmosomes (Figure 1A and B).

The gap junction provides intercellular communication via small molecules and ions that pass through a channel generated by a family of proteins called connexins, allowing electrical/metabolic synchronization between cells. Connexin 43 (Cx43) is the most abundant connexin isotype localized in gap junctions of the heart.

Figure 1. Intercellular mechanical and electrical junction of the cardiomyocyte. (A) Schematic representation of junctional components. (B) Transmission electron microscopy of cardiomyocyte intercalated disc. (B) (From Sheikh et al., 2009)
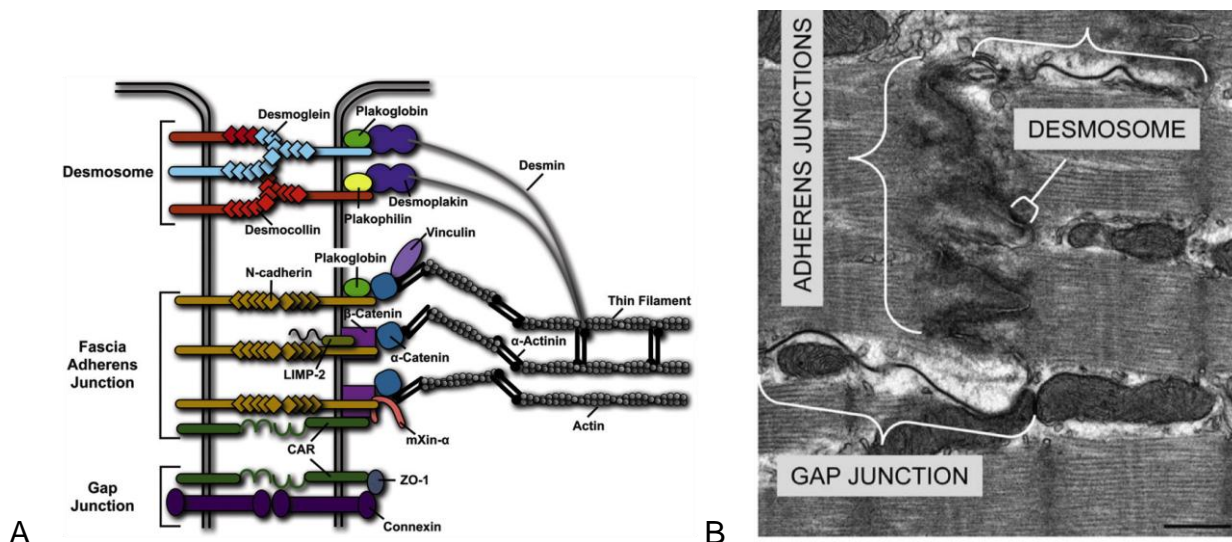
The adherens junction provides strong cell-cell adhesion, which is mediated by the cadherin/catenin complex via linkage to the actin cytoskeleton. In the classic adherens

junctions, the cytoplasmic tail of N-cadherin interacts with either β-catenin or PG. β-Catenin or PG links cadherins to α-catenin, and α-catenin interacts with either the cadherin/catenin complex or the actin cytoskeleton.

The desmosome include proteins from at least three distinct gene families: cadherins, armadillo proteins and plakins (Garrod et al., 2002). Desmosomal cadherins, DSG2 and DSC2 form extracellular connections by homophilic and heterophilic binding with cadherins on neighboring cells. The cytoplasmic tails of desmosomal cadherins bind to the armadillo proteins PG and PKP-2, which in turn bind to the plakin protein DP. DP links desmosomes to intermediate-filament desmin, playing a key role in ensuring mechanical integrity and intercellular force transmission of tissues which undergo high mechanical stress, such as epidermis and heart (Cheng and Koch, 2004; MacRae et al., 2006; Stokes 2007).

It is not surprising, therefore, that human diseases related to mutations in desmosomal proteins manifest clinically as cardiac or cutaneous diseases whose phenotypic expression is determined by the specific tissue distribution of the mutant protein and by the severity of the mutation.

Recent evidence has emerged to suggest that these junctions are more structurally and functionally complex than once thought. A study of the ultrastructure of the adult mammalian heart supports the notion that desmosome and adherens junctions are not morphologically distinct; rather, the cardiac intercalated disc shows (in addition to gap junctions) the "area composita" with mixed characteristics of the 2 types of mechanical junctions and colocalisation of the usually distinct components of desmosomes and adherens junctions. In area composita desmosomal proteins are therefore indirectly involved in supporting the myofibrillar actin anchorage in N-cadherin mediated cell–cell adhesion complexes (Franke et al., 2006). Recognition of the "area composita" and the determination of interactions between

17

intercellular adhesion molecules and gap junctions suggests that these may be 3 elements of a single functional unit. Moreover, there is growing evidence that other molecules, not directly involved in intercellular coupling, also reside at the intercalated disc. Among them is NaV1.5, the major a-subunit of the cardiac sodium channel (Kucera et al., 2002).

Clinical features and natural history

The phenotype of ARVC is highly variable, ranging from the asymptomatic to a severely symptomatic state due to arrhythmias (palpitations, dizziness related to syncopal episodes or aborted SCD) (Basso et al., 2009). Often the first and only symptom is SCD. Although mutations are present throughout the earliest stages of cardiac development, clinical symptoms are manifested in the early adulthood. ARVC clinically manifests sooner and more severely in athletes but also in individuals not physically active, and can be identified later in life. Sex influence with greater clinical severity in males has been described (Blomstrom-Lundqvist et al, 1987). More recently, although men are more frequently affected than women, gender appears a priori not to harbor adverse effects on long-term survival (Bauce et al., 2008). Exercise may be a precipitating factor, suggesting adrenergic inputs as a culprit in generating these tachycardias, that may be due to increased sympathetic tone.

Based on the long-term clinical follow-up, the natural history of ARVC was distinguished in four phases in the past (Thiene et al., 1990):

1.   in the first subclinical phase, the patients are usually asymptomatic, but may be at risk of SCD, especially during exercise. The structural changes in the early "concealed" phase, when present, are of small extent and may locate at the inferior, apical, and infundibular walls of the RV (triangle of dysplasia).

2.   In the second, "overt" electrical phase, symptomatic ventricular arrhythmias of RV

origin, usually triggered by effort, are observed, while the morphological and functional changes in the RV are more apparent.

3. The third phase is characterized by diffuse damage of the RV, accounting for severe pump failure, while LV function is preserved by comparison.

4. In the fourth, advanced phase, there is severe, diffuse biventricular involvement, mimicking dilated cardiomyopathy. Endocavitary mural thrombosis may develop within aneurysms or in the atrial appendages, when heart failure is complicated by atrial fibrillation, leading to thromboembolism. In such conditions, contractile dysfunction may require cardiac transplantation.

SCD can occur at any time during the disease course, and the incidence of SCD varies from 0.1% to 3.0% per year (Basso et al., 2012), but may be higher in adolescents and young adults, in whom the disease is concealed.

SCD is generally the result of an abrupt ventricular tachyarrhythmia that compromises cardiac output. Despite great advances in the treatment of SCD using implantable cardioverter defibrillators (ICDs), the incidence of SCD continues to rise, probably due to our inability to clearly identify all high-risk patients who will benefit from ICDs, and uncomplete understanding of the arrhythmic mechanisms in ARVC.

In the fully expressed form, the diagnosis of ARVC is not difficult. However, the classical findings may not be apparent in the early stages of the disease, during which patients may still be at risk of ventricular arrhythmias, leading to diagnostic difficulties. So the main clinical targets are early detection of concealed forms and risk stratification for preventive strategies.

Diagnosis

Diagnosis of ARVC carries serious implications both for the affected patient and also for family members, especially because SCD can be the first manifestation of the disorder. In many cases, families first become aware of ARVC when an index case dies suddenly and the disease is diagnosed at autopsy.

Several factors, including marked phenotypic variation, incomplete and low (30%) penetrance, and age-related disease development and progression contribute to the complexity of clinical diagnosis (Sen-Chowdhry et al., 2005).

In 1994 a Task Force proposed criteria, encompassing structural, histological, electrocardiographic, arrhythmic and genetic factors, that are used as a standard in clinical diagnostics (McKenna et al., 1994). According to this classification, the presence of two major criteria or one major and two minor criteria or four minor criteria are required in order to confirm ARVC. Despite a standardized approach designed to facilitate assessment, arriving at a definitive diagnosis remains challenging in many individuals. The original criteria focused on the diagnosis of overt and severe disease and lacked sensitivity for early forms common among family members.

The diagnostic criteria have been recently revised by an international Task Force (Marcus et al., 2010), to incorporate new –predominantly electrophysiological - knowledge and technology (i.e.MRI), to enhance the detection of "nonclassic" patterns of ARVC through advanced cardiac imaging and to include quantitative parameters, aiming to increase sensitivity while maintaining the already high specificity of the 1994 guidelines. These new criteria are particularly useful for the identification of early phenotypes, such as in cases of familial disease. Moreover, it appears that the revised criteria can better identify individuals who carry disease-causing mutations in one or more desmosomal genes.

The diagnostic criteria are divided in six categories: depolarization/conduction abnormalities, repolarization abnormalities,ventricular arrhythmias, right ventricular structural or functional characteristics as demonstrated by imaging techniques, histological criteria, and familial occurrence of ARVC or presence of mutations associated with ARVC (Figure 2). Clinical suspicion of ARVC is the most important factor in diagnosis (Basso et al., 2009). This condition should be considered in any young healthy patient who presents with frequent palpitations, lightheadedness, or syncope in the absence of a clear precipitating cause. Other warning signs include a positive family history of SCD and an abnormal ECG.

Most of the patients are evaluated for the above-mentioned symptoms and undergo screening Holter or excersise testing, which shows multifocal premature ventricular contractions, short runs of nonsustained ventricular tachycardia, or sustained ventricular tachycardia of left bundle branch block morphology, which prompts further diagnostic workup.

Figure 2. Schematic diagram of the recently modified diagnostic criteria for ARVC (From Paul et al, 2012)
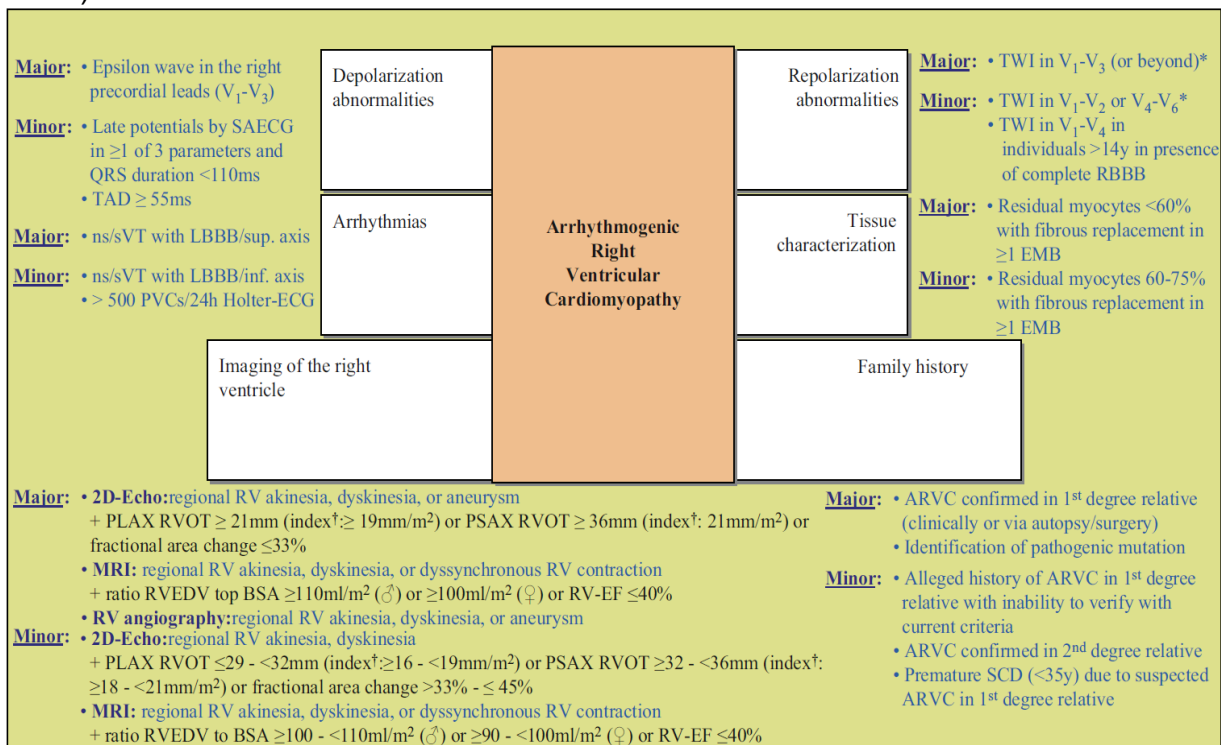
Electrocardiography

It is one of the key screening diagnostic modalities, resulting abnormal in 70% of cases. The diagnosis of ARVC can often be suspected on the basis of ECG abnormalities. Precordial T-wave inversion in V1-V3 is the most common finding. A unique finding is the presence of the "Epsilon Wave" in the right precordial leads, which represents a relative prolongation of the QRS complex as a result of slow conduction in the diseased RV free wall. The presence of a QRS greater than 110 ms along with precordial T wave inversion is said to have high sensitivity and specificity for ARVC. Among electrocardiographic parameters, right precordial QRS prolongation, QRS dispersion, and late potentials on signal-averaged ECG (SAECG), have been associated with an increased arrhythmic risk in ARVC.

Holter monitoring and excersise testing may show ventricular tachycardia of left bundle branch block morphology with a superior axis orientation, which helps to differentiate it from RV outflow tract tachycardias, which are more benign and have an inferior axis orientation.

Echocardiography

2-D Echocardiography is the standard modality used for diagnosis of ARVC. Echocardiography is noninvasive and represents the first-line approach in evaluating patients with suspected ARVC or in screening family members.

Findings include RV enlargement or multiple outpouchings and dyskinetic areas which cause RV dysfunction. Diastolic bulging of the infero-basal wall, structural abnormalities of the moderator band, isolated dilatation of the RV outflow tract, apical dyskinesia, and trabecular disarrangement have also been reported.

Echocardiography has value in overt cases and may be negative in cases with localized disease not associated with significant RV morphologic change. Moreover, conventional

echocardiography cannot be detect LV involvement in ARVC because of the relatively late appearance of overt LV structural and functional abnormalities (Marcus et al., 2007; Corrado et al., 2011).

Magnetic Resonace Imaging and Computerized Tomography

Computerized tomography (CT) and MRI provide better structural evaluation and offer the advantage of noninvasive tissue characterization.

CT features of ARVC are a localized or diffuse RV involvement and dilatation, thinning of the free wall, and hypokinesis. The distinguishing feature is the marked increase in subepicardial fat delineated by densitometric analysis of the CT image.

As an imaging modality, MRI offers many advantages for the evaluation of ARVC, including noninvasive detection of structural changes in vivo, avoidance of exposure to ionizing radiation, and visualization of the RV without restriction by acoustic windows. Moreover, MRI plays a pivotal role, especially thanks to its unique ability to detect LV involvement and early and subtle cases of ARVC which may otherwise be misdiagnosed (Hunold et al, 2005; Sen-Chowdhry et al., 2008; Marra Perazzolo M et al. 2012), using the late enhancement technique even in the setting of preserved morpho-functional features. Cine-MRI may be of value in estimating RV volume and wall motion abnormalities with akinesia, dyskinesia and aneurysms. However, recent studies have shown a high degree of interobserved variability in assessing fatty deposition, which may be observed even in normal hearts.

It is becoming clear that this non-invasive tool is a valuable diagnostic tool that complements echocardiography and substantially enhances the sensitivity of clinical diagnosis, particularly in early disease (Sen-Chowdhry et al., 2006).

Endomyocardial Biopsy

In patients suspected of ARVC by clinical and diagnostic modalities, transvenous endomyocardial biopsy may help to confirm the diagnosis, through histological demonstration of fibro-fatty myocardial replacement. Biopsy may give false negative results in cases with localized involvement. The major limitation is that the biopsy is usually obtained from the septum, which is spared in ARVC leading to a false negative result (Basso et al., 2008; Marcus et al., 2010). Samples should be retrieved from the RV free wall, since the fibro-fatty replacement is usually transmural and thus detectable from the endocardial approach.

A residual amount of myocardium <60%, due to fibrous or fibro-fatty replacement, has been proven to have a high diagnostic accuracy and is now considered a major criterion for ARVC diagnosis. To improve the diagnostic sensitivity for ARVC, an endomyocardial biopsy procedure guided either by voltage mapping or by MRI has been suggested (Avella et al., 2008). Moreover, biopsy is essential to rule out the so-called ARVC "phenocopies", such as myocarditis, sarcoidosis or idiopathic RV outflow tract tachycardia (Corrado et al., 2005; Corrado et al., 2008; Vasaiwala et al., 2009; Corrado et al., 2009; Ladyjanskaia et al., 2010). Very recently, a new diagnostic test based on immunohistochemical desmosomal analysis of human myocardial samples obtained by endomyocardial biopsy has been shown to be sensitive and moderately specific in diagnosing ARVC (Asimaki et al., 2009). This study showed that the immunoreactive signal level for the desmosomal protein PG was reduced at intercalated discs in patients with ARVC, not only in diseased RV myocardium, but also in normal-appearing LV and interventricular septum, potentially expanding the diagnostic utility of a conventional endomyocardial biopsy.

However, the extent to which this test may be used in the routine diagnosis of early-stage disease in the clinical setting remains to be seen. A more complete understanding of the

specificity of this test in the full spectrum of ARVC will be required.

Electrophysiologic Study

Emerging data suggest an increasing role for endocardial voltage mapping in identifying the presence of scarring in the RV in early phases of the disease. The technique has the potential to accurately identify the presence, location and extent of the pathologic substrate of ARVC to be targeted by endomyocardial biopsy and ablation, by demonstration of low voltage RV regions, corresponding to areas of myocardial depletion and correlating with the histopathologic finding of myocardial atrophy and fibro-fatty replacement at endomyocardial biopsy (Corrado et al., 2005).

Electrophysiologic testing with programmed electrical stimulation (PES) should be performed to define the morphologic characteristic of the arrhythmia, and if possible, a precise region of origin in the RV. This can guide drug suppression trials and/or radiofrequency ablation of the arrhythmogenic focus.

Differential Diagnosis

The main differential diagnoses of ARVC are idiopathic RV outflow tract tachycardia, sarcoidosis, idiopathic dilated cardiomyopathy, and isolated myocarditis. Although it is not difficult to diagnose a manifest case of ARVC, differentiation of ARVC at its early stages from idiopathic RV outflow tract tachycardia, a usually benign and nonfamilial arrhythmic condition, remains a clinical challenge. If clinical doubts remain after traditional examinations (ECG, Holter) and imaging techniques (echocardiogram, MRI), RV voltage mapping seems to be a useful emerging tool to differentiate between the two entities.

Cardiac sarcoidosis, a disorder in which noncaseating granulomas focally replace the

myocardium, and ARVC can manifest very similarly. The discrimination between these entities is very challenging at times, notably because of common RV and occasionally just mild to moderate LV involvement. the revised diagnostic ARVC criteria do not reliably differentiate cardiac sarcoidosis from ARVC. Additional testing (endomyocardial biopsy, electroanatomical mapping, MRI), to specifically exclude sarcoidosis is of major relevance, as treatment differs fundamentally (Corrado et al., 2009; Ladyjanskaia et al., 2010; Dechering et al., 2012; Steckman et al., 2012).

The Brugada syndrome has been considered a subliminal form of ARVC (Martini et al., 2004; Corrado, Basso et al., 2010). In some cases of Brugada syndrome, subtle structural interstitial changesin the RV, that are undetectable by routine diagnostic procedures, may underlie both the ECG changes and the propensity for life-threatening arrhythmias (Coronel et al., 2005). Prior to the introduction of the Brugada syndrome, Martini et al. (1989) presented a patient with right precordial ST-segment elevation and idiopathic ventricular fibrillation. One patient demonstrated what was later to be called the Brugada ECG pattern. Careful clinical re-evaluation demonstrated enlargement of the right ventricular outflow tract and right ventricular wall motion abnormalities. This caused the authors to conclude that a concealed form of ARVC was present in this patient. Since, more histological findings consistent with ARVC have been demonstrated at autopsy series of patients with the Brugada ECG (Corrado et al., 1996, 2001; Tada et al., 1998). The largest series was presented by Corrado et al. (2001) and consisted of 13 young SCD victims with a Brugada ECG pattern on their last recorded ECG. Of these patients, 12 demonstrated structural heart disease consistent with ARVC at autopsy. Similar to Brugada syndrome patients (Matsuo et al., 1999), most of these patients died at night or at rest (Tada et al., 1998; Corrado et al., 2001). Furthermore, polymorphic VTs as observed in the Brugada syndrome were recorded in some these ARVC patients (Corrado et

al., 2001). Secondly, sodium channel blockers can induce the Brugada ECG pattern ~1 in 6 patients previously diagnosed with ARVC (Peters et al., 2004; Peters, 2008). These data indicate the Brugada ECG pattern, the associated ventricular arrhythmias are present and can be modulated by INa in some ARVC patients (Hoogendijk 2012).

Role of Genetic Analysis

A key clinical application of genetic analysis includes confirmatory testing of proband cases to facilitate interpretation of investigations (Basso et al., 2011). Moreover, genotyping relatives with non-overt forms of ARVC and before a malignant clinical phenotype is manifest may be crucial in preventing SCD, through serial clinical follow-up (electrocardiogram, echocardiogram, 24-hour Holter, early recognition of symptoms), lifestyle modifications (restriction from extreme activity), and prophylactic therapy when needed (antiarrhythmic drugs, ICDs).

Despite its reliability, genetic sequencing is an effort- and cost-intensive process, especially in the investigation of ARVC, in which potentially large numbers of genes are involved (Sen-Chowdhry et al., 2007). Recommending genetic testing in patients with ARVC and their first-degree relatives has to be linked to specific guidelines (e.g., genetic pre-/posttest counseling, standardized protocols of laboratory analyses) (Ackerman et al., 2011; Charron et al., 2010; Hofman et al., 2010). Genetic testing for ARVC gene variants is supportive, but should not to be mistaken for the ultimate diagnostic tool, since genetic heterogeneity, clinical variant phenotypic presentation, and variable disease progression still complicate the understanding of the disease (Kapplinger et al., 2011).

The negative genetic examination is not incompatible with the diagnosis of the disease.

Treatment

The main goal of a management strategy is to prevent SCD. Currently, antiarrhythmic drugs, catheter ablation, and ICDs are the 3 main therapies available for patients with ARVC (Thiene, Rigato et al., 2012; Basso et al., 2012).

In addition, patients should avoid competitive sports and any activity that causes palpitations, presyncopal or syncopal episodes (Corrado et al., 2003).

Left cardiac sympathetic denervation, which is a safe and effective antifibrillatory therapeutic option for channelopathies, has been recently suggested as a potential adjuvant treatment in patients with cardiomyopathies and malignant ventricular arrhythmias, which may be exacerbated specifically by sympathetic activation (Coleman et al., 2012).

Antiarrhythmic agents

Antiarrhythmic drug therapy is applied with varying rates of efficacy in the treatment of ventricular tachycardia (Basso et al., 2012). Patients with ARVC and no history of syncope or cardiac arrest, but with premature ventricular contractions or short ventricular runs do not usually have an increased risk of arrhythmias and therefore do not require specific antiarrhythmic treatment. In patients with sustained ventricular tachycardia, the aim of antiarrhythmic drug therapy is the prevention of SCD. Not much data are available concerning the use of pharmacologic agents in the treatment of patients with ARVC for the prevention of SCD. To date, prospective, randomized studies on antiarrhythmic drug efficacy in ARVC are not available. The largest experience of pharmacologic therapy in ARVC comes from Germany, with 191 patients and 608 drug tests (Wichter et al., 1992; Wichter et al., 2005). Sotalol was the most effective drug, with an a 68% overall acute efficacy rate. In a small subset of patients with non reentrant VT and possible triggered activity or autonomic

abnormal automaticity, verapamil and beta-blockers had efficacy rates of 44% and 25%. Amiodarone alone or in combination with beta-blockers was also effective, while class I antiarrhythmic drugs were only in a minority of patients (18%). Anyway, in long-term, sotalol or non pharmacologic treatments are preferentially used due to the high incidence of serious side effects of amiodarone.

The next largest study comes from the North American Registry, in which 108 patients were prospectively collected and put on antiarrhyhmic drug at the discretion of the treating physician (Marcus et al., 2009). Noteworthy, 95 had ICD and the majority (61%) was treated with beta-blockers, including atenolol, metoprolol, bisoprolol and carvedilol. The authors did not observe a clinical significant benefit to prevent VT or VF with beta-blockers as compared with patients not taking antiarrhythmic drugs or beta-blockers, although a trend in reduction on ICD shocks was noted.

Catheter ablation

The role of catheter ablation using three-dimensional electroanatomic mapping systems in ARVC remain poorly defined, and is frequently used as a palliative measure for patients with with localized forms of the disease and drug-refractory or incessant ventricular tachyarrhythmias or frequent ICD discharges. The progressive pathology of ARVC suggests that catheter ablation would not be a long-term curative procedure (Dalal et al., 2007). The recognition that the epicardial scar is usually much more extensive then the endocardial area of involvement has resulted in evolution of ablation strategies to involve both the epicardium and the endocardium. Preliminary results are encouraging with success rates of 85% at 3 years (Bai et al., 2011) and no VT recurrence after 18+/-13 months in 77% of treated patients in the Marchlinski series (Marchlinski et al., 2004). More recently, Philips et

al, by reporting the outcome of catheter ablation of VT in 87 ARVC patients, demonstrated that, despite the better results with the epicardial approach and the use of 3D electroanatomic mapping, recurrence rates remain considerable; a cumulative freedom from VT following epicardial ablation of 64% and 45% at 1 and 5 years was found, which was significantly longer than with the endocardial approach (p=0.02) (Philips et al., 2012). Epicardial ablation is not without hazard because of myocardial perforation, tamponade, etc., and should be done in selected centers that have considerable experience with this approach (Sacher et al., 2010).

Implantable Cardioverter-Defibrillator

ARVC patients are often considered for ICD implantation after an aborted cardiac arrest or after a syncope related to ventricular tachyarrhythmias (Zipes et al., 2006). It is widely accepted that ICD therapy improves long-term prognosis and survival in ARVC patients at high risk of SCD (Corrado et al., 2003; Wichter et al., 2004; Roguin et al., 2004; Hodgkinson et al., 2005; Corrado et al., 2010). In this high risk group of patients, the rate of appropriate ICD intervention against life-threatening ventricular tachyarrhythmias is 8-10% per year and the estimated mortality reduction at 36 months of follow-up ranges from 24 to 35% (Corrado et al., 2010). However, the significant rate of inappropriate interventions and complications, as well as the psychological repercussions mostly in the younger age group, strongly suggests the need to accurately stratify the individual arrhythmic risk before device implantation (James et al., 2012).

ICD implantation for primary prevention in the general ARVC population seems to be unjustified (Corrado et al., 2010). Few data are available to guide the prophylactic indications for ICD implantation in ARVC patients (Corrado et al., 2003; Hodgkinson et al., 2005; Berul et

al., 2008). In the future, it is likely that genetics will play a more important role in decision-making.

Cardiac transplantation

When the disease has progressed to right ventricular or biventricular failure, treatment consists of the current therapy for heart failure, including diuretics, beta-blockers, angiotensin-converting enzyme inhibitors, and anticoagulants.

In the case of intractable right heart failure, cardiac transplantation may be the only alternative (Thiene et al., 1998).

Recent Insights

While RV involvement in "classic" ARVC is the most common and well-described manifestation of the disease, recent evidence has shown that both RV and LV are often affected in these patients. As such, a descriptive change to Arrhythmogenic Cardiomyopathy has been suggested to better reflect the pathology (Basso et al., 2010; Sen-Chowdhry et al., 2007; Sen-Cowdhry et al., 2010; Jacoby and McKenna, 2012; Rizzo et al., 2012).

Three distinct patterns of disease expression exist: (1) "classic" ARVC, characterized by RV preponderance throughout the disease course; (2) "left dominant arrhythmogenic cardiomyopathy (LDAC)" characterized by early and predominant LV involvement (Sen-Cowdhry et al., 2008); and (3) a biventricular variant, which is characterized by parallel involvement of both ventricles.

ARVC is characterized by electrical instability presenting ventricular arrhythmias of RV origin. Therefore, the role of an arrhythmogenic co-factor of LV involvement of the disease remains to be established, but may reflect a greater involvement of total myocardial mass by the

disease process. The clinical implication being that the morphologic arrhythmogenic site of origin will respond to treatment differently in this subset of patients with coexisting LV dysfunction. This has led to the impression that for ARVC patients with progressive LV involvement and drug-resistant arrythmia, other treatment options such as the ICD or cardiac transplantation should be considered.
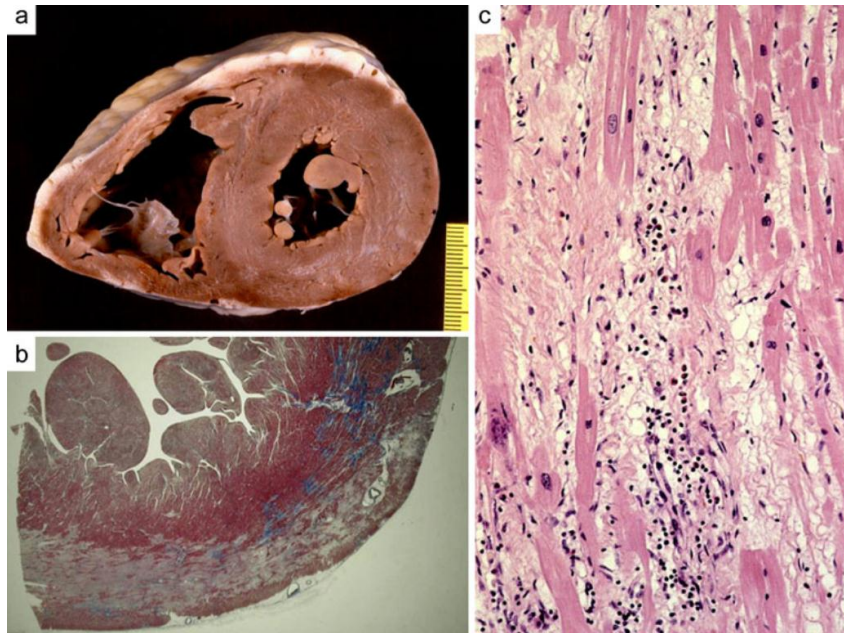
LV Involvement

It was originally thought that LV involvement developed only as a feature of advanced disease in ARVC. Basso et al. reported evidence of left ventricular involvement in 47% of the cases (Basso et al., 1996). Corrado et al. reported in their series of 34 patients that 75% had LV involvement (Corrado et al, 1997).

Recently a new clinical entity Left Dominant Arrhythmogenic Cardiomyopathy (LDAC) was defined (Sen-Chowdhry et al., 2008), characterized by: (a) unexplained ventricular arrhythmia of right bundle block configuration, (b) unexplained T-wave inversion in inferior or lateral leads, (c) mild LV dilation and/or systolic impairment, (d) myocyte loss with fibrofatty or fibrotic replacement confirmed by biopsy or late gadolinium enhancement in the LV on MRI. Pathologically, the heart in LDAC shows lesions composed of relatively more fibrosis and less fat in subepicardial or midmyocardial areas of the postero-inferior LV free wall (Figure 3). MRI showing late enhancement following infusion of gadolinium appears to be the best clinical tool to document these lesions. The most common mutations linked to LDAC are dominant mutations in the gene encoding DSP. Unfortunately, the international task force criteria established for the diagnosis of ARVC do not apply to LDAC, which remains an underrecognized condition that, apparently, is often mistaken for dilated cardiomyopathy or myocarditis.

Figure 3. Early stage of ARVC in a 15-year-old asymptomatic boy carrying a desmoplakin mutation who died suddenly at rest. a Cross section of the heart showing a whitish midmural–subepicardial band in the postero-lateral left ventricular wall, in the absence of wall thinning, aneurysm and RV abnormalities. b Panoramic histologic view of the posterolateral left ventricular wall, showing a subepicardial band of acute–subacute myocyte necrosis with loose fibrous tissue and granulation tissue (trichrome Heidenhain ×3). C Myocyte necrosis and myocytolysis associated with polymorphous inflammatory infiltrates, together with early fibrous and fatty tissue repair (haematoxylin–eosin ×40). (From Rizzo et al., 2012).

Biventricular Involvement

This occurs when the same disease process characteristic of ARVC affects the LV causing progressive fibrofatty infiltration leading to LV dysfunction. This may lead to an erroneus diagnosis of dilated cardiomyopathy, although evidence of fibrous and fatty infiltration in the LV should lead to the correct diagnosis. In a study of 200 patients with ARVC, MRI revealed evidence of biventricular involvement in 56% of the patients and predominant LV disease in 5% (Sen-Chowdhry et al., 2007). The occurrence of biventricular disease is also supported by animal models and genomics data, which have revealed that only a small number of genes are differentially regulated between the RV and LV in ARVC (Gaertner et al., 2012).

In such instances, histological examination is the only way of conclusively establishing the

diagnosis of ARVC. Histologically, ARVC patients with biventricular involvement need to be distinguished from myocarditis with fatty infiltration.

Pathophysiological mechanisms

Though the genes and causative mutations have been identified in ARVC, the pathogenesis of the condition is obscure.

To explain the loss of the ventricular myocardium and the replacement by fibrous and fatty tissue, several etiopathogenetic theories have been advanced (Basso et al., 2009; Basso et al., 2010).

In the disontogenetic theory, the absence of myocardium is considered to be the consequence of a congenital aplasia or hypoplasia of the RV myocardium, like in Uhl's anomaly (Uhl 1952). The use of the term "dysplasia" is in agreement with this view. In contrast, in ARVC there are always residual myocytes within fat and fibrous tissue between the epicardial and endocardial layers. In ARVC, myocardial atrophy is the consequence of cell death occurring after birth, progressive with time.

In the inflammatory theory, the fibrofatty replacement is viewed as a healing process in the setting of chronic myocarditis. The loss of the RV myocardium might be the consequence of an inflammatory injury followed by fibrofatty repair. Thus, an infectious and/or immune myocardial reaction might intervene in the etiology and pathogenesis of the disease (Thiene et al., 1991). Cardiotropic viruses have been reported in the myocardium of some patients with ARVC, thus supporting an infective pathogenesis (Bowles et al., 2002; Calabrese et al., 2006). However, the viral agent might be just an innocent bystander or play a secondary but still important role. According to the latter hypothesis, the genetically dystrophic myocardium could favour viral settlement (superimposed myocarditis), leading to progression or the

precipitation of the disease phenotype. Noteworthy, similar pathological features of inflammation have been described in spontaneous animal models of ARVC, with a clinical picture dominated by right heart failure and ventricular arrhythmias at risk of SCD (Fox et al., 2000; Basso et al., 2004). Recently, inflammatory infiltrates are considered as the consequence of myocyte degeneration and death rather than the result of a superimposed viral myocarditis. Pilichou et al., in an experimental animal model, showed that myocyte necrosis is the key initiator of myocardial injury in ARVC, triggering progressive myocardial damage, with inflammatory response followed by injury repair with fibrous tissue replacement, supporting the reactive nature of myocarditis (Pilichou et al., 2009).

The role of inflammation in ARVC is unresolved, although inflammation may contribute to disease progression in ARVC. Campian et al. assessed cardiac inflammation non-invasively with the combined analysis of plasma inflammatory cytokine levels and cardiac 67Ga scintigraphy, showing that ARVC patients had significantly higher plasma levels than controls of the pro-inflammatory cytokines interleukin (IL)-1b, IL-6 and tumor necrosis factor TNF-alpha as well as a significantly higher 67Ga uptake in the RV wall (Campian et al., 2010). Moreover, myocardial expression of IL-17 and TNF-alpha was recently observed in patients with ARVC (Asimaki et al., 2011). The clinical implications of these findings remain to be clarified. Inflammation probably play a major part in triggering life-threatening arrhythmias and can be associated with abrupt acceleration of biventricular cardiac failure that leads to the hypothesis that ARVC is a genetic disease in which environmental factors can trigger heart failure as well as ventricular arrhythmias. An increase of C-reactive protein has been reported in patients who have recent ventricular tachycardia as compared with ARVC patients referred without arrhythmias (Bonny et al., 2010). Of interest is the observation by Hoffman et al. that inflammation may lead to the production of early after depolarizations which may be a

mechanism for ventricular arrhythmias (Hoffman et al, 1997).

To try to explain the fibro-fatty phenomenon, a transdifferentiation theory has been also advanced, according to which cardiomyocytes transform into fibrocytes and/or adipocytes (d'Amati et al., 2000). The transdifferentiation theory is based on the hypothesis that myocardial cells can change from muscle to fibrous and adipose tissue and the observation that in one patient, "transitional cells" at the interface between cardiac muscle and adipose tissue expressed both desmin, which is characteristic of muscle tissue, and vimentin, expressed only in adipocytes. However, this theory is questionable due to the limited dedifferentiation capabilities of adult cardiomyocytes.

In the degenerative or dystrophic theory (Basso et al., 1996), the loss of the myocardium is considered to be a consequence of progressive, genetically determined, myocyte death, either by apoptosis or necrosis (Mallat et al., 1996; Valente et al., 1998), and fibrofatty replacement, as observed in the skeletal muscle of patients with Duchenne's and Becker's diseases. The acquired nature of the disease (postnatal phenotype expression) is corroborated by the age range of the affected patients (15 to 65 years), the nearly preserved distance of the epicardium from the endocardium without apposition of the two layers, and, most important, the observation of patchy myocyte death associated with inflammatory infiltrates and fibrofatty repair in various stages of healing. The cell death could enhance the electrical vulnerability of the ventricles, thus accounting for the onset of life-threatening arrhythmias.

Nowadays, desmosomal dysfunction is considered the final common pathway of ARVC pathogenesis (Basso et al., 2011). Genetic mutations responsible for ARVC result in haploinsufficiency and reduced expression of desmosomal proteins, which may predispose mechanical cell contacts to rupture, potentially triggered by mechanical stress of the RV (such

as that occurring during exercise or sports activity). Degeneration and death of the cardiomyocytes is the pathological consequence of these mutations in adhesion proteins, with the subsequent progressive replacement by fatty and fibro-fatty tissue. Mechanical overload of the cell–cell junction is considered to trigger the pathophysiological myocardial changes in ARVC (Delmar et al., 2010). Patients with ARVC are particularly prone to disease exacerbations in response to strenuous exercise, emphasizing the importance of biomechanical determinants of disease. The observation that the thin walled RV and the thinnest segment of the LV (posterior wall) are most often involved may reflect these areas being more vulnerable to physical stress or stretch, where, according to Laplace's law, wall tension is particularly high (Thiene et al., 2012). The septum is thicker, and this may explain why it is rarely involved.

Signaling pathways have been implicated in ARVC pathogenesis (Basso et al., 2011). Although desmosomes are traditionally considered specialized structures which provide mechanical attachment between cells, they are emerging as mediators of intra- and intercellular signal transduction pathways (Huber et al., 2003; Desai et al., 2009; Green et al., 2010). It is suggested that PG is involved in a final common pathway of defects in the desmosomal mechanical junction via its signalling role. Immunohistochemical and molecular studies of intercellular junction proteins demonstrated PG redistribution from intercellular junctions to other locations within the cell in nearly every case of ARVC (Kaplan et al., 2004; Asimaki et al., 2009). When PG translocates to the nucleus, it competes and opposes the action of β-catenin and downregulates the canonical Wnt/b-catenin signaling pathway (Garcia-Gras et al., 2006), driving adipogenesis and fibrogenesis in cardiac tissue. Moreover, redistribution of PG from junctions to intracellular pools with impaired mechanical coupling might account for abnormal electrical coupling by gap junction remodeling, providing

evidence that a mutation in a single desmosomal protein may perturb the subcellular distribution of another intercellular junction protein which is not genetically altered.

Models of ARVC

Because it is difficult to obtain cardiac tissue from mutation-positive patients, the effects of desmosomal gene mutations have mostly been studied in artificial expression systems by use of transfected cell cultures and animal models of the disease.

Overexpression of mutant desmosomal genes or introduction of mutant desmosomal genes in mice and other animal model systems (zebrafish) have contributed to understand the pathophysiological processes leading to both cardiomyopathy and an increased susceptibility to cardiac arrhythmias (Macrae, 2010; Pilichou et al., 2009; Lodder and Rizzo, 2012).

Since keratinocytes express all cardiac-specific isoforms of desmosomal proteins, it is likely that changes in myocardial expression of desmosomal proteins, as a result of mutations, are mirrored by similar changes in the epidermis (Desai et al., 2009).

ARVC appears to occur spontaneously in Boxer dogs and is associated with a high incidence of ventricular arrhythmias and SCD, although the genetic basis of the disease in these animals is unknown. Afflicted Boxers show loss of gap junctions, suggesting that, as in human ARVC, the disease in Boxers is associated with a significant remodeling of the structures involved in cell-cell communication and supporting the notion that loss of gap junctions may represent a substrate in the development of ARVC-related ventricular arrhythmias (Oxford et al., 2007).

A variety of animals have been used to examine the pathological effects of mutations at both the whole organism/organ level and the cellular and molecular level.

With the advent of genetically modified mouse models, inherited mutations identified in

humans with cardiomyopathy are now modeled in transgenic or knock-in mice that may recapitulate the clinical features of the disease (Berul, 2003). It is important to note that transgenic mouse models may have limitations from alterations in gene expression besides the targeted gene. Likewise, single gene knockout models may introduce compensatory changes in other related structural genes, which may confound phenotypic results. However, animal models of ARVC continue to provide valuable insights into our understanding of the disease.

Mutations in the gene encoding DSP are a classic example of desmosomal dysfunction leading to ARVC phenotype.

Using the human squamous carcinoma line SCC9 as a cellular model of desmosome formation, it was demonstrated that the N-terminal mutants V30M and Q90R failed to localize to the plasma membrane, whereas the C-terminal R2834H mutation did not affect the function of the N-terminus (Yang et al, 2006).

DSP targeted deletion mice (DSP −/−) die at embryonic day 6.5 of malformations in the extra-embryonic tissue before assessment of a cardiac phenotype is possible (Gallicano et al., 1998). To overcome this problem the extra-embryonic phenotype was rescued by tetraploid aggregation. The resulting embryos die around embryonic day E11. At E10 they show severe cardiac malformation although desmosomal-like structures appear to be present by transmission electron microscopy (Gallicano et al., 2001).

The embryonic lethality of the DSP−/− mice is partially circumvented in the cardiac specific, αMHCcre induced, targeted deletion of DSP (Garcia-Gras et al., 2006). Cardiac-restricted deletion of DSP impaired cardiac morphogenesis and caused embryonic lethality in homozygous knockout mice (DSP-/-). Histopathologic evaluation revealed poorly formed hearts with no chamber specification and poorly organized myocytes with large areas of

patchy fibrosis. Furthermore, an excess number of cells resembling adipocytes, dispersed between myocytes, were also detected. Heterozygous DSP-deficient mice exhibited excess adipocytes and fibrosis, increased apoptosis, defective cardiac contractility and ventricular arrhythmias, recapitulating the human ARVC phenotype. In addition to these pathologic abnormalities, the authors showed that PG interacts and competes with β-catenin, the effector of the canonical Wnt signalling, having a negative effect on this pathway. They were able to show that PG was translocated to the nucleus in DSP-deficient mice and that expression levels of gene targets of the canonical Wnt/β-catenin pathway were reduced.

Another animal model of mutant DSP was recently described (Yang et al., 2006). This model, a transgenic mouse with cardiac-restricted overexpression of a C-terminal DSP mutant (R2834H), resulted in viable mice that developed ventricular dilatation and biventricular cardiomyopathy, with histological evidence of cardiomyocyte apoptosis, cardiac fibrosis and lipid accumulation. The mutant mice also displayed ultrastructural abnormalities of the intercalated discs.

PKP2 is the only member of the plakophilin family to be expressed in the heart, and serves to tether desmosomal proteins (Hatzfeld et al, 2007; Rohr et al, 2007). Grossmann et al. generated a mouse model with targeted deletion of PKP2. The heterozygous mice carrying one wild type copy of PKP2 were completely viable without any cardiac phenotype. Mouse homozygous for the deletion (PKP2−/−) die during embryonic development, showing abnormal heart morphogenesis, with myocardial wall thinning and aneurysm formation followed by blood leakage, cardiac rupture and death on around embryonic day E11.5 (Grossmann et al., 2004).

PG is another essential desmosomal protein which, when absent, causes an ARVC phenotype in mice. The first mouse model involving a desmosomal protein

described the targeted deletion of Pg by two independent groups in 1996 (Bierkamp et al., 1996; Ruiz et al., 1996). Homozygous targeted deletion of PG leads to embryonic lethality between embryonic day 9.5 and 16 due to cardiac malformations: thin cardiac walls and less trabeculation; in addition mice showed a blistering skin phenotype. Heterozygous animals appeared healthy and fertile. However, closer inspection of these mice showed that PG+/- mice at 10 months after birth had enlarged RV, increased spontaneous ventricular arrhythmias and right ventricular conduction slowing. No replacement fibrosis and remodeling of the junctions was observed, Cx43 localization and distribution were normal on immunofluorescence microscopy. All observed changes were exacerbated when mice were subjected to exercise training (Kirchhof et al., 2006). Load reducing therapy is able to prevent these symptoms of ARVC in PG+/- mice (Fabritz et al., 2011).

To circumvent the problem of neonatal lethality, a cardiac specific targeted deletion of PG was developed under the control of αMHCcre. PGf/f αMHCcre mice have about 30% of the WT protein as measured by Western blot, no PG was detectable by immunofluorescence on cardiac sections. Phenotypically these mice largely recapitulate the human ARVC phenotype: SCD, progressive dilation, and fibrosis in the cardiac walls (both in the LV and the RV). No cardiac fat deposition was observed. With transmission electron microscopy the structure of the desmosomes seemed to be disrupted: other desmosomal proteins appeared to be absent from the intercalated disc (Li et al., 2011). Cell death in the PGf/f αMHCcre mice was at least partially through myocyte apoptosis in addition to myocyte necrosis.

Interestingly, increased β-catenin staining was observed at the intercalated disc suggesting partial rescue by this close relative of PG. To test whether the lack of fast spontaneous death in these mice was due to a partial rescue by β-catenin, double-targeted mice were created, carrying both a floxed PG gene and a floxed β-catenin locus (PGf/f ; β-cateninf/f). Crossing

with αMHC/MerCreMer mice and subsequent tamoxifen injections effected specific targeted deletion. Double-targeted mice showed a strong arrhythmogenic phenotype, with 100% of the double-targeted animals dying of SCD between 3 and 5 months after tamoxifen injections. In contrast to either single targeted deletion and wild type littermates of which 4–9% died within 6 months of tamoxifen injection (Swope et al., 2012).

Two lines overexpressing wild type and mutant PG were generated (Lombardi et al., 2011); both showed similar levels of increased incidence of SCD, an indication that even moderate levels of overexpression of PG disturb the balance of the mechanical interaction and signaling functions of PG independent of the introduced truncating mutation.

Mutations in DSG2 have been associated with ARVC. Most of the mutations are located in the extracellular portion of the protein, but no clear correlation has been observed between specific mutations and clinical features. A few functional studies on the molecular pathology of DSG2 mutations in ARVC have been reported.

Transgenic mice with cardiac overexpression of flag tagged Dsg2 both wild type (Tg-WT) and N271S-Dsg2 mutant (Tg-NS) were generated; the murine N271S mutation is the mouse homolog of the human ARVC mutation DSG2–N266S.

While mice overexpressing of wild type Dsg2 were indistinguishable from their wild type littermates at 2 months of age, Tg-Ns mice developed spontaneous ventricular arrhythmias, conduction slowing, ventricular dilatation and aneurysms, and replacement fibrosis, leading to SCD from a less than 2 weeks of age. The disease process was triggered by myocyte necrosis followed by calcification and fibrous tissue replacement (Pilichou et al., 2009). Immunohistochemical staining for PG, PKP2, DSP, and Cx43 at the intercalated discs appeared to be normal in this animal model.

The phenotype was dependent on the level of expression of the transgene, with those

animals expressing high levels of the N271S mutation being at a significantly higher risk of sudden death at a young age (30% death rate by 3.6 weeks of age).

These findings are consistent with the results obtained in mice carrying a targeted deletion in the extracellular adhesion domain of Dsg2. Approximately 30% of the mice homozygous for the mutation survived embryonic development. These mice develop left and right ventricular dilatation, fibrosis, calcification, and spontaneous death similar to the Tg-NS mice (Krusche et al., 2011). Detailed investigation of this model by transmission electron microscopy revealed a widening of the intercellular space at the intercalated disc and loss of desmosomal structure close to macroscopically visible lesions of the heart (Kant et al., 2012). Cadherin domains are important for calcium-dependent rod-like structures. Aminoacid changes may thus destabilize the rod structure and influence inter-cellular binding (Syrris et al., 2007).

At present, there is no mouse model of DSC2 mutations.

In addition to mouse models, embryonic morpholino knockdown has been used in zebrafish to evaluate the effects of gene inhibition on embryogenesis. A morpholino is a synthetic antisense oligonucleotide with a high affinity for RNA, which acts as a blocker of translation and/or mRNA splicing (Chen et al., 2004). Morpholino-induced knockdown of PG or DSC2 expression in zebrafish resulted in significant effects on cardiogenesis (Heuser et al., 2006; Martin et al., 2009). Zebrafish with reduced PG expression (morphants) developed small hearts, cardiac edema and valvular dysfunction (Martin et al., 2009). Morphants exhibited a reduced number of desmosome and adherens junctions in the intercalated discs. Heuser et al. performed morpholino knockdown of DSC2 in zebrafish. Morphants exhibited hearts with edema, bradycardia, reduced desmosomal areas, loss of desmosomal midlines and reduced contractility. Rescue of the morphant phenotype by co-injection of wild-type human DSC2

mRNA implicated DSC2 as a protein that is crucial for desmosomal function (Heuser et al., 2006).

Whereas zebrafish morpholino models may offer insights into cardiac development and desmosomal organization in the absence of specific ARVC-associated genes, they have limitations because the morphology of the fish heart is very different from the human heart. Moreover, morpholino studies are limited typically to the embryonic stage and to knockdown models, whereas the knock-in animal models offer a more accurate representation of the pathophysiology of human disease.

Cellular models provide an important tool for understanding the molecular/cellular phenotype associated with ARVC. In studies where parallel investigations have been conducted in expression systems and in transgenic mice, the results between the 2 experimental models have been remarkably consistent (Garcia-Gras et al., 2006; Yang et al., 2006) Cellular models have confirmed that disruption of the desmosome alters the integrity of the gap junction plaque, as originally shown in human hearts with Naxos disease and with Carvajal syndrome and then in samples obtained from patients carrying mutations in other desmosomal genes.

Loss of PKP2 expression in cultured cardiac myocytes associates with loss of immunoreactive Cx43 from the site of cell– cell apposition, a decrease in Cx43 abundance, and an increased presence of Cx43 in the intracellular space (Oxford et al., 2007). Biochemical analysis has demonstrated that PKP2 coimmunoprecipitates not only with Cx43 but also with the major subunit of the cardiac sodium channel, Nav1.5 (Sato et al., 2009). Voltage clamp experiments revealed that loss of PKP2 expression also leads to a decrease in amplitude of the sodium current in adult cardiac myocytes. Optical mapping studies showed that PKP2 knockdown associates with a significant decrease in conduction

velocity in cardiac cell monolayers and an increased propensity to reentrant arrhythmias, likely resulting from the combination of decreased electric coupling and impaired sodium current density.

Although animal models have provided some useful insights into the pathogenesis of ARVC, significant differences between the electrophysiological properties of animal and human hearts limits the interpretation of such data. In addition, the lack of good in vitro sources of living human cardiomyocytes hinders the study of this disease. In recent years, several groups have successfully modelled a number of inherited cardiac ion channel diseases, mostly different subtypes of long-QT syndrome, through the generation of patient-specific induced pluripotent stem cell (iPSC)-derived cardiomyocytes (Moretti et al., 2010). There is the exciting possibility of using iPSC-derived cardiomyocytes from patients with ARVC as a cellular model to study the disease. iPSC-derived cardiomyocytes from ARVC patients would exhibit altered desmosomal protein localization at the intercalated disc. Successful generation of such a model would offer the possibility to further understand the pathogenesis of the disease as well as to evaluate future novel clinical applications in diagnosis and management (Ma et al. 2012; Hoekstra et al., 2012).

Current insights into mechanisms of arrhythmogenesis

The normal cardiac electrical cycle begins with diastolic depolarization of the cells within the sinoatrial node which generates an action potential (AP) and spreads to depolarize the surrounding atrial myocardium. The electrical impulse is then conducted through the atrioventricular node, down the His bundle to the bundle branches and distributed to the working myocardium of the ventricles through the Purkinje fiber network. The efficient cardiac contractile function is highly dependent upon the coordinated excitation-contraction coupling of the myocardial tissue. This is achieved by the different junctional complexes within the intercalated discs. Aberrant cell-cell coupling is associated with an increased risk of arrhythmias and SCD.

The mechanisms underlying arrhythmogenesis in ARVC have been partially elucidated (Figure 4) thanks also to current animal models (Wolf et al., 2008).

Figure 4 Substrates and pathophysiologic mechanisms of ventricular arrhythmias in the different phases of ARVC.
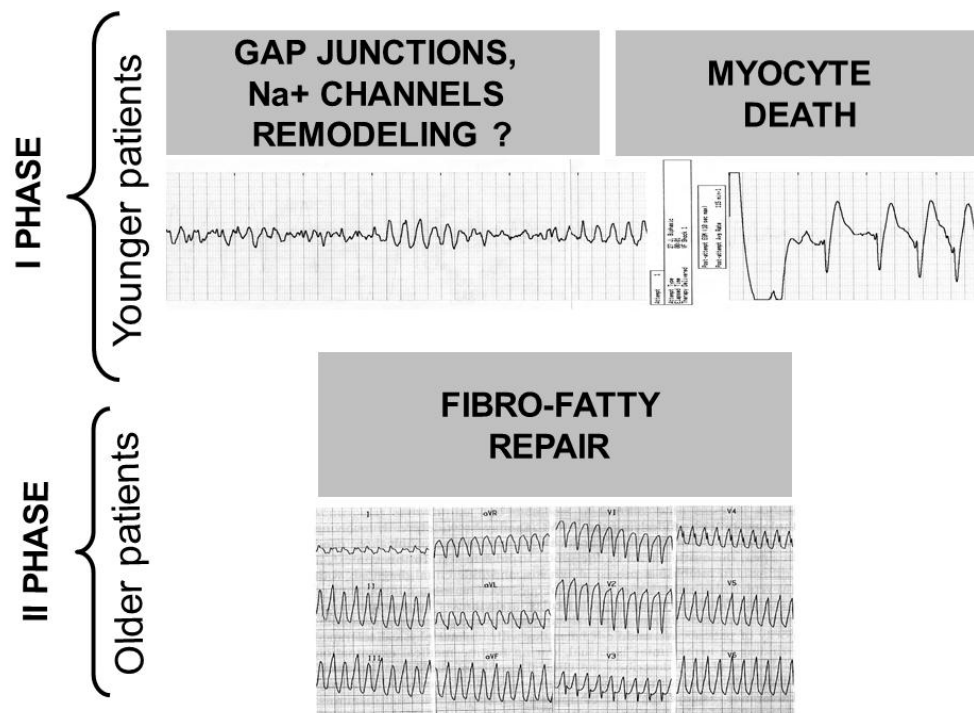
In ARVC, the electric isolation of cardiomyocytes by surrounding scar tissue may provide the substrate for slow conduction and promote reentrant arrhythmias. In the clinical setting, late potentials, detected with signal-averaged ECG, are considered a noninvasive marker of slow conduction areas in ARVC due to fibrofatty replacement and thus can be used to identify the patients at risk (Turrini et al., 1994).Less clear is the nature of the arrhythmogenic substrate during the concealed phase of the disease (in the absence of overt structural damage), during which ARVC is more reminiscent of the ion channelopathies (Saffitz 2011). Arrhythmias may occur early in the natural history of ARVC, often preceding structural remodeling of the myocardium (Bauce et al., 2005;

Sen-Chowdhry et al., 2010). An increased susceptibility to arrhythmia has also been noted in mice with ARVC-linked mutations in which structural remodeling is absent (Muthappan et al., 2008).

Gap junction remodelling may be considered as an alternative pathway to intraventricular slow conduction enhancing the risk of ventricular arrhythmias.

Impaired desmosomal structure and function may affect other cell-to-cell contact structures in the myocardium. There is increasing evidence that components of the desmosome are essential for the proper function and distribution of the Cx43, supporting the notion of a molecular crosstalk between desmosomal and gap junction proteins (Kaplan et al., 2004; Sato et al., 2009; Delmar et al., 2010). A common observation in ARVC is remodeling of cardiac gap junctions early in the disease, with a diminished expression of the major gap junction protein Cx43 at the intercalated discs, which establish the mechanical and electrical coupling between adjacent cells (Saffitz 2009).

The described case of a child with Naxos disease presenting ventricular arrhythmias before

the development of pathologic changes of myocardium provided evidence to support this

hypothesis. Immunohistochemical and electron microscopy studies in Naxos disease

revealed reduced localisation of mutant PG to cell–cell junctions, diminished expression of the

Cx43, and a decreased number and size of gap junctions (Kaplan et al., 2004). More recently,

similar changes in the various junctional proteins were observed in the classic form of ARVC

without cardiocutaneous manifestations (Fidler et al., 2009). These studies showed a link

between desmosomal and gap junction integrity and were the first to postulate failure of this

interaction as a potential pathophysiologic mechanism in ARVC.

Decreased gap junction-mediated electrical coupling could be an adjuvant to

arrhythmogenesis, though it is unlikely to be the only cause. Simulation experiments (Wilders

2012) demonstrated that a 50% reduction in gap junctional conductance gives rise to

relatively small changes in conduction velocity.

The gap junction remodeling observed in the endomyocardial biopsy samples (indicated by

reduced immunoreactive signal for Cx43) may act synergistically with the histologic

abnormalities characteristic of ARVC to enhance conduction heterogeneity and increase the

risk of arrhythmia (Basso et al, 2006; Kaplan et al, 2004; Boukens et al., 2009).

Given the relatively small effects of gap junctional remodeling on conduction velocity, other

factors, like changes in electrical properties (sodium current) of the cardiac myocytes,

may contribute to arrhythmogenesis (Sato et al., 2009, 2011).

The proposal of electrical disturbances at the early stage of the disease is an attractive one in

the light of the recent data showing cross talk between the mechanical junctions, the gap

junctions and the Na+ channel complex (Sato et al., 2009, 2011; Basso et al., 2011) (Figure

5).

There is new evidence in support of the hypothesis that Na current is affected by desmosomal

mutations. Nav1.5, the major α subunit of the cardiac sodium channel (Roden et al., 2002), fundamental to the electrical behavior of the single myocyte, functionally and physically interacts with other intercalated disc proteins. As such, loss of PKP2 affects gap junction-mediated coupling (Oxford et al., 2007) as well as sodium channel function (Sato et al., 2009); loss of N-cadherin expression affects gap junctions (Li et al., 2005) and also the function of Kv1.5 channels (Cheng et al., 2011); loss of intercellular contact leads to a decrease in sodium current (Lin et al, 2011); expression of AnkG, a protein associated with the sodium channel complex, is necessary for proper intercellular adhesion strength and for proper electrical coupling (Lowe et al., 2008); finally, expression of Cx43, a protein previously associated only with gap junctions, is required for the normal function of sodium and potassium currents (Danik et al., 2008; Jansen et al., 2011). These observations suggest that mutations in any individual component of the complex is sufficient to compromise junctional structures, resulting in defects in tissue integrity, development, and differentiation (Delmar and McKenna, 2010).

Further evidence for the involvement of sodium current in ARVC comes from a recent study by Gomes et al., who studied RV biopsies from three ARVC patients and observed NaV1.5 mislocalization in biopsies from two early-stage patients. On the other hand, in the same study no difference was observed in sodium current properties. Moreover, no indications of altered Na current characteristics could be found recently in a murine model of heterozygous desmoplakin knockout (Gomes et al.,2012).

Figure 5. Hypothesized intracellular desmosome crosstalk. Possible targets include intercalated-disc proteins (ion channels or gap-junctional proteins) and nuclear-signaling proteins (From Basso et al., 2011).
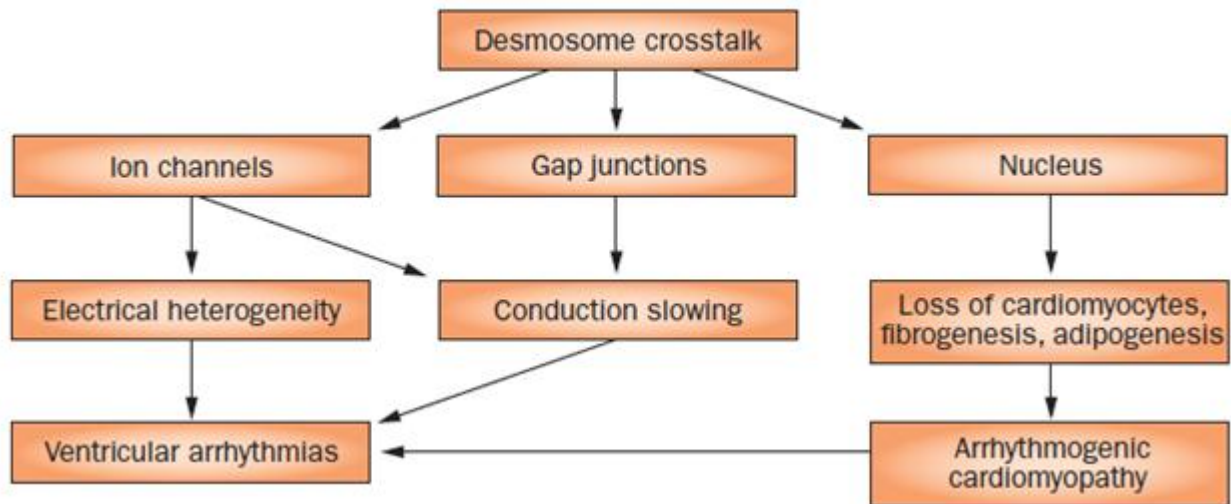
ORIGINAL CONTRIBUTION

Mutations in genes encoding desmosomal proteins have been implicated in the pathogenesis of arrhythmogenic right ventricular cardiomyopathy (ARVC). However, the consequences of these mutations in early disease stages are unknown.

We investigated whether mutation-induced intercalated disc remodelling impacts on electrophysiological properties before the onset of cell death and replacement fibrosis.

We here dissect the early stages of disease development in mice overexpressing a Dsg2 mutation associated with ARVC in humans to:

- assess whether intercalated disc remodelling is observed, and time of onset of intercalated disc remodelling remodeling, if present;

- characterize arrhythmia susceptibility consequent to overexpression of mutant Dsg2

- explore the relative contribution of cell uncoupling in alterations of sodium current (action potential upstroke velocity changes; Na+ channel performance)

- evaluate whether this interaction account for slow conduction and increased arrhythmia susceptibility at disease stages preceding the onset of replacement fibrosis.

MATERIAL AND METHODS

Animal Husbandry and Mouse Lines Used

We studied the effects of heart specific overexpression of mutant Dsg2 in young mice before the development of gross and histological abnormalities. The transgenic mouse models with heart-specific overexpression of either mutant (Dsg2-N271S) or wild-type (Tg-WT) Dsg2 were generated previously (Pilichou et al, 2009). Of the two Dsg2-N271S lines we generated, which respectively had high (Tg-NS/H) and low (Tg-NS/L) overexpression of the transgene, the Tg-NS/L line was used in this study. Although both lines i.e. Tg-NS/H and Tg-NS/L, develop an ARVC phenotype, the latter line was selected as it develops the phenotype at a slower pace which makes it more amenable for the dissection of the early, pre-cardiomyopathic, phenotype of the model. Tg-WT and wild-type (WT) mice were used as controls in all experiments throughout the study. The mice were studied at three different ages: <2 weeks, 3- 4 weeks and 6-9 weeks. At least 4 mice of each group were studied except where specifically indicated otherwise. Mice were sacrificed by cervical dislocation after sedation with O_2/CO_2 for 1 min. All experiments were approved by the local animal welfare committee and followed Dutch law concerning experimental animal welfare and conformed with the Guide or the Care and Use of Laboratory Animals published by the US National Institutes of Health (NIH Publication No. 85-23, revised 1996) (PHS assurance number A5549-01).

Morphological Analysis

For pathological studies hearts were isolated and snap-frozen immediately after excision in liquid nitrogen and stored at -80°C. In parallel, tissue samples were fixed in 4% paraformaldehyde (in PBS) for light microscopy or in glutaraldehyde for electron microscopy

(see below). 7-µm-thick paraffin embedded sections were cut and routinely stained with hematoxylin and eosin (HE) and Heidenhain's trichrome to examine the myocardium and to detect the presence and amount of necrosis, inflammation and fibrosis.

Transmission Electron Microscopy

Transmission Electron Microscopy was used to characterize the desmosomes and the other intercellular junctions in situ as described before (Franke et al, 2006). In short: small pieces of LV tissue were fixed in 2.5% glutaraldehyde for 20 min, post-fixation was performed with 2% OsO_4 in cacodylate buffer for 2 hr on ice, followed by washes at 4°C in distilled water and overnight heavy metal staining (0.5% uranyl acetate in distilled water). After 3 washes in distilled water, samples were dehydrated in an ethanol series and propylenoxide before being embedded in Epon. Ultrathin sections for TEM were made with a Reichert-Jung microtome (Ultracut, Leica, Bensheim, Germany). For contrast enhancement, the sections were stained with 2% uranyl acetate in methanol for 15 min and with lead citrate for 5 min. Electron micrographs were taken using a Philips CM10 transmission electron microscope by a systematic random sampling and analyzed by two independent expert pathologists (S.R & C.B.) blinded to the genotype of the mouse. For evaluation ~100 intercalated discs were analyzed per mouse. Morphometric analysis of intercalated discs was performed according to a previously described method (Basso et al, 2006). The percentage of intercellular widened junctions (space>30 nm; Fawcett et al.,1969) of the total number of examined intercalated discs was calculated; the interobserver correlation coefficient between S.R. and C.B. was 0.945 (95% C.I. 0.936-0.958).

Electrical analysis

The electrical properties of the heart were studied in vivo by surface electrocardiograms (ECG), ex vivo in Langendorff-perfused hearts by epicardial mapping and in isolated cardiomyocytes by patch-clamp analysis.

Surface ECGs

Mice were anesthetized using isoflurane inhalation (0.8–1.0% volume in oxygen), efficacy of the anaesthesia was monitored by watching breathing speed and tail suspension. Four-lead surface ECGs were recorded from subcutaneous 23-gauge needle electrodes attached to each limb using the Powerlab acquisition system (ADInstruments). Lead II was analyzed for heart rate (RR interval) and PR, QRS, and QT duration using Chart5 Pro analysis software (ADInstruments). QT intervals in mice were corrected for heart rate using the following formula: QTc = QT/(RR/100)1/2 (RR in ms).

Epicardial mapping experiments

Mice were anesthetized by an intraperitoneal injection of pentobarbital, after which the heart was excised, cannulated, mounted on a Langendorff perfusion set-up, and perfused at 37°C with a solution containing (in mMol) 128 NaCl, 4.7 KCl, 1.45 $CaCl_2$, 0.6 $MgCl_2$, 27 $NaHCO_3$, 0.4 NaH_2PO_4, and 11 glucose (pH maintained at 7.4 by equilibration with a mixture of 95% O_2 and 5% CO_2). Ventricular extracellular epicardial electrograms were recorded from the RV and LV using a 247-point multi-electrode (unipolar 19×13 electrode grid, inter-electrode spacing 300 µm) during sinus rhythm and ventricular pacing from the centre of the electrode (basic cycle length of 120 ms; twice the diastolic stimulus current threshold). The effective refractory period (ERP) was determined by reducing the coupling interval of a premature

stimulus (after 16 stimuli at basic cycle length 120 ms) in steps of 5 ms until activation of the ventricle failed. Electrograms were acquired using a custom-built 256-channel data acquisition system. Activation maps were constructed from local activation times determined by the time between the stimulus artefact and the maximal negative dV/dt as measured from the unipolar electrograms using custom software. Ventricular activation time was determined as the difference between the first and last moment of activation measured under the recording electrode grid. Maximal conduction velocities in both longitudinal and transverse directions were measured from RV and LV activation maps. Inducibility of ventricular arrhythmias was assessed using a stimulation protocol with up to three extrastimuli, followed by burst pacing at the shortest possible coupling intervals.

Cellular electrophysiology

Cell preparation. Mouse ventricular myocytes were isolated by enzymatic dissociation as described previously in detail (Berecki et al, 2010). In short, excised hearts were perfused in a Langendorff system (37°C) for 5 minutes with normal Tyrode's solution containing (in mMol): 140 NaCl, 5.4 KCl, 1.8 $CaCl_2$, 1 $MgCl_2$, 5.5 glucose, 5 HEPES; pH 7.4 (NaOH). Subsequently, the heart was perfused for 8 minutes with a nominally Ca^{2+}-free Tyrode's solution, i.e. normal Tyrodes's solution with 1 µmol/L $CaCl_2$, after which the enzyme Liberase TM (Roche; 0.02 mg/mL) and elastase were added for 10 minutes. After the digestion period, LV tissue was gently triturated in the nominally Ca^{2+}-free enzyme solution to obtain single cardiomyocytes. Then, the nominally Ca^{2+}-free Tyrode's solution was refreshed two times (at 20°C) with nominally Ca^{2+}-free Tyrode solution to which bovine serum albumin (BSA, 50 mg/mL) was added. Finally, Ca^{2+} concentration was increased by replacing the nominally Ca^{2+}-free Tyrode's with normal Tyrode's solution. Single cells were stored at RT for at least

45 min before they were put into a recording chamber on the stage of an inverted microscope. Cells were allowed to adhere for 5 min after which superfusion was started. Quiescent, rod-shaped cells with clear cross-striations and smooth surface were selected for measurements.

Data acquisition and analysis. Action potentials (APs) and Na^+ current (I_{Na}) were recorded with the amphotericin-B-perforated patch-clamp and ruptured patch-clamp technique, respectively, using an Axopatch 200B Clamp amplifier (Molecular Devices Corporation, Sunnyvale, CA, USA). Voltage control, data acquisition, and analysis were performed using custom software. Potentials were corrected for the estimated change in liquid junction potential. Adequate voltage control was achieved with low-resistance pipettes (1.5-2.5 MΩ), and series resistance was compensated by $\geq$80%. Signals were filtered (low-pass, 5 kHz) and digitized at 40 and 20 kHz for AP and I_{Na} measurement, respectively. Cell membrane capacitance (C_m) was determined as described previously (Verkerk et al., 2004).

Current-clamp experiments. APs were measured at 36°C using normal Tyrode's solution; pipette solution contained (in mMol): 125 K-gluconate, 20 KCl, 10 NaCl, 0.22 amphotericin-B, 10 HEPES; pH 7.2 (KOH). APs were elicited at 4 Hz by 3 ms, 1.2$\times$ threshold current pulses through the patch pipette. We analyzed resting membrane potential (RMP), maximal AP upstroke velocity (V_{max}), AP amplitude (APA), and AP duration at 20, 50 and 90% repolarization (APD_{20}, APD_{50}, and APD_{90}, respectively). Data from 10 consecutive APs were averaged.

Voltage-clamp experiments. I_{Na} was measured at RT with a bath solution containing (in mMol): 7.0 NaCl, 133 CsCl, 1.8 $CaCl_2$, 1.2 $MgCl_2$, 11.0 glucose, 5.0 HEPES; pH 7.4 (CsOH). Nifedipine (5 μM) was added to block the L-type Ca^{2+} current. Pipettes were filled with (in mMol): 3.0 NaCl, 133 CsCl, 2.0 $MgCl_2$, 2.0 Na_2ATP, 2.0 TEACl, 10 EGTA, 5.0 HEPES; pH 7.3 (CsOH). I_{Na} was measured using a two-step protocol, with a holding potential of -120 mV and

a cycle time of 5 seconds (see Figure 6D). During the first depolarizing pulse (P1) of the voltage clamp protocol, I_{Na} activates; the second pulse (P2) is used for measuring voltage dependency of inactivation. Current densities were calculated by dividing current amplitudes by C_m. Voltage-dependence of (in)activation was determined by fitting a Boltzmann function ($y= [1+\exp\{ (V-V_{1/2})/k\}]$) to the individual curves, yielding half-maximal voltage $V_{1/2}$ and slope factor k.

Antibodies

For immunofluorescence microscopy and Western blotting, the following primary antibodies against desmosomal and other junctional and cytoskeletal proteins were used: murine monoclonal and rabbit polyclonal antibodies specific to N-cadherin, pan-cadherin, γ-catenin, connexin-43 and Flag M5 (all purchased from Sigma), $Na_V1.5$ (Alomone, rabbit),desmocollin-2, desmoglein-2 (clone DG310), plakoglobin (clone PG 5.1), desmoplakins, plakophilin-2, α- and β-catenin (all purchased by Progen Biotechnik, Heidelberg); Calnexin (1:500; Santa Cruz Biotechnology, Inc.); M2 anti-Flag (Stratagene). For immunofluorescence primary antibody complexes were visualized with secondary antibodies coupled to Donkey-anti-mouse or Donkey-anti-rabbit Alexa488, and Alexa568 (Molecular Probes). 4',6-Diamidino-2-phenylindol (DAPI; Sigma) or Sytox Orange nucleic acid stain (S11368, Invitrogen) was used to label nuclei. For Western blot analysis, horseradish peroxidase-conjugated secondary antibodies against mouse and rabbit (NA9310 & NA9340 GE-health sciences) were used.

Immunofluorescence microscopy

Cryosections of 5-µm were fixed in methanol (5 min) followed by acetone (20 sec), at −20°C, air-dried and rehydrated in PBS. Permeabilization was done in 0.2% Triton X-100 for 5 min.

Primary antibodies were applied for 1 hr at RT, followed by 3 washes in PBS (5 min each), incubation with the secondary antibodies (30 min, RT) and 3 × 5 min washes with PBS. Sections were mounted with 50% glycerol in PBS. Images were recorded with a confocal laser scanning microscopy (Leica CTR 5500).

Protein Isolation and Western blot analysis

LV tissue from a snap frozen mouse heart was homogenized in ice-cold RIPA buffer (50 mM Tris HCl pH 7.6, 150 mM NaCl, 1% NP-40, 0.5% sodium deoxycholate, 0.1% SDS) supplemented with protease inhibitors (Complete Mini; Roche) and Sodium Orthovanadate (final concentration 0.5 mM) using magnalyser ceramic beads (Roche scientific, 03358941001) for 30". The unsoluable parts were spun down (30 sec at 4°C, 13000 rpm), the supernatant was transferred to a fresh tube and protein concentrations were determined using a BCA protein assay kit (Thermo Fisher Scientific).

For Western blot analysis, LV protein (60 ug) was run on denaturing SDS-page gels. The gels were blotted on a pre-equilibrated PVDF Immobilon-P membrane (Millipore) by means of a semidry system. Blots were cut at appropriate heights and probed with primary antibodies. HRP conjugated secondary antibodies were detected with ECL-Plus (Amersham). Chemiluminescent signals were visualized using a digital image analyzer (LAS-4000 Lite; Fujifilm) and quantified using the Aida software package (Aida Image Analyzer v.4.26).

Co-immunoprecipitation

Aliquots of 100 µg LV whole cell lysate protein of 3-4 week old mice were incubated rotating overnight at 4°C with washed agarose beads with either conjugated M2 Flag antibody or protein A (both Sigma) and 1 µl of normal mouse IgG (Santa Cruz) in 1ml of

PBS supplemented with protease inhibitors (Complete Mini; Roche) and 0.5 mM Sodium Orthovanadate (PBS++). Beads were washed 3 times with 1 ml of PBS++, and the bound proteins were eluted with Flag peptide (Sigma). Untreated protein and elutes from both precipitations were treated with Laemli buffer and analysed by Western blot as described above.

Statistical analysis

Data are expressed as mean ± SEM. Values are considered significantly different if $P<0.05$ in an unpaired two sided t-test or in Two-Way Repeated Measures of Analysis of Variance (Two-Way Repeated Measures ANOVA) followed by pairwise two sided comparison using the Student-Newman-Keuls test, after testing for normal distribution of the data. Minimal sample sizes were calculated prior to the experiments based upon a power calculation with a $(1-\beta) = 80\%$, $\alpha=5\%$, mean control = 7.0, mean observed = 9.5 and SD = 1.0 (effect size of 2.5, which represents the expected effect sizes for the electrical mapping) which gives n = 4 animals per test group. The intraclass correlation coefficient was used to test the interobserver variability in the morphometric measurements. Statistical tests were performed using the PASW statistics software, version 18.0.2 (IBM, New York, USA) and SigmaStat, version 3.1 (Aspire Software International, Ashburn, VA, USA).

RESULTS

Absence of cardiomyopathic changes in Tg-NS/L mice younger than 6 weeks of age

The early phase of the disease was studied by investigating mice at three different age

groups: (i) < 2 weeks of age, (ii) 3-4 weeks of age, and (iii) 6-9 weeks. On gross examination

and histologically, hearts from Tg-NS/L mice at all three age groups appeared normal, with

no evidence of replacement-type fibrosis (Figure 6). Other cardiomyopathic

changes, consistent with those we previously reported for Tg-NS/H mice (Pilichou et al, 2009)

and which included necrosis, focal myofibrillar lysis, dilated sarcoplasmatic reticulum and T-

tubules, and mitochondrial clustering, were observed exclusively in Tg-NS/L mice ≥ 6 weeks

of age. These analyses established that Tg-NS/L mice <6 weeks of age were devoid of

cardiomyopathic changes allowing for the examination of the early electrophysiological

phenotype prior to and in the absence of cardiac remodeling.

Figure 6. Hematoxylin and eosin (HE) and Heidenhain's trichrome staining of transverse section of the heart of Tg-NS/L mouse aged 3 weeks: note the absence of myocyte death, inflammation, and fibrosis.
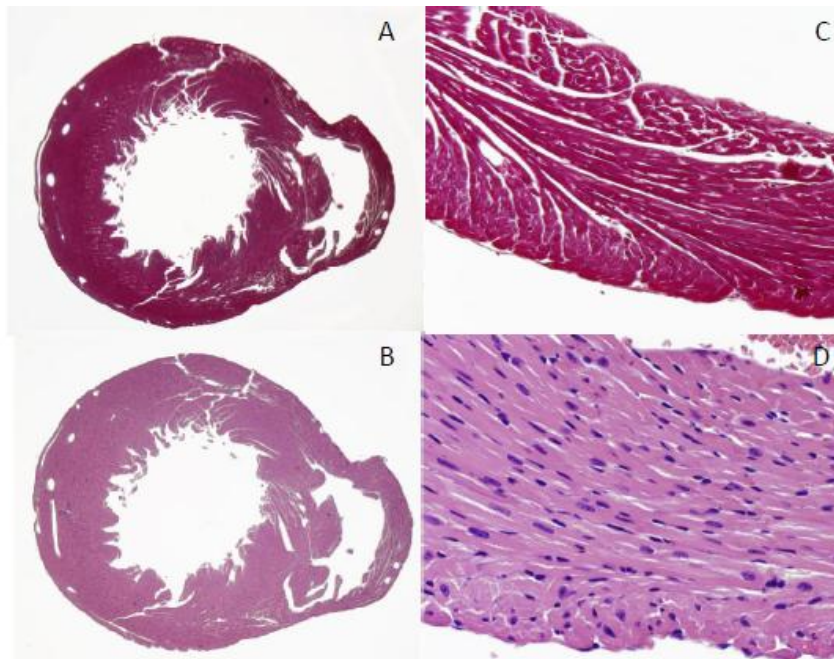
Widening of intercellular space at the desmosome/adherens junctions

We next examined intercalated disc structures in detail by TEM. No consistent

differences were observed in the general organization of the cell-cell junctions between Tg-

NS/L and control mice. Gap junctions appeared structurally normal in all groups (Figure 7).

In addition to desmosomes, gap junctions and adherens junctions, intermediate structures

were observed that displayed features of both desmosomal and adherens junctions

concurring with recent reports describing this "area composita" (Franke et al., 2006; Li et al.,

2010).

Separation of the opposed membranes, resulting in larger intercellular spaces, was

observed at the level of desmosomes/adherens junctions. These changes were seen in

otherwise morphologically normal cardiomyocytes in all Tg-NS/L mice ≥3 weeks of age and

in 1 out of 4 Tg-NS/L mice <2 weeks old (Figure 7). None of the control mice (Tg-WT, WT)

displayed any intercellular space widening. Morphometric analysis showed that the average

intercellular space was significantly widened in Tg-NS/L mice at 3-4 weeks compared to

controls (Figure 8A). The percentage of widened cellular junctions increased with age (Figure

8B).

In some Tg-NS/L cardiomyocytes with intercellular space widening, myofibrils appeared to

have undergone focal lysis at their points of attachment to desmosomes/adherens junctions

(Figure 7E).

Figure 7 (*next page*) At ultrastructural level, widening of the intercellular space at the level of
the desmosomes/adherens junctions compared with WT mice (A) and Tg-WT (B) is visible in
Tg-NS/L mice both at 3-4 weeks (D, E) and at 6-9 weeks (F). This feature is observed also in
a Tg-NS/L mouse aged <2 weeks (C). The structure of the gap-junctions is preserved in both
Tg-NS/L and Tg-WT mice at all ages (B-F). Scale bars 500 nm

A — WT 3 wks
B — Tg-WT 3 wks
C — Tg-NS/L <2 wks
D — Tg-NS/L 3 wks
E — Tg-NS/L 3 wks
F — Tg-NS/L 6 wks
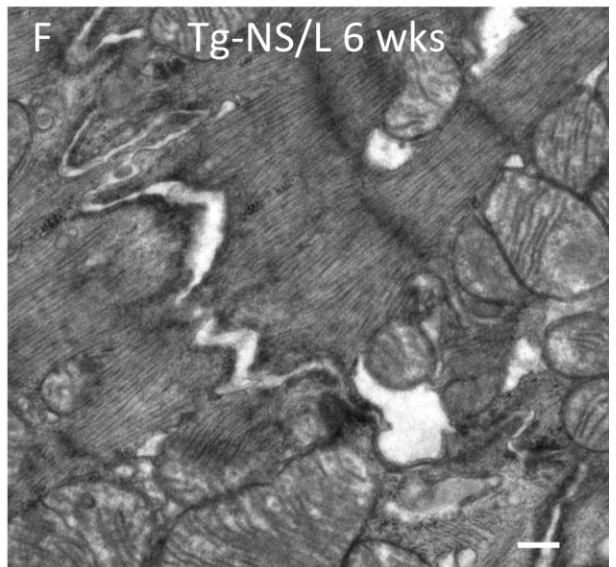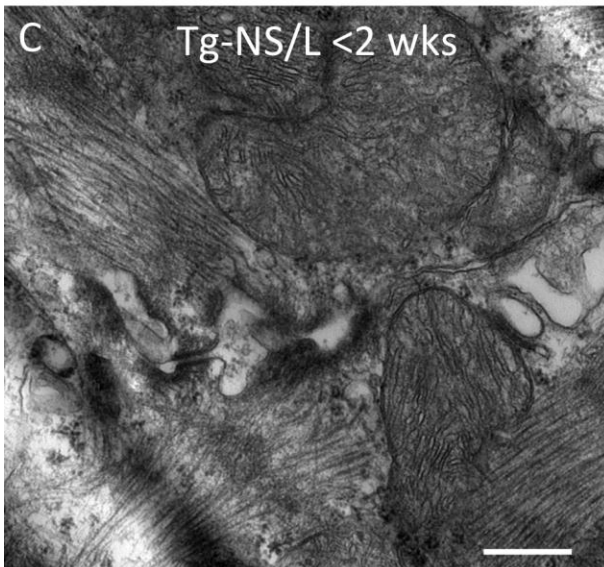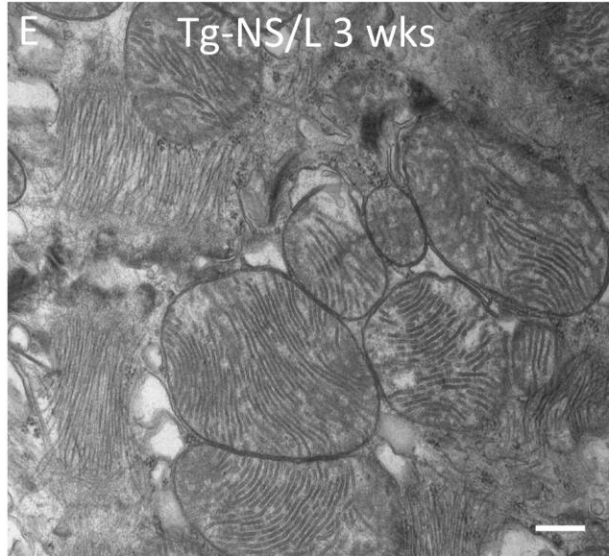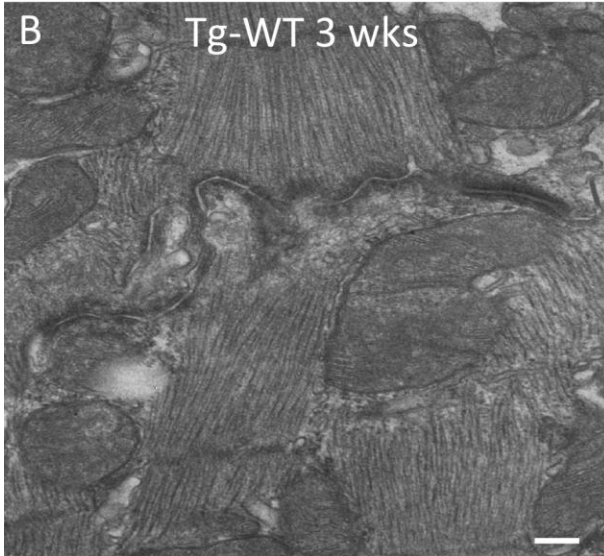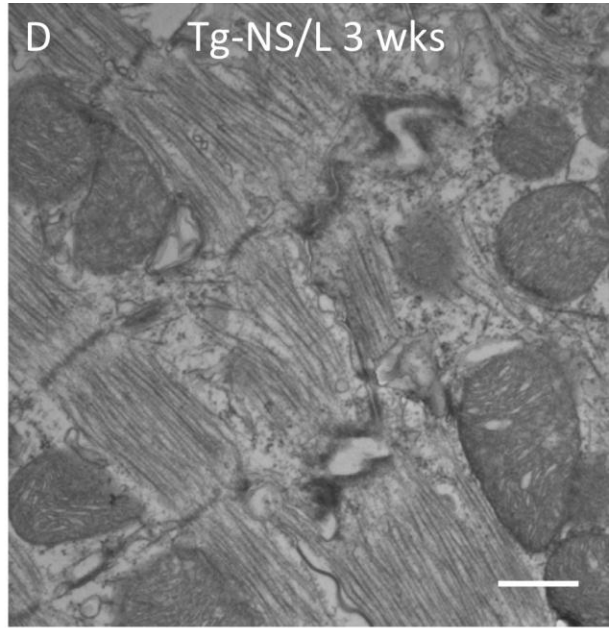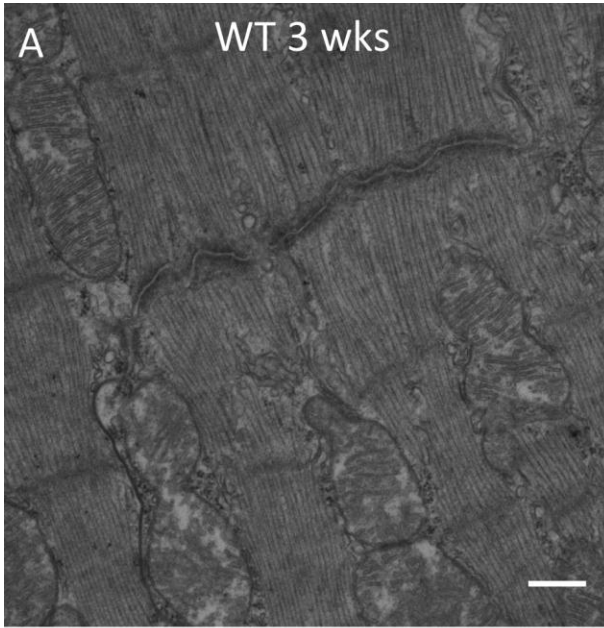
Figure 8. Quantification of intercellular widening in nm in WT, Tg-WT & Tg-NS/L (**A**) and percentage of widened intercellular junctions in Tg-NS/L mice <2 weeks, 3-4 weeks, and >6 weeks (**B**) * denotes $p < 0.05$ of Tg-NS/L vs WT and Tg-WT; * denotes $p < 0.05$ vs <2 weeks, # denotes $p < 0.05$ vs 3 weeks
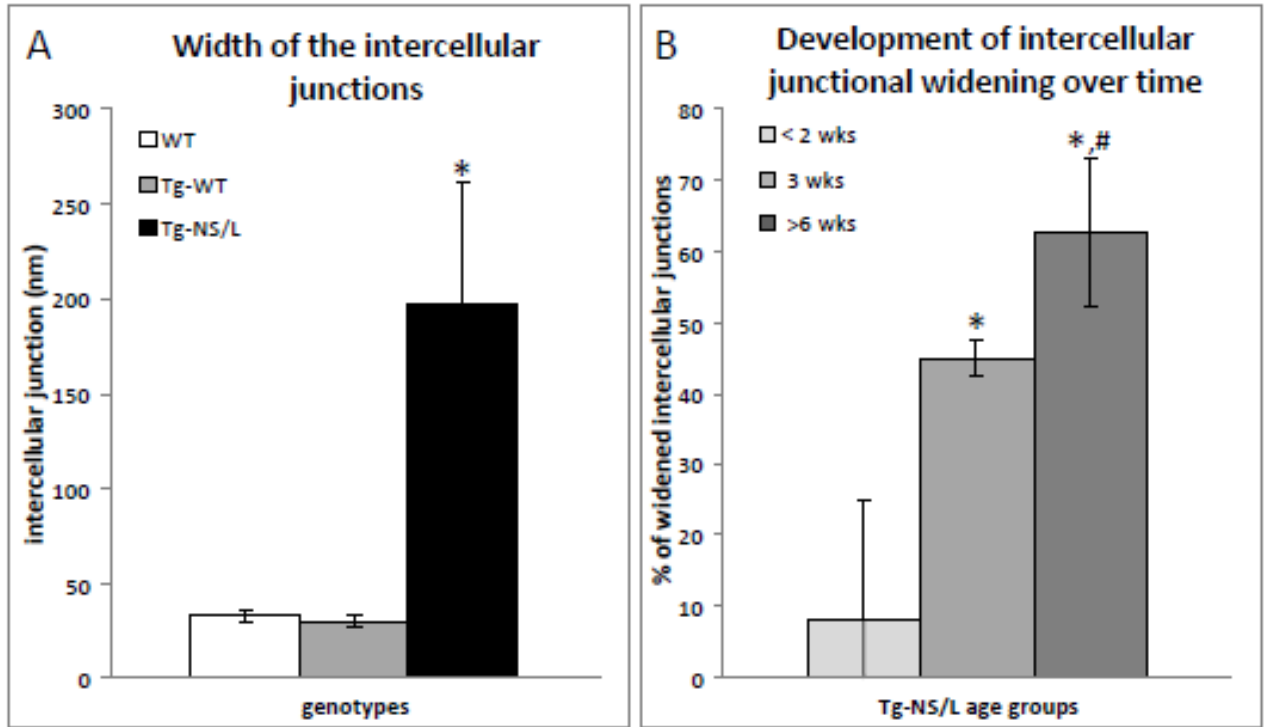
Conduction slowing in Tg-NS/L hearts from 3-4 weeks of age

To investigate the occurrence of electrophysiological abnormalities prior to the development of cardiomyopathic changes, we first performed surface ECG measurements in anaesthetized mice. In mice aged 3-4 weeks, no statistically significant differences in heart rate (RR interval), QRS-duration, PR-interval, and QTc-interval were observed between Tg-NS/L and controls (Figure 9 A-B and Table 1). However, fractionation of the QRS complex was observed in some Tg-NS/L mice aged 3-4 weeks, indicating the presence of discrete ventricular conduction slowing (Figure 9A). In the 6-9 weeks age group, Tg-NS/L mice developed significant QRS prolongation and abnormal QRS morphology (including marked fractionation), in addition to spontaneous ventricular rhythm disturbances consisting of single or multiple ventricular extra systoles and short runs of non-sustained ventricular tachycardia (Figure 9A,B,D). No spontaneous arrhythmias were observed in Tg-NS/L mice aged 3-4 weeks.

We next performed epicardial mapping in isolated Langendorff-perfused hearts from WT, Tg-WT and Tg-NS/L mice of the three age groups to further assess cardiac conduction in detail. In mice aged <2 weeks, no significant differences were found between the groups for left (LV) or right (RV) ventricular activation time or effective refractory periods, but a tendency towards lower longitudinal and transversal conduction velocities was observed in Tg-NS/L mice compared to controls (Figure 10A-D, Table 2). In contrast, a significantly prolonged epicardial LV activation time in addition to decreased LV conduction velocity was observed in Tg-NS/L mice from the age of 3-4 weeks onwards compared to controls. Both longitudinal and transversal conduction velocities were equally affected, as indicated by the unaltered L/T ratio (Table 2). In the RV, activation time and conduction velocity was only significantly prolonged at the age of >6 weeks. Arrhythmia

inducibility was tested using up to 3 extra stimuli and burst pacing. No arrhythmias could be

induced in WT, Tg-WT or Tg-NS/L mice younger than 2 weeks. In contrast, ventricular

arrhythmias were inducible in almost half of all Tg-NS/L mice aged 3-4 weeks and >6 weeks,

but only sporadically in control mice of the same age groups (Table 2).

Table 1. Surface ECG results

	WT	Tg-WT	Tg-NS/L	p ANOVA
Age 3-4 weeks:				
Number of mice (n)	7	7	12	
Age (weeks)	3.8 ± 0.3	3.7 ± 0.2	3.8 ± 0.1	0.934
Heart rate	364.3 ± 18.8	331.0 ± 26.6	352.7 ± 15.3	0.549
PR-interval (ms)	32.8 ± 0.6	34.8 ± 1.6	33.1 ± 1.4	0.634
QRS-duration (ms)	9.0 ± 0.3	9.0 ± 0.3	9.3 ± 0.3	0.658
QTc-interval (m/s)	40.6 ± 1.5	45.1 ± 1.8	43.9 ± 1.2	0.158
Arrhythmias	0/7	0/7	0/12	
Age 6-9 weeks:				
Number of mice (n)	10	9	12	
Age (weeks)	7.4 ± 0.5	7.9 ± 0.5	7.2 ± 0.2	0.502
Heart rate	390.6 ± 16.1	385.5 ± 16.6	394.5 ± 10.0	0.905
PR-interval (ms)	35.5 ± 1.3	33.8 ± 2.2	32.3 ± 0.7	0.176
QRS-duration (ms)	10.3 ± 0.4	10.6 ± 0.3	11.7 ± 0.4#$	**0.033**
QTc-interval (m/s)	42.5 ± 1.0	44.7 ± 3.4	46.3 ± 2.2	0.321
Arrhythmias	0/10	1/9	9/12	

Data are presented as mean ± SEM
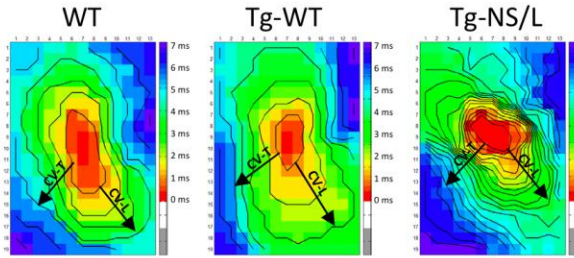#p<0.05 vs WT; $p<0.05 vs Tg-WT

Figure 9 A. Surface ECG examples of WT, Tg-WT, and Tg-NS/L mice (scale bar: 20 ms). In a subset of Tg-NS/L mice aged 3-4 weeks, discrete fractionation of the QRS complex was observed (top right example). In the 6-9 weeks age group, Tg-NS/L mice developed significant QRS prolongation and abnormal QRS morphology (including substantial fractionation of the QRS complex). B. Average values (mean±SEM) for QRS-duration in WT, Tg-WT, and Tg-NS/L mice in age groups 3-4 weeks (n=7, 7, 12 resp.) and 6-9 weeks (n=10, 9, 12 resp.) (# denotes $p<0.05$ vs. WT; $ denotes $p<0.05$ vs. Tg-WT). C. Examples of spontaneous ventricular rhythm disturbances observed in Tg-NS/L mice aged 6-9 weeks, including single or multiple ventricular extra systoles and short runs of non-sustained ventricular tachycardia (scale bar: 100 ms).
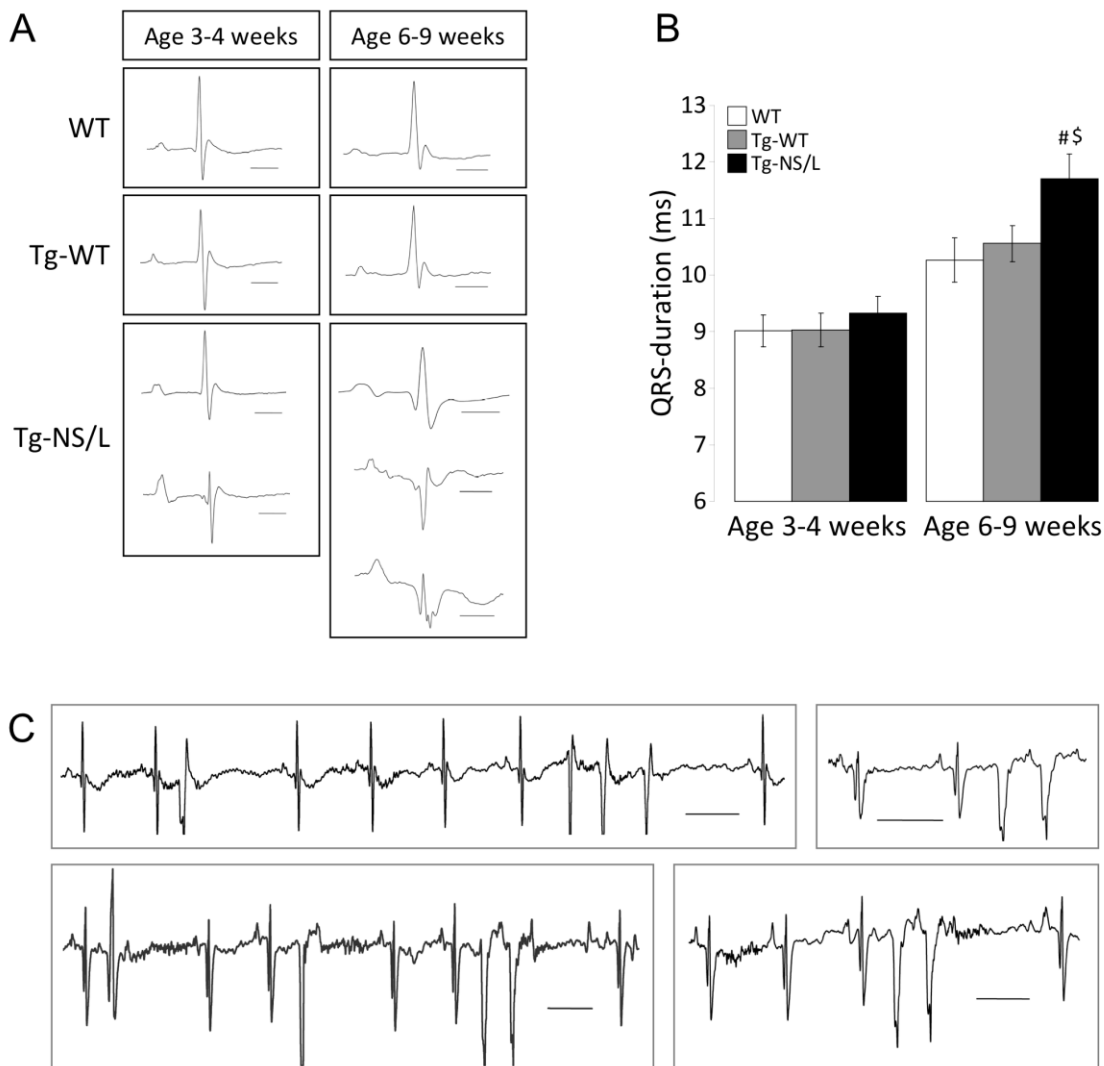
Table 2. Epicardial mapping result.

	WT	Tg-WT	Tg-NS/L	p ANOVA
Age <2 weeks:				
Number of mice (n)	6	4	5	
LV ERP (ms)	42.7±3.0	42.5±7.2	48.6±5.2	0.616
RV ERP (ms)	46.7±6.0	45.0±6.4	40.4±1.9	0.677
LV activation time (ms)	6.7±0.6	6.5±0.9	7.3±0.4	0.629
RV activation time (ms)	7.2±0.8	7.1±1.1	6.9±0.4	0.966
LV long CV (cm/s)	73.4±3.2	74.1±5.8	69.0±3.5	0.606
LV trans CV (cm/s)	39.7±1.5	39.8±3.5	35.7±3.1	0.503
LV l/t ratio	1.9±0.1	2.0±0.1	2.0±0.1	0.358
RV long CV (cm/s)	64.9±3.1	64.2±4.5	60.0±4.4	0.644
RV trans CV (cm/s)	37.7±2.0	39.2±5.7	37.0±2.0	0.899
RV l/t ratio	1.7±0.1	1.7±0.2	1.6±0.1	0.748
Inducible arrhythmias	0/6	0/4	0/5	
Age 3-4 weeks:				
Number of mice (n)	5	6	6	
LV ERP (ms)	42.8±3.6	42.5±2.9	48.8±3.8	0.360
RV ERP (ms)	44.2±5.4	41.2±2.4	48.0±4.5	0.504
LV activation time (ms)	7.1±0.3	7.4±0.6	12.1±1.8#$	**0.014**
RV activation time (ms)	6.8±0.5	7.1±0.4	7.7±0.5	0.418
LV long CV (cm/s)	82.2±1.5	78.3±5.7	60.6±3.7#$	**0.006**
LV trans CV (cm/s)	39.5±1.0	37.2±1.8	28.4±2.8#$	**0.005**
LV l/t ratio	2.1±0.0	2.1±0.1	2.2±0.2	0.766
RV long CV (cm/s)	63.9±1.8	60.8±1.1	57.8±2.7	0.129
RV trans CV (cm/s)	39.5±0.7	37.3±1.4	36.5±2.3	0.450
RV l/t ratio	1.6±0.0	1.6±1.1	1.6±1.1	0.934
Inducible arrhythmias	0/5	1/6	3/6	
Age >6 weeks:				
Number of mice (n)	6	5	6	
LV ERP (ms)	53.6±4.1	52.0±2.6	49.3±4.8	0.729
RV ERP (ms)	43.0±2.5	48.6±4.3	45.3±4.4	0.580
LV activation time (ms)	8.5±0.6	8.1±0.6	10.9±0.9#$	**0.032**
RV activation time (ms)	8.6±0.3	8.3±0.4	10.6±0.8#$	**0.008**
LV long CV (cm/s)	75.2±4.3	75.3±3.0	60.9±2.8#$	**0.020**
LV trans CV (cm/s)	35.6±2.0	37.3±1.5	27.7±1.9#$	**0.006**
LV l/t ratio	2.1±0.1	2.0±0.1	2.2±0.1	0.224
RV long CV (cm/s)	59.4±1.0	59.4±1.3	53.2±2.8	**0.050**
RV trans CV (cm/s)	37.0±1.3	35.5±1.5	30.8±1.7#	**0.024**
RV l/t ratio	1.6±0.0	1.7±0.1	1.7±0.1	0.344
Inducible arrhythmias	1/6	1/5	2/6	

Figure 10 *(next page)* A. Typical examples of LV activation maps of isolated Langendorff-perfused hearts from WT, Tg-WT, and Tg-NS/L mice aged 3-4 weeks. Arrows indicate directions and distances used for measurements of longitudinal (CV-L) and transversal (CV-T) conduction velocities. Crowding of isochrones (1 ms) in the Tg-NS/L heart indicates areas of conduction slowing. B. Average values (mean±SEM) for LV and RV total activation time C. and D. Average values (mean±SEM) for LV and RV longitudinal and transversal conduction velocities B-D. in hearts from WT, Tg-WT, and Tg-NS/L mice aged <2 weeks (n=6, 4, 5 resp.), 3-4 weeks (n=5, 6, 6 resp.), and >6 weeks (n=6, 5, 6 resp.) (* denotes $p<0.05$ vs. WT; $ denotes $p<0.05$ vs. Tg-WT). E. Examples of ventricular arrhythmias induced in isolated Langendorff-perfused hearts of Tg-NS/L mice aged 3-4 weeks (scale bar: 100 ms). Top panels show induction of non-sustained polymorphic ventricular tachycardia induced by either 3 extrasimuli (top left panel) or burst pacing (top right panel). The lower panel depicts an example of a sustained monomorphic ventricular tachycardia induced through burst pacing.
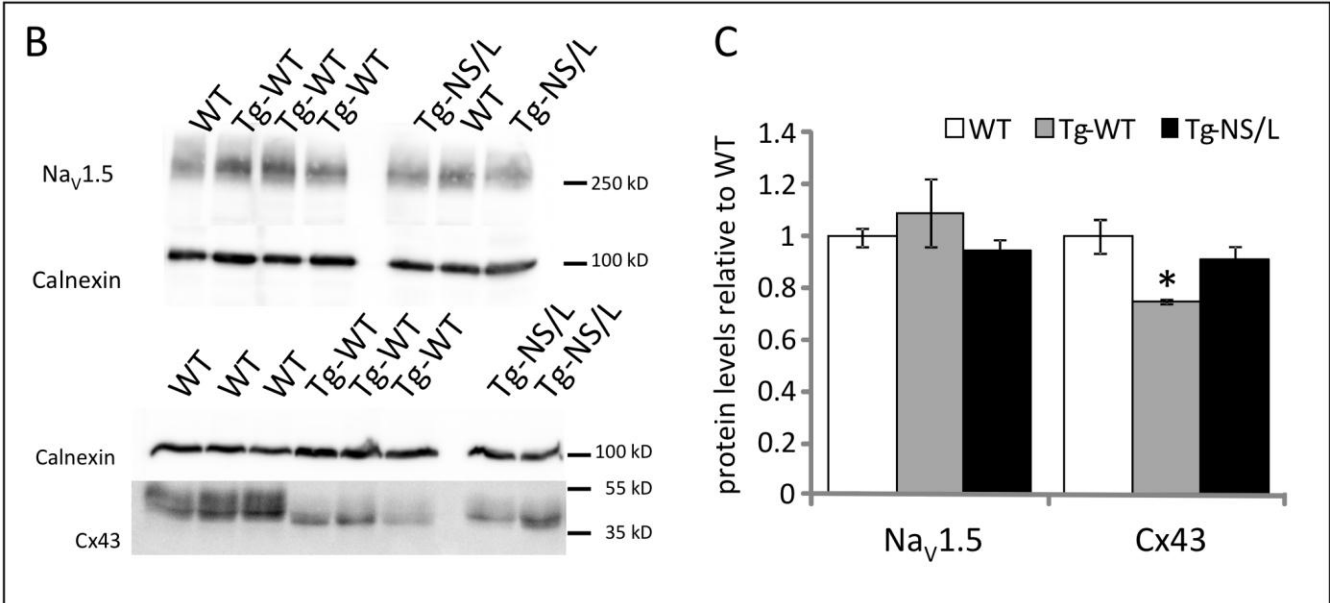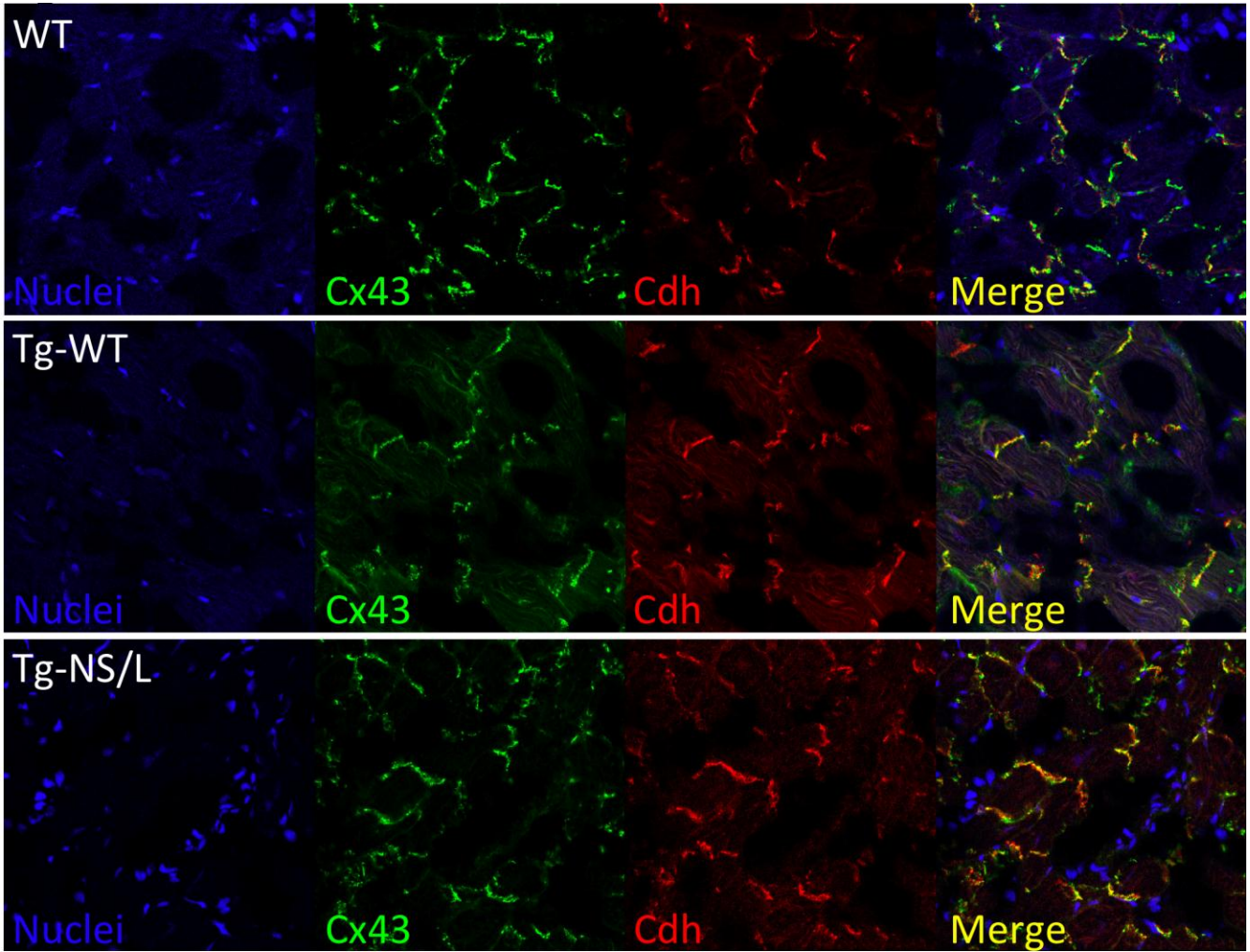
A

WT   Tg-WT   Tg-NS/L

B

C

D

E

Basic stimulation (120 ms)   S1 S2 S3

Burst pacing   Non-sustained ventricular tachycardia

Burst pacing   Sustained ventricular tachycardia

69
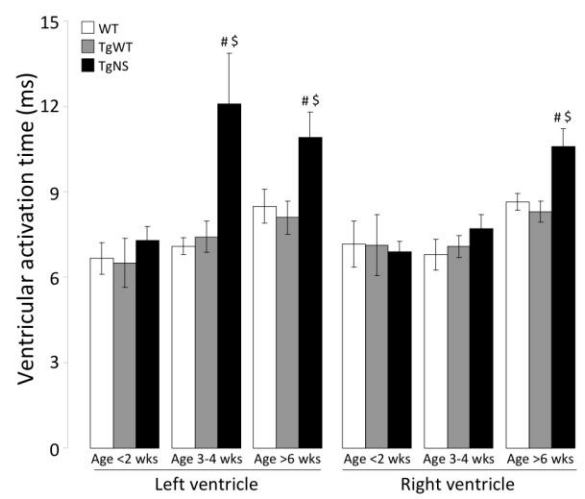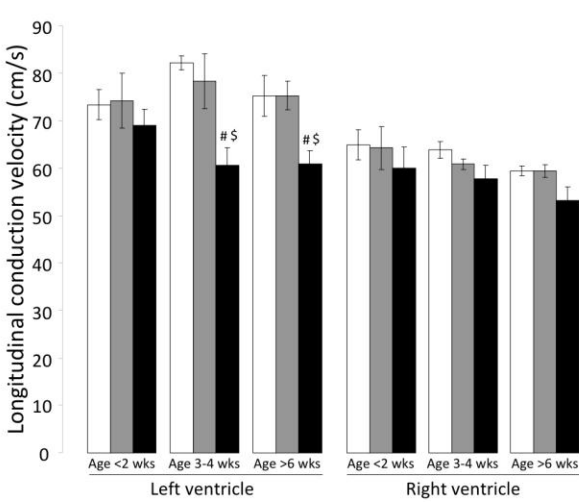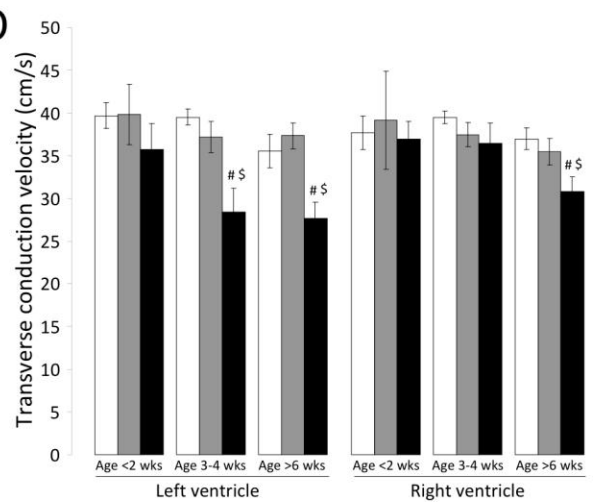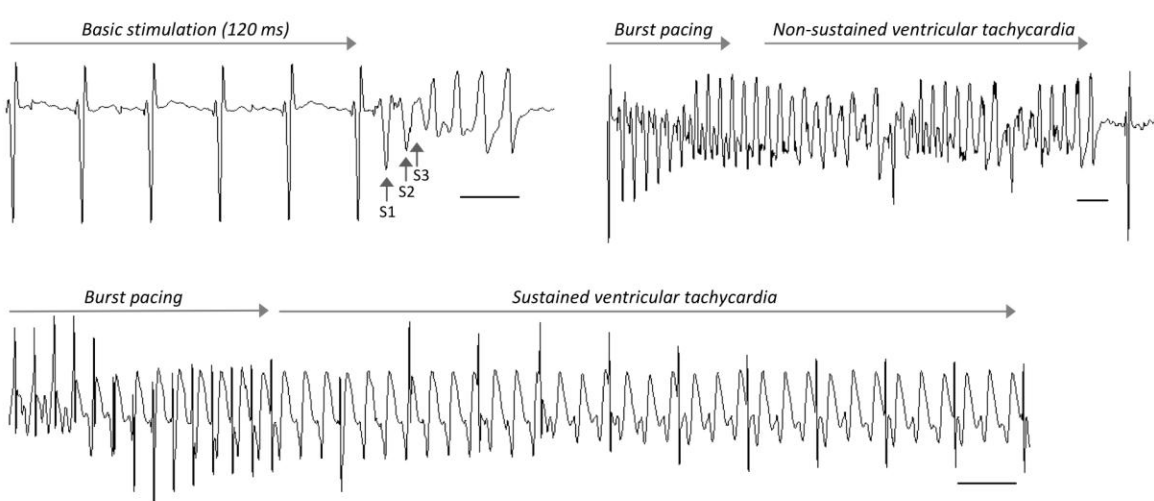
Localization and levels of the intercalated disc proteins

We hypothesized that the conduction slowing observed in hearts at 3-4 weeks of age, i.e. prior to the onset of cardiomyopathic changes, could be related to altered localization or reduced levels of components of the intercalated disc. We used immunofluorescence to characterize the distribution of intercalated disc proteins in Tg-NS/L mice and control mice. A normal immunoreactive signal was detected for Flag-tagged Desmoglein-2, Desmocollin-2, Plakophilin-2 (Pkp2), Plakoglobin (PG), Desmoplakin and NaV1.5 as well as for the classical adherens junction proteins N- and pan-Cadherin and α- and β-Catenin and the gap junctional Connexin43 (Cx43) (Figure 11 and 12). Note the normal co-localization of Cx43 with pan-Cadherin in all three genotype groups; no clear lateralization of Cx43 was observed (Figure 11A).

On Western blot analysis in 3-4 week old hearts, no differences were observed in the levels of PG, Pkp2, NaV1.5, Pan-Cadherin and Cx45 between the three genotype groups (Figure 11B and 13). However we observed a significantly reduced level of Cx43 in Tg-WT compared to WT hearts (Figure 11B,C). Additionally we observed a shift in the height of the Cx43 bands from predominantly phosphorylation state P2 in WT to P1 and P0 in both Tg-WT and Tg-NS/L lines (Figure 11B).

Figure 11 *(next page)* A. Immunohistochemistry of Cx43 (green) and pan-Cadherin (Cdh, red) on LV tissue of WT, Tg-WT and Tg-NS/L mice at 3-4 weeks B. Western blot analysis of whole cell lysate of hearts of WT, Tg-WT, and Tg-NS/L mice aged 3-4 weeks for Calnexin, NaV1.5 and Cx43 C. Quantification of the NaV1.5 and Cx43 Western Blot signals (n=3) relative to Calnexin normalized for WT, error bars denote standard errors, * denotes $p < 0.05$ vs. WT.

B

| | WT | Tg-WT | Tg-WT | Tg-WT | | Tg-NS/L | WT | Tg-NS/L |

Na$_V$1.5 ——— 250 kD

Calnexin ——— 100 kD

| | WT | WT | WT | Tg-WT | Tg-WT | Tg-WT | | Tg-NS/L | Tg-NS/L |

Calnexin ——— 100 kD

——— 55 kD

Cx43 ——— 35 kD

C
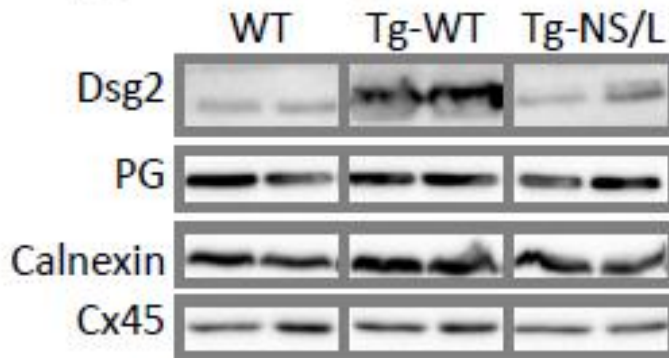
Figure 12. Immunohistochemistry of N-Cadherin, Plakophilin-2, Desmoplakin, Plakoglobin Desmoglein and Nav1.5 on LV tissue of WT, Tg-WT and Tg-NS/L mice at 3-4 weeks.
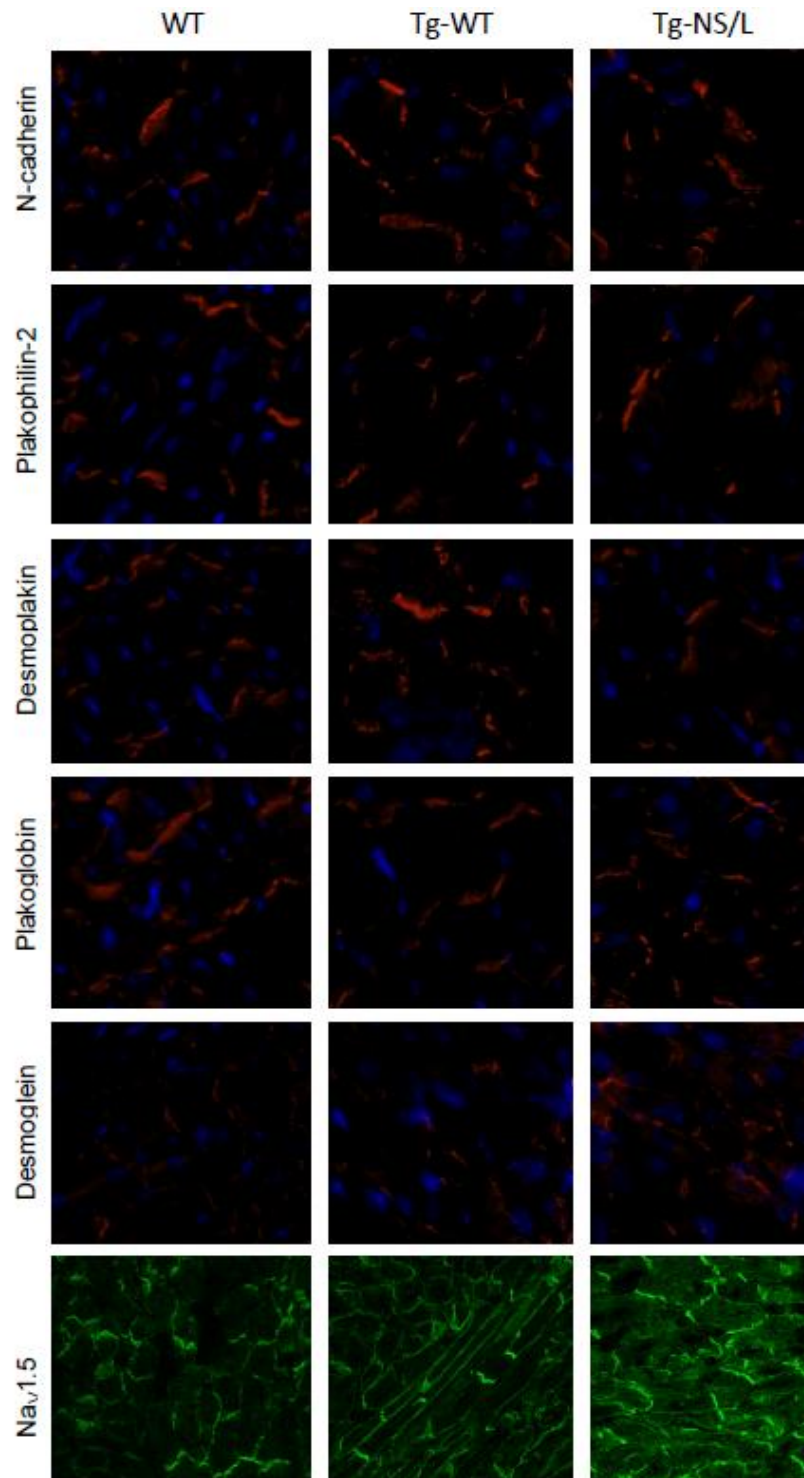
Figure 13. Western blot analysis of whole cell lysate of hearts of WT, Tg-WT, and Tg-NS/L mice aged 3-4 weeks for Dsg2, Plakoglobin (PG), Calnexin and Cx45.


Reduced action potential upstroke velocity in isolated cardiomyocytes

In parallel, we investigated the possible cellular electrophysiological changes underlying the ventricular conduction slowing in the 3-4 week old Tg-NS/L. AP and INa characteristics of LV cardiomyocytes isolated from 3-4 week old mice were measured using patch clamp methodology. Figure 14A shows typical APs of Tg-WT and Tg-NS/L myocytes; Figure 14B summarizes the average AP characteristics of WT, Tg-WT and Tg-NS/L myocytes. No differences were noticed between Tg-NS/L, Tg-WT and WT in resting membrane potential (RMP), AP amplitude (APA) and AP duration (APD) at 20, 50 and 90% repolarization (APD20, APD50, and APD90, respectively). However, cardiomyocytes from Tg-NS/L mice showed a significantly lower AP upstroke velocity (Vmax) compared with age-matched WT and Tg-WT mice (Figure 14B). On average, Vmax in Tg-NS/L myocyte was reduced with ≈17±4% . The AP upstroke is predominantly determined by Na+ influx through voltage gated Na+ channels. The observed lower Vmax thus indicates that cardiomyocytes of Tg-NS/L mice have a reduced functional Na+ channel availability (Berecki et al, 2010).

The reduced functional Na+ channel availability during the AP upstroke may be due to a

decrease of INa density and/or changes in voltage-dependency of (in)activation. Voltage-

clamp experiments performed at RT using a double pulse protocol (Figure 15D) demonstrated

no differences in the voltage dependencies of the activation (Figure15A) and inactivation

(Figure 15B) of INa. Figure 15 C shows the current-voltage relationships of INa in WT, Tg-WT

and Tg-NS/L myocytes. Maximal peak currents were smaller in Tg-NS/L myocytes

compared to WT and Tg-WT myocytes (Figure 15E). On average, the maximal peak current

was ≈19±6% lower; thus the reduction in INa density was in the same order as the Vmax

reduction.

Figure 14 A. Representative action potentials (APs) of LV cardiomyocytes isolated from a Tg-
NS/L (light grey) and Tg-WT (black) mouse heart of 3-4 weeks. Inset: First derivatives of the
AP upstrokes. B. Average AP characteristics of Tg-NS/L (n=3, n=11), Tg-WT (n=3, n=13),
and WT (n=3, n=11) cardiomyocytes age 3-4 weeks. RMP=resting membrane potential;
APA=maximal AP amplitude; Vmax=maximal upstroke velocity; APD20, APD50 and,
APD90=AP duration at 20, 50, and 90% repolarization, respectively.
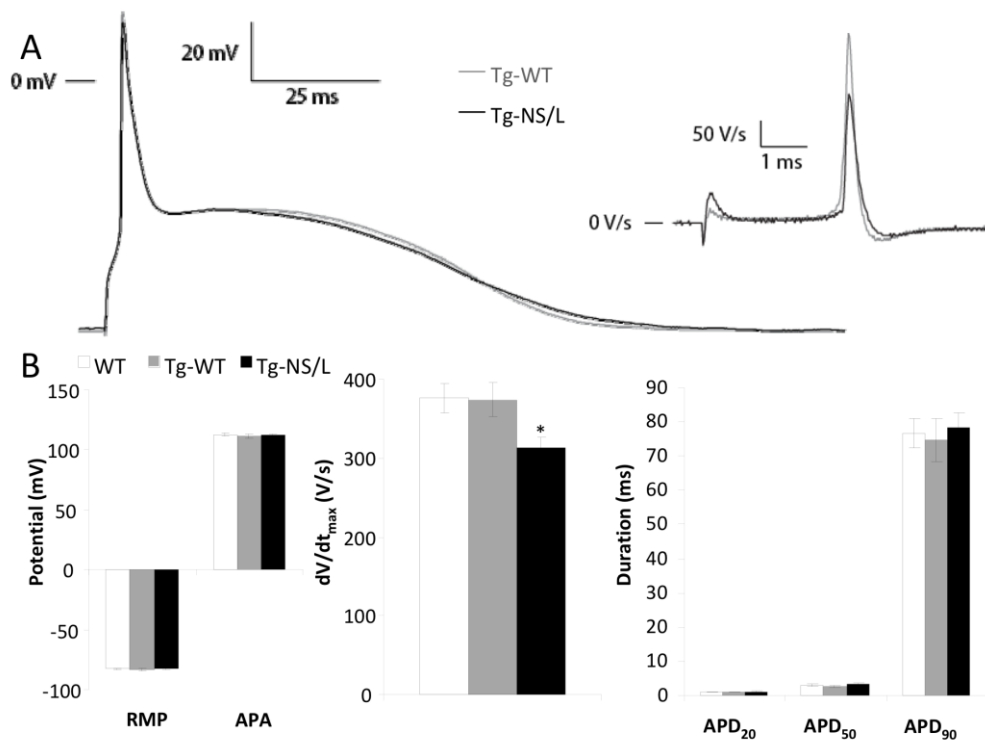
Figure 15. Na+ current (INa) characteristics in in WT, Tg-WT, and Tg-NS/L myocytes. A. Voltage dependency of activation. B. Voltage dependency of inactivation C Current-voltage relationships of INa. D. Voltage clamp protocol. E. Average maximal peak currents, * denotes $p<0.05$ vs. WT.
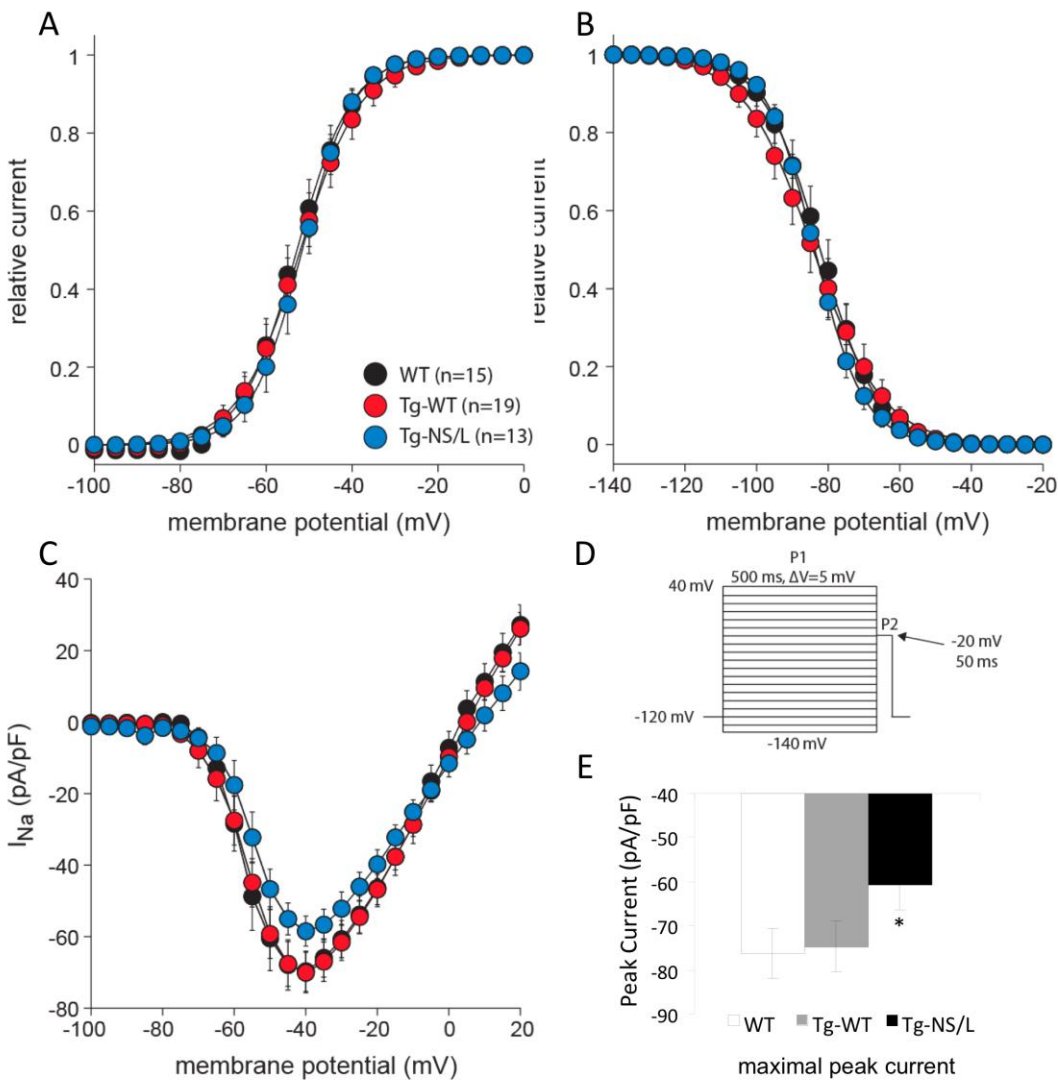
Physical interaction between Dsg2 and NaV1.5

Since our electrophysiological studies showed a reduced INa density in Tg-NS/L mice,

and, considering the fact that recent studies in rat neonatal cardiomyocytes have

demonstrated that desmosomal proteins interact with the Na+ channel complex (Sato et al,

2011; Sato et al, 2009; Delmar et al, 2011), we next sought to investigate the possible in vivo

interaction between Dsg2 and NaV1.5 by co-immunoprecipitation. We made use of the Flag-

tag epitope present on the Dsg2 protein overexpressed in Tg-WT and Tg-NS/L mice to

efficiently and specifically pull down Dsg2 from whole cell protein extracts of the LV of

transgenic mice. This demonstrated an interaction between Flag-tagged Dsg2 and NaV1.5 in

both Tg-WT and Tg-NS/L hearts (Figure 16).

Figure 16. Co-immunoprecipitation of NaV1.5 with Flag-Dsg2 in Tg-WT mice of 3-4 weeks: Western blot for NaV1.5 and Flag tagged on whole cell lysate (In), whole cell lysate precipitated with normal mouse IgG (IgG, negative control) and whole cell lysate precipitated with M2 α-flag (Flag).
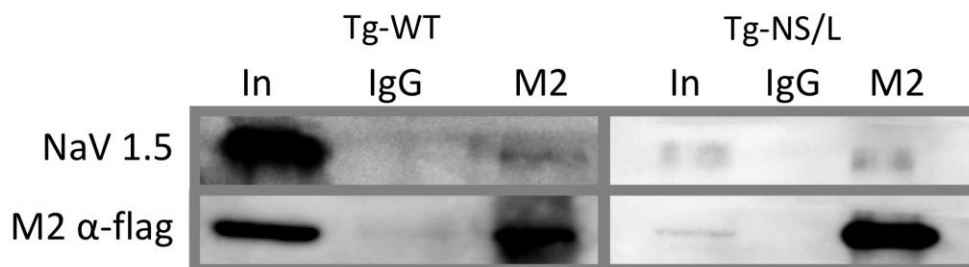
DISCUSSION

We demonstrated for the first time that a mutation in a structural component of cardiac desmosomes impacts on ventricular conduction and arrhythmia susceptibility even before the onset of necrosis and replacement fibrosis. These effects occur through a reduction in AP upstroke velocity due to a reduced INa density. Furthermore, we show for the first time that the cardiac Na+ channel in an in vivo murine model forms part of a macromolecular complex that includes Dsg2. This structural link between the desmosomal protein complex and the NaV1.5 channel may explain the conduction disturbances and arrhythmias seen early in the ARVC disease process. These data have been recently published (Rizzo, Lodder et al., 2012)

Our findings provide support to the recent proposition that at the intercalated disc, cross-talk exists between structures previously perceived as being independent (Delmar et al., 2004). In a series of recent studies, the Delmar group demonstrated interactions between Pkp2, Cx43, NaV1.5 and AnkG, thus connecting the desmosomes to the gap junctions and the Na+ channel complex (Sato et al., 2009; Sato et al., 2011). In these previous studies disruption of these protein complexes by downregulation of Pkp2 and/or AnkG in cultured neonatal rat cardiomyocytes led to reduced Na+ channel availability. The data presented in the current study now shows that Dsg2 interacts with NaV1.5 in the mouse heart in vivo. This observation, coupled to the reduced action potential upstroke velocity due to reduced INa density point to this functional link as the basis for the observed reduction in conduction velocity. It will be interesting to study the temporal and spatial changes in these interactions, as well as the interaction with the other molecules in this protein complex, these studies are unfortunately impossible with co-immunoprecipitation, but will need real time in vivo imaging of the components of intercalated disc.

Unexpectedly, Cx43 protein levels were found to be significantly reduced in Tg-WT, furthermore a shift towards less-phosphorylated (P0, P1) forms of Cx43 was observed. Nevertheless Cx43 sub-cellular localization and distribution within the myocardium did not appear to be altered compared to WT mice, in particular no clear lateralization, which has been reported to correlate to the phoshporylation state of Cx43 (Marquez-Rosado et al., 2011), was observed. Previously, homogeneous reduction of Cx43 has been shown to be well tolerated. For instance, no differences in cardiac conduction were observed in mice carrying a heterozygous deletion of Cx43 (Jansen et al., 2011; Stein et al., 2011). The observed reduction of ~25% of Cx43 in both Tg-NS/L and Tg-WT mice is therefore not expected to influence conduction parameters. Corroborating this, no differences on surface ECG and in epicardial mapping were observed between Tg-WT and WT animals.

However, we cannot exclude the possibility that the observed reduction in Cx43 levels sensitizes the hearts of the Tg-NS/L mice to the consequences of the Dsg2 mutation. The fact that no other changes in level and localization of intercalated disc proteins were seen in Tg-NS/L mice at 3-4 weeks indicates that the observed changes in conduction are due to subtle changes of protein-protein interactions of the intercalated disc proteins rather than gross changes in their level and localization.

One of the earliest signs of disease observed in the Tg-NS/L mice was a widening of the intercalated disc space at the level of the desmosome/adherens junction with focal lysis of the myofilaments, as previously described in humans (Basso et al., 2006). In our previous studies on Tg-NS/H mice (Pilikhou et al, 2009), which have a faster disease development, the widening of the intercellular space was detected only in the setting of concomitant necrosis and inflammation and as such was interpreted as a secondary phenomenon. In the current study, the use of the Tg-NS/L line, which is characterized by a later disease onset, allowed us

to show that intercalated disc space widening is an early feature of the disease and precedes cell injury and inflammation. Such intercalated disc widening could be explained by the fact that the N271 residue, located between the second and third extracellular cadherin domains of Dsg2, has been shown to be critical for co-ordination of Ca2+ binding, a phenomenon essential to the adhesive intercellular interactions of junctional cadherins (Nagar et al., 1996). Similar observations were also made by Kant et al. who studied mice carrying a deletion of the adhesive extracellular domain of Dsg2 (Kant et al., 2012). They suggested that mutant Dsg2 results in compromised adhesion at intercalated disc and mechanical cell stress during postnatal heart development, eventually inducing cardiomyocyte death, inflammation and fibrotic replacement. These features are similar to those observed in our Tg-NS/L mouse model, showing an age-related development of structural lesions, although in the current investigation we focused on the early stages when the heart is still grossly and histologically normal.

In 3-4 week-old mice, intercellular space widening coincided with the onset of conduction slowing. Here, two scenarios are possible. In one, desmosomal interactions (Nagar et al., 1996) are weakened by the N271S mutation leading to intercellular space widening, consequently disrupting the multiprotein Na+ channel complex. In a second scenario, the Dsg2 mutation leads to a conformational change affecting the functional interaction between the desmosomal complex and the Na+ channel complex independent of the intercellular space widening.

The conduction slowing and increased arrhythmia inducibility in the 3-4 week old Tg-NS/L mice point to electrical instability prior to overt structural changes. However no spontaneous arrhythmias were observed at this age on surface ECG, although we cannot exclude their occurrence since long-term telemetric ECG recordings are not feasible at this young age.

Clearly the observed conduction slowing likely sensitizes the Tg-NS/L mice for development

of spontaneous arrhythmias at more advanced disease stages. Our experimental findings of

altered ventricular conduction and increased arrhythmia susceptibility even before

the onset of necrosis and replacement fibrosis support the hypothesis that conduction

disturbances and electrical instability could develop in human carriers of ARVC gene

mutations without structural changes (pre-clinical phase of ARVC). This finding underlines

the need of a diagnostic tool targeting conduction changes, especially in the cardiological

screening of first-degree relatives of ARVC probands carrying gene mutations.

Epicardial mapping in Tg-NS/L mice indicates that the LV is more affected than the RV.

This is in line with the increasing recognition of biventricular involvement in ARVC (Basso et

al., 2009; Pilichou et al., 2006; Bauce et al., 2005; Sen-Chowdhry et al., 2007; Sen-Chowdhry

et al., 2008).

The relative rarity of the left-dominant involvement in published ARVC populations is likely

a consequence of restrictive inclusion criteria and low sensitivity of diagnostic tools (Marcus et

al., 2010). In the setting of family history of ARVC, even signs of isolated LV involvement

should be carefully investigated, as they could be the only marker of the underlying

genetically determined cardiomyopathy (Bauce et al., 2005; Sen-Chowdhry et al., 2007).

Noteworthy, all the reported experimental animal models irrespective of the affected gene

show both LV and RV involvement (Pilichou et al., 2011).

In summary, we here dissect the early stages of disease development in mice

overexpressing a Dsg2 mutation associated with ARVC in humans. Intercellular space

widening at the level of the intercalated discs (desmosomes/adherens junctions) and a

concomitant reduction in action potential upstroke velocity as a consequence of reduced

functional Na+ channel availability leads to slowed conduction and increased arrhythmia

susceptibility at disease stages preceding the onset of replacement fibrosis.

The demonstration of an in vivo interaction between Dsg2 and NaV1.5 provides a molecular pathway for the observed electrical disturbances during the early ARVC disease process.

Recently, similar results of Na-current deficit have been reported by Cerrone et al. (2012) in a murine model of plakophilin-2 haploinsufficiency, suggesting that Na-current dysfunction may contribute to generation and/or maintenance of arrhythmias in PKP2-deficient hearts.

Although ARVC is associated with a clear reduction in intercellular coupling and probably also in membrane excitability, which is largely determined by the fast sodium current, it remains questionable whether the observed changes, either alone or in combination, can explain the arrhythmogenic nature of early-stage ARVC. The recent study by Noorman and colleagues (2012) on heart samples of patients with ARVC revealed by immunocytochemistry a reduction of NaV1.5 and Cx43, suggesting a powerful and dangerous arrhythmogenic combination, although validation is necessary.

Knowledge of the early disease stages would help in risk assessment and designing more effective treatments.

Whether sodium channel blockers (including flecainide) would aid in the evaluation of arrhythmia risk in patients suspect of ARVC, is an interesting area that deserves further investigation.

REFERENCES

Ackerman MJ, Priori SG, Willems S, Berul C, Brugada R, Calkins H, Camm AJ, Ellinor PT, Gollob M, Hamilton R, Hershberger RE, Judge DP, Le Marec H, McKenna WJ, Schulze-Bahr E, Semsarian C, Towbin JA, Watkins H, Wilde A, Wolpert C, Zipes DP. HRS/EHRA expert consensus statement on the state of genetic testing for the channelopathies and cardiomyopathies this document was developed as a partnership between the Heart Rhythm Society (HRS) and the European Heart Rhythm Association (EHRA). Heart Rhythm. 2011;8:1308-39

Angst BD, Marcozzi C, Magee AI. The cadherin superfamily: diversity in form and function. J Cell Sci 2001; 114:629-641

Asimaki A, Syrris P, Wichter T, Matthias P, Saffitz JE, McKenna WJ. A novel dominant mutation in plakoglobin causes arrhythmogenic right ventricular cardiomyopathy. Am J Hum Genet 2007;81:964 –973

Asimaki A, Tandri H, Huang H, Halushka MK, Gautam S, Basso C, Thiene G, Tsatsopoulou A, Protonotarios N, McKenna WJ, Calkins H, Saffitz JE. A new diagnostic test for arrhythmogenic right ventricular cardiomyopathy. N Engl J Med 2009;360:1075–1084

Asimaki A, Tandri H, Duffy ER, Winterfield JR, Mackey-Bojack S, Picken MM, Cooper LT, Wilber DJ, Marcus FI, Basso C, Thiene G, Tsatsopoulou A, Protonotarios N, Stevenson WG, McKenna WJ, Gautam S, Remick DG, Calkins H, Saffitz JE. Pathogenic Links to Arrhythmogenic Right Ventricular CardiomyopathyAltered Desmosomal Proteins in

Granulomatous Myocarditis and Potential Pathogenic Links to Arrhythmogenic Right Ventricular Cardiomyopathy. Circ Arrhythm Electrophysiol. 2011;4:743-752

Avella A, d'Amati G, Pappalardo A, Re F, Silenzi PF, Laurenzi F, DE Girolamo P, Pelargonio G, Dello Russo A, Baratta P, Messina G, Zecchi P, Zachara E, Tondo C. Diagnostic value of endomyocardial biopsy guided by electroanatomic voltage mapping in arrhythmogenic right ventricular cardiomyopathy/dysplasia. J Cardiovasc Electrophysiol. 2008;19:1127-34

Awad MM, Dalal D, Cho E, Amat-Alarcon N, James C, Tichnell C, Tucker A, Russell SD, Bluemke DA, Dietz HC, Calkins H, Judge DP. DSG2 mutations contribute arrhythmogenic right ventricular dysplasia/ cardiomyopathy. Am J Hum Genet 2006;79:136–42

Awad MM, Calkins H, Judge DP. Mechanisms of disease: molecular genetics of arrhythmogenic right ventricular dysplasia/cardiomyopathy. Nat Clin Pract Cardiovasc Med 2008; 5, 258–267

Bai R, Di Biase L, Shivkumar K, Mohanty P, Tung R, Santangeli P, Saenz LC, Vacca M, Verma A, Khaykin Y, Mohanty S, Burkhardt JD, Hongo R, Beheiry S,Dello Russo A, Casella M, PelargonioG, Santarelli P, Sanchez J, Tondo C, Natale A. Ablation of ventricular arrhythmias in arrhythmogenic right ventricular dysplasia/cardiomyopathy: Arrhythmia-free survival after endo-epicardial substrate based mapping ablation. Circulation 2011;4:478-485

Basso C, Thiene G, Corrado D, Angelini A, Nava A, Valente M. Arrhythmogenic right ventricular cardiomyopathy: dysplasia, dystrophy or myocarditis? Circulation 1996; 94:983–91

Basso C, Fox PR, Meurs KM, Towbin JA, Spier AW, Calabrese F, Maron BJ, Thiene G.. Arrhythmogenic right ventricular cardiomyopathy causing sudden cardiac death in boxer dogs: a new animal model of human disease. Circulation 2004, 109: 1180–85

Basso C, Thiene G. Adipositas cordis, fatty infi ltration of the right ventricle, and arrhythmogenic right ventricular cardiomyopathy. Just a matter of fat? Cardiovasc Pathol 2005; 14: 37–41

Basso C, Czarnowska E, Della Barbera M, Bauce B, Beffagna G, Wlodarska EK, Pilichou K, Ramondo A, Lorenzon A, Wozniek O, Daliento L, Danieli GA, Valente M, Nava A, Thiene G, Rampazzo A. Ultrastructural evidence of intercalated disc remodeling in arrhythmogenic right ventricular cardiomyopathy. An electron microscopy investigation on endomyocardial biopsies. Eur Heart J 2006; 27:1847-1854

Basso C, Ronco F, Marcus F, Abudureheman A, Rizzo S, Frigo AC, Bauce B, Maddalena F, Nava A, Corrado D, Grigoletto F, Thiene G. Quantitative assessment of endomyocardial biopsy in arrhythmogenic right ventricular cardiomyopathy/dysplasia: an in vitro validation of diagnostic criteria. Eur Heart J 2008;29:2760–71

Basso C, Corrado D, Marcus F, Nava A, Thiene G. Arrhythmogenic right ventricular cardiomyopathy. Lancet 2009; 373:1289–1300

Basso C, Corrado D, Thiene G. Arrhythmogenic right ventricular cardiomyopathy: what's in a name? From a congenital defect (dysplasia) to a genetically determined cardiomyopathy

(dystrophy). Am J Cardiol. 2010;106:275-277

Basso C, Bauce B, Corrado D, Thiene G. Pathophysiology of arrhythmogenic cardiomyopathy. Nature Reviews Cardiology, 2011; 9:223–233

Basso C, Corrado D, Bauce B, Thiene G. Arrhythmogenic right ventricular cardiomyopathy. Circ Arrhythm Electrophysiol. 2012;5:1233-46

Bauce B, Basso C, Rampazzo A, Beffagna G, Daliento L, Frigo G, Malacrida S, Settimo L, Danieli G, Thiene G, Nava A. Clinical profile of four families with arrhythmogenic right ventricular cardiomyopathy caused by dominant desmoplakin mutations. Eur Heart J 2005;26:1666-1675

Bauce B, Frigo G, Marcus FI, Basso C, Rampazzo A, Maddalena F, Corrado D, Winnicki M, Daliento L, Rigato I, Steriotis A, Mazzotti E, Thiene G, Nava A. Comparison of clinical features of arrhythmogenic right ventricular cardiomyopathy in men versus women. Am J Cardiol. 2008;102:1252-7

Bauce B, Nava A, Beffagna G, Basso C, Lorenzon A, Smaniotto G, De Bortoli M, Rigato I, Mazzotti E, Steriotis A, Marra MP, Towbin JA, Thiene G, Danieli GA, Rampazzo A. Multiple mutations in desmosomal proteins encoding genes in arrhythmogenic right ventricular cardiomyopathy/dysplasia. Heart Rhythm 2010; 7: 22-29

Beffagna G, Occhi G, Nava A, Vitiello L, Ditadi A, Basso C, Bauce B, Carraro G, Thiene G,

Towbin JA, Danieli GA, Rampazzo A. Regulatory mutations in transforming

growth factor-beta3 gene cause arrhythmogenic right ventricular cardiomyopathy type 1.

Cardiovasc Res 2005; 65:366–373

Beffagna G, De Bortoli M, Nava A, Salamon M, Lorenzon A, Zaccolo M, Mancuso L, Sigalotti

L, Bauce B, Occhi G, Basso C, Lanfranchi G, Towbin JA, Thiene G, Danieli GA, Rampazzo A.

Missense mutations in desmocollin-2 N-terminus, associated with arrhythmogenic right

ventricular cardiomyopathy, affect intracellular localization of desmocollin-2 in vitro. BMC Med

Genet. 2007;8:65

Berecki G, Wilders R, de Jonge B, van Ginneken AC, Verkerk AO. Re-evaluation of

the action potential upstroke velocity as a measure of the Na+ current in cardiac

myocytes at physiological conditions. PloS one 2010;5:e15772

Berul CI. Electrophysiological phenotyping in genetically engineered mice. Physiol Genomics

2003; 13, 207–216

Berul CI, Van Hare GF, Kertesz NJ, Dubin AM, Cecchin F, Collins KK, Cannon BC, Alexander

ME, Triedman JK, Walsh EP, Friedman RA. Results of a multicenter retrospective implantable

cardioverter-defibrillator registry of pediatric and congenital heart disease patients. J Am Coll

Cardiol 2008; 51: 1685–1691

Bhuiyan ZA, Jongbloed JD, van der Smagt J, Lombardi PM, Wiesfeld AC, Nelen M, Schouten

M, Jongbloed R, Cox MG, van Wolferen M, Rodriguez LM, van Gelder IC, Bikker H,

Suurmeijer AJ, van den Berg MP, Mannens MM, Hauer RN, Wilde AA, van Tintelen JP. Desmoglein-2 and desmocollin-2 mutations in Dutch arrhythmogenic right ventricular dysplasia/cardiomyopathy patients: results from a multicenter study. Circ Cardiovasc Genet 2009;2:418 – 427

Bierkamp C, Mclaughlin KJ, Schwarz H, Huber O, Kemler R. Embryonic heart and skin defects in mice lacking plakoglobin. Dev Biol. 1996;180:780-5

Blomstrom-Lundqvist C, Sabel K, and Olsson S. A long term follow-up of 15 patients with arrhythmogenic right ventricular dysplasia. Br Heart J 1987; 58, 477–488

Bonny A, Lellouche N, Ditah I, Hidden-Lucet F, Yitemben MT, Granger B, Larrazet F, Frank R, Fontaine G. C-reactive protein in arrhythmogenic right ventricular dysplasia /cardiomyopathy and relationship with ventricular tachycardia. Cardiol Res Pract 2010

Boukens BJ, Christoffels VM, Coronel R, Moorman AF. Developmental basis for electrophysiological heterogeneity in the ventricular and outflow tract myocardium as a substrate for life-threatening ventricular arrhythmias. Circ Res 2009; 104, 19–31

Bowles NE, Ni J, Marcus F, Towbin JA. The detection of cardiotropic viruses in the myocardium of patients with arrhythmogenic right ventricular dysplasia/cardiomyopathy. J Am Coll Cardiol 2002; 39: 892–95

Calabrese F, Basso C, Carturan E, Valente M, Thiene G. Arrhythmogenic right ventricular cardiomyopathy/dysplasia: is there a role for viruses? Cardiovasc Pathol 2006; 15: 11–17

Campian ME, Verberne HJ, Hardziyenka M, de Groot EA, van Moerkerken AF, van Eck-Smit BL, Tan HL. Assessment of inflammation in patients with arrhythmogenic right ventricular cardiomyopathy/dysplasia. Eur J Nucl Med Mol Imaging 2010; 37: 2079–2085

Cerrone M, Noorman M, Lin X, Chkourko H, Liang FX, van der Nagel R, Hund T, Birchmeier W, Mohler P, van Veen TA, van Rijen HV, Delmar M. Sodium current deficit and arrhythmogenesis in a murine model of plakophilin-2 haploinsufficiency. Cardiovasc Res. 2012;95:460-8

Charron P, Arad M, Arbustini E, Basso C, Bilinska Z, Elliott P, Helio T, Keren A, McKenna WJ, Monserrat L, Pankuweit S, Perrot A, Rapezzi C, Ristic A, Seggewiss H, van Langen I, Tavazzi L. Genetic counselling and testing in cardiomyopathies: a position statement of the European Society of Cardiology Working Group on Myocardial and Pericardial Diseases. Eur Heart J. 2010; 31:2715-2726

Chen E, Ekker SC. Zebrafish as a genomics research model. Curr Pharm Biotechnol 2004;5:409–413

Cheng L, Yung A, Covarrubias M, Radice GL. Cortactin is required for N-cadherin regulation of Kv1.5 channel function. J Biol Chem 2011;286:20478 – 20489

Cheng X, Koch PJ. In vivo function of desmosomes. J Dermatol 2004, 31:171-187

Clarkson E, Costa CF, Machesky LM. Congenital myopathies: Diseases of the actin cytoskeleton. J Pathol. 2004;204:407-417

Coleman MA, Bos JM, Johnson JN, Owen HJ, Deschamps C, Moir C, Ackerman MJ. Videoscopic left cardiac sympathetic denervation for patients with recurrent ventricular fibrillation/malignant ventricular arrhythmia syndromes besides congenital long-QT syndrome. Circ Arrhythm Electrophysiol. 2012;5:782-8

Coonar AS, Protonotarios N, Tsatsopoulou A, Needham EW, Houlston RS, Cliff S, Otter MI, Murday VA, Mattu RK, McKenna WJ. Gene for arrhythmogenic right ventricular cardiomyopathy with diffuse nonepidermolytic palmoplantar keratoderma and woolly hair (Naxos disease) maps to 17q21. Circulation 1998; 97: 2049 – 2058

Coronel R, Casini S, Koopmann TT, Wilms-Schopman FJ, Verkerk AO, de Groot JR, Bhuiyan Z, Bezzina CR, Veldkamp MW, Linnenbank AC, van der Wal AC, Tan HL, Brugada P, Wilde AA, de Bakker JM. Right ventricular fibrosis and conduction delay in a patient with clinical signs of Brugada syndrome: a combined electrophysiological, genetic, histopathologic, and computational study. Circulation. 2005;112:2769-77

Corrado D, Thiene G, Nava A, Rossi L. Sudden death in young competitive athletes: clinicopathologic correlations in 22 cases. Am J Med 1990, 89:588-596

Corrado D, Nava A, Buja G, Martini B, Fasoli G, Oselladore L, Turrini P, and Thiene G. Familial cardiomyopathy underlies syndrome of right bundle branch block, ST segment

elevation and sudden death. J. Am. Coll. Cardiol. 1996; 27: 443–448

Corrado D, Basso C, Thiene G, McKenna WJ, Davies MJ, Fontaliran F, Nava A, Silvestri F, Blomstrom-Lundqvist C, Wlodarska EK, Fontaine G, Camerini F. Spectrum of clinicopatho-logic manifestations of arrhythmogenic right ventricular cardiomyopathy/dysplasia: a multicenter study. J Am Coll Cardiol. 1997; 30:1512–20

Corrado D, Basso C, Buja G, Nava A, Rossi L, Thiene G. Right bundle branch block, right precordial ST-segment elevation, and sudden death in young people. Circulation 2001; 103: 710–717

Corrado D, Leoni L, Link MS, Della Bella P, Gaita F, Curnis A, Salerno JU, Igidbashian D, Raviele A, Disertori M, Zanotto G, Verlato R, Vergara G, Delise P, Turrini P, Basso C, Naccarella F, Maddalena F, Estes NA 3rd, Buja G, Thiene G. Implantable cardioverter-defibrillator therapy for prevention of sudden death in patients with arrhythmogenic right ventricular cardiomyopathy/dysplasia. Circulation 2003; 108: 3084–3091

Corrado D, Basso C, Rizzoli G, Schiavon M, Thiene G. Does sports activity enhance the risk of sudden death in adolescents and young adults? J Am Coll Cardiol. 2003;42:1959-63

Corrado D, Basso C, Leoni L, Tokajuk B, Bauce B, Frigo G, Tarantini G, Napodano M, Turrini P, Ramondo A, Daliento L, Nava A, Buja G, Iliceto S, Thiene G. Three-dimensional electroanatomic voltage mapping increases accuracy of diagnosing arrhythmogenic right ventricular cardiomyopathy/dysplasia. Circulation. 2005;111:3042-50

Corrado D, Basso C, Pavei A, Michieli P, Schiavon M, Thiene G. Trends in sudden cardiovascular death in young competitive athletes after implementation of a preparticipation screening program. JAMA 2006; 296: 1593–1601

Corrado D, Basso C, Leoni L, Tokajuk B, Turrini P, Bauce B, Migliore F, Pavei A, Tarantini G, Napodano M, Ramondo A, Buja G, Iliceto S, Thiene G. Three-dimensional electroanatomical voltage mapping and histologic evaluation of myocardial substrate in right ventricular outflow tract tachycardia. J Am Coll Cardiol. 2008;51:731-9

Corrado D, Thiene G. Cardiac sarcoidosis mimicking arrhythmogenic right ventricular cardiomyopathy/dysplasia: the renaissance of endomyocardial biopsy? J Cardiovasc Electrophysiol. 2009;20:477-9

Corrado D, Calkins H, Link M, Leoni L, Favale S, Bevilacqua M, Basso C, Ward D, Boriani G, Ricci R, Piccini JP, Dalal D, Santini M, Buja G, Iliceto S, Estes NA 3rd, Wichter T, McKenna WJ, Thiene G, Marcus FI. Prophylactic implantable defibrillator in patients with arrhythmogenic right ventricular cardiomyopathy/dysplasia and no prior ventricular fibrillation or sustained ventricular tachycardia. Circulation. 2010;122;1144-1152

Corrado D, Basso C, Buja G, Nava A, Rossi L, Thiene G. Right bundle branch block, right precordial ST-segment elevation, and sudden death in young people. Circulation. 2001; 103: 710–717

Corrado D, Basso C, Thiene G. Arrhythmogenic cardiomyopathy. Cardiac Electrophysiology Clinics. WB Saunders, Philadelphia, 2011

Cox MG, van der Zwaag PA, van der Werf C, van der Smagt JJ, Noorman M, Bhuiyan ZA, Wiesfeld AC, Volders PG, van Langen IM, Atsma DE, Dooijes D, van den Wijngaard A, Houweling AC, Jongbloed JD, Jordaens L, Cramer MJ, Doevendans PA, de Bakker JM, Wilde AA, van Tintelen JP, Hauer RN. Arrhythmogenic right ventricular dysplasia/cardiomyopathy: pathogenic desmosome mutations in index-patients predict outcome of family screening: Dutch arrhythmogenic right ventricular dysplasia/ cardiomyopathy genotype-phenotype follow-up study. Circulation. 2011;123:2690-700

Dalal D, Jain R, Tandri H, Dong J, Eid SM, Prakasa K, Tichnell C, James C, Abraham T, Russell SD, Sinha S, Judge DP, Bluemke DA, Marine JE, Calkins H. Long-term efficacy of catheter ablation of ventricular tachycardia in patients with arrhythmogenic right ventricular dysplasia/cardiomyopathy. J Am Coll Cardiol. 2007;50:432–440

Dalla Volta S, Battaglia G, Zerbini E. "Auricularization" of right ventricular pressure curve. Am Heart J 1961; 61:25-33

d'Amati G, di Gioia CR, Giordano C, Gallo P. Myocyte transdifferentiation: a possible pathogenetic mechanism for arrhythmogenic right ventricular cardiomyopathy.
Arch Pathol Lab Med 2000; 124: 287–90

Danik SB, Rosner G, Lader J, Gutstein DE, Fishman GI, Morley GE. Electrical remodeling contributes to complex tachyarrhythmias in connexin43-deficient mouse hearts. FASEB J 2008;22:1204 – 1212

Dechering DG, Kochhäuser S, Wasmer K, Zellerhoff S, Pott C, Köbe J, Spieker T, Piers SR, Bittner A, Mönnig G, Breithardt G, Wichter T, Zeppenfeld K, Eckardt L. Electrophysiological characteristics of ventricular tachyarrhythmias in cardiac sarcoidosis versus arrhythmogenic right ventricular cardiomyopathy.Heart Rhythm. 2012 [Epub ahead of print]

Delmar M. The intercalated disk as a single functional unit. Heart Rhythm 2004;1:12-13

Delmar M, McKenna WJ. The cardiac desmosome and arrhythmogenic cardiomyopathies. Circ.Res. 2010; 107: 700–714

Delmar M. Desmosome–Ion Channel Interactions and Their Possible Role in Arrhythmogenic Cardiomyopathy. Pediatr Cardiol 2012; 33:975–979

den Haan AD, Tan BY, Zikusoka MN, Lladó LI, Jain R, Daly A, Tichnell C, James C, Amat-Alarcon N, Abraham T, Russell SD, Bluemke DA, Calkins H, Dalal D, Judge DP. Comprehensive desmosome mutation analysis in North Americans with arrhythmogenic right ventricular dysplasia/cardiomyopathy. Circ Cardiovasc Genet 2009;2:428 – 435

Desai BV, Harmon RM, Green KJ. Desmosomes at a glance. J Cell Sci 2009:122: 4401-4407

Fabritz L, Hoogendijk MG, Scicluna BP, van Amersfoorth SC, Fortmueller L, Wolf S, Laakmann S, Kreienkamp N, Piccini I, Breithardt G, Noppinger PR, Witt H, Ebnet K, Wichter T, Levkau B, Franke WW, Pieperhoff S, de Bakker JM, Coronel R, Kirchhof P. Load-reducing therapy prevents development of arrhythmogenic right ventricular cardiomyopathy in plakoglobin-deficient mice. J Am Coll Cardiol. 2011;57:740-50

Fawcett DW, McNutt NS. The ultrastructure of the cat myocardium. I. Ventricular papillary muscle. J Cell Biol 1969;42:1-45

Fidler LM, Wilson GJ, Liu F, Cui X, Scherer SW, Taylor GP, Hamilton RM. Abnormal connexin43 in arrhythmogenic right ventricular cardiomyopathy caused by plakophilin-2 mutations. J Cell Mol Med. 2009;13:4219-28

Fontaine G, Guiraudon G, Frank R. Mechanism of ventricular tachycardia with and without associated chronic myocardial ischemia: surgical management based on epicardial mapping. In: Narula OS, ed. Cardiac arrhythmias. Baltimore1979:516-23

Fox PR, Maron BJ, Basso C, Liu SK, Thiene G. Spontaneously occurring arrhythmogenic right ventricular cardiomyopathy in the domestic cat: a new animal model similar to the human disease. Circulation 2000; 102: 1863–70

Franke WW, Borrmann CM, Grund C, Pieperhoff S. The area composita of adhering junctions connecting heart muscle cells of vertebrates. I. Molecular definition in intercalated disks of cardiomyocytes by immunoelectron microscopy of desmosomal

proteins. Eur J Cell Biol 2006;85:69-82

Gaertner A, Schwientek P, Ellinghaus P, Summer H, Golz S, Kassner A, Schulz U, Gummert J, Milting H. Myocardial transcriptome analysis of human arrhythmogenic right ventricular cardiomyopathy. Physiol Genomics 2012; 44: 99–109

Gallicano GI, Kouklis P, Bauer C, Yin M, Vasioukhin V, Degenstein L, Fuchs E. Desmoplakin is required early in development for assembly of desmosomes and cytoskeletal linkage. J Cell Biol. 1998;143:2009-22

Gallicano GI, Bauer C, Fuchs E. Rescuing desmoplakin function in extra-embryonic ectoderm reveals the importance of this protein in embryonic heart, neuroepithelium, skin and vasculature. Development. 2001;128:929-41

Garcia-Gras E, Lombardi R, Giocondo MJ, Willerson JT, Schneider MD, Khoury DS, Marian AJ. Suppression of canonical Wnt/beta-catenin signaling by nuclear plakoglobin recapitulates phenotype of arrhythmogenic right ventricular cardiomyopathy. J Clin Invest 2006;116:2012–2021

Garrod DR, Merritt AJ, Nie Z. Desmosomal adhesion: structural basis, molecular mechanism and regulation. Mol Membr Biol 2002; 19:81-94

Gehmlich K, Syrris P, Peskett E, Evans A, Ehler E, Asimaki A, Anastasakis A, Tsatsopoulou A, Vouliotis AI, Stefanadis C, Saffitz JE, Protonotarios N, McKenna WJ. Mechanistic insights

into arrhythmogenic right ventricular cardiomyopathy caused by desmocollin-2 mutations. Cardiovasc Res. 2011; 90: 7787

Gerull B, Heuser A, Wichter T, Paul M, Basson CT, McDermott DA, Lerman BB, Markowitz SM, Ellinor PT, MacRae CA, Peters S, Grossmann KS, Drenckhahn J, Michely B, Sasse-Klaassen S, Birchmeier W, Dietz R, Breithardt G, Schulze-Bahr E, Thierfelder L. Mutations in the desmosomal protein plakophilin-2 are common in arrhythmogenic right ventricular cardiomyopathy. Nat Genet 2004; 36:1162-1164

Gomes J, Finlay M, Ahmed AK, Ciaccio EJ, Asimaki A, Saffitz JE, Quarta G, Nobles M, Syrris P, Chaubey S, McKenna WJ, Tinker A, Lambiase PD. Electrophysiological abnormalities precede overt structural changes in arrhythmogenic right ventricular cardiomyopathy due to mutations in desmoplakin-A combined murine and human study. Eur Heart J. 2012; 33: 1942–1953

Green KJ, Getsios S, Troyanovsky S, Godsel LM. Intercellular junction assembly, dynamics, and homeostasis. Cold Spring Harb Perspect Biol. 2010;2:a000125

Groeneweg JA, van der Zwaag PA, Jongbloed JD, Cox MG, Vreeker A, de Boer RA, van der Heijden JF, van Veen TA, McKenna WJ, Peter van Tintelen J, Dooijes D, Hauer RN. Left-Dominant Arrhythmogenic Cardiomyopathy in a Large Family: Associated Desmosomal or Non-Desmosomal Genotype? Heart Rhythm. 2012 [Epub ahead of print]

Grossmann KS, Grund C, Huelsken J, Behrend M, Erdmann B, Franke WW, Birchmeier W.

Requirement of plakophilin 2 for heart morphogenesis and cardiac junction formation. J Cell Biol 2004; 167:149–160

Hamid MS, Norman M, Quraishi A, Firoozi S, Thaman R, Gimeno JR, Sachdev B, Rowland E, Elliott PM, McKenna WJ. Prospective evaluation of relatives for familial arrhythmogenic right ventricular cardiomyopathy/dysplasia reveals a need to broaden diagnostic criteria. J Am Coll Cardiol 2002;40:1445–1450

Hatzfeld M. Plakophilins: multifunctional proteins or just regulators of desmosomal adhesion? Biochim Biophys Acta 2007;1773, 69–77

Heuser A, Plovie ER, Ellinor PT Grossmann KS, Shin JT, Wichter T, Basson CT, Lerman BB, Sasse-Klaassen S, Thierfelder L, MacRae CA, Gerull B. Mutant desmocollin-2 causes arrhythmogenic right ventricular cardiomyopathy. Am J Hum Genet 2006, 79:1081-1088

Hodgkinson KA, Parfrey PS, Bassett AS, Kupprion C, Drenckhahn J, Norman MW, Thierfelder L, Stuckless SN, Dicks EL, McKenna WJ, Connors SP. The impact of implantable cardioverter-defibrillator therapy on survival in autosomal-dominant arrhythmogenic right ventricular cardiomyopathy (ARVD5). J Am Coll Cardiol 2005; 45: 400–408

Hoekstra M, Mummery CL, Wilde AA, Bezzina CR, Verkerk AO. Induced pluripotent stem cell derived cardiomyocytes as models for cardiac arrhythmias. Front Physiol. 2012;3:346

Hofman N, van Langen I, Wilde AA. Genetic testing in cardiovascular diseases. Curr Opin Cardiol. 2010;25:243-8

Hoffman BF, Feinmark SJ, Guo SD. Electrophysiologic effects of interactions between activated canine neutrophils and cardiac myocytes. J Cardiovasc Electro-physiol 1997;8: 679–687

Hoogendijk MG. Diagnostic dilemmas: overlapping features of brugada syndrome and arrhythmogenic right ventricular cardiomyopathy. Front Physiol. 2012;3:144

Huber O. Structure and function of desmosomal proteins and their role in development and disease. Cell Mol Life Sci. 2003; 60:1872-1890

Hunold P, Wieneke H, Bruder O, Krueger U, Schlosser T, Erbel R, et al. Late enhancement: a new feature in MRI of arrhythmogenic right ventricular cardiomyopathy? J Cardiovasc Magn Reson. 2005;7:649-55

Huttin O, Mandry D, Brembilla-Perrot B. Arrhythmogenic right ventricular cardiomyopathy: magnetic resonance imaging does not detect early stages of the disease. Int J Cardiol. 2011;147:167-9

Itzhaki I, Maizels L, Huber I, Zwi-Dantsis L, Caspi O, Winterstern A, Feldman O, Gepstein A, Arbel G, Hammerman H, Boulos M, Gepstein L. Modelling the long QT syndrome with induced pluripotent stem cells. Nature 2011;471:225-229

Jacoby D, McKenna WJ. Genetics of inherited cardiomyopathy. Eur Heart J. 2012;33:296-304

James TN. Normal and abnormal consequences of apoptosis in the human heart: from postnatal morphogenesis to paroxysmal arrhythmias. Circulation 1994;90:556-73

Jansen JA, Noorman M, Musa H, Stein M, de Jong S, van der Nagel R, Hund TJ, Mohler PJ, Vos MA, van Veen TA, de Bakker JM, Delmar M, van Rijen HV. Reduced heterogeneous expression of Cx43 results in decreased Nav1.5 expression and reduced sodium current which accounts for arrhythmia vulnerability in conditional Cx43 knockout mice. Heart Rhythm 2012 [Epub ahead of print]

James CA, Tichnell C, Murray B, Daly A, Sears SF, Calkins H. General and disease-specific psychosocial adjustment in patients with arrhythmogenic right ventricular dysplasia/ cardiomyopathy with implantable cardioverter defibrillators: a large cohort study. Circ Cardiovasc Genet. 2012;5:18-24

Kant S, Krull P, Eisner S, Leube RE, Krusche CA. Histological and ultrastructural abnormalities in murine desmoglein 2-mutant hearts. Cell Tissue Res 2012; 348: 249–259

Kaplan SR, Gard JJ, Protonotarios N. Remodeling of myocyte gap junctions in arrhythmogenic right ventricular cardiomyopathy due to a deletion in plakoglobin (Naxos disease). Heart Rhythm. 2004;1:3–11

Kaplan SR, Gard JJ, Carvajal-Huerta L, Ruiz-Cabezas JC, Thiene G, Saffitz JE. Structural and molecular pathology of the heart in Carvajal syndrome. Cardiovasc Pathol 2004; 13:26-32

Kapplinger JD, Landstrom AP, Salisbury BA, Callis TE, Pollevick GD, Tester DJ, Cox MG, Bhuiyan Z, Bikker H, Wiesfeld AC, Hauer RN, van Tintelen JP, Jongbloed JD, Calkins H, Judge DP, Wilde AA, Ackerman MJ. Distinguishing arrhythmogenic right ventricular cardiomyopathy/dysplasia-associated mutations from background genetic noise. J Am Coll Cardiol. 2011;57:2317-27

Kirchhoff S, Kim JS, Hagendorff A, Thonnissen E, Kruger O, Lamers WH, Willecke K. Abnormal cardiac conduction and morphogenesis in connexin40 and connexin43 double-deficient mice. Circ Res. 2000;87:399 – 405

Kirchhof P, Fabritz L, Zwiener M, Witt H, Schäfers M, Zellerhoff S, Paul M, Athai T, Hiller KH, Baba HA, Breithardt G, Ruiz P, Wichter T, Levkau B. Age- and training-dependent development of arrhythmogenic right ventricular cardiomyopathy in heterozygous plakoglobin-deficient mice. Circulation 2006; 114, 1799–1806

Klauke B, Kossmann S, Gaertner A, Brand K, Stork I, Brodehl A, Dieding M, Walhorn V, Anselmetti D, Gerdes D, Bohms B, Schulz U, Zu Knyphausen E, Vorgerd M, Gummert J, Milting H. De novo desmin-mutation N116S is associated with arrhythmogenic right ventricular cardiomyopathy. Hum Mol Genet 2010; 19: 4595 – 4607

Kostis WJ, Tedford RJ, Miller DL, Schulman SP, Tomaselli GF. Troponin-I elevation in a young man with arrhythmogenic right ventricular dysplasia/cardiomyopathy. J Interv Card Electrophysiol 2008;22:49–53

Krusche CA, Holthofer B, Hofe V, Van De Sandt AM, Eshkind L, Bockamp E, Merx MW, Kant, S, Windoffer R, and Leube RE. Desmoglein 2 mutant mice develop cardiac fibrosis and dilation. Basic Res Cardiol. 2011; 106, 617–633

Kucera JP, Rohr S, Rudy Y. Localization of sodium channels in intercalated disks modulates cardiac conduction. Circ Res 2002; 91:1176–1182

Ladyjanskaia GA, Basso C, Hobbelink MG, Kirkels JH, Lahpor JR, Cramer MJ, Thiene G, Hauer RN, V Oosterhout MF. Sarcoid myocarditis with ventricular tachycardia mimicking ARVD/C. J Cardiovasc Electrophysiol. 2010;21:94-8

Lahtinen AM, Lehtonen A, Kaartinen M, Toivonen L, Swan H, Widén E, Lehtonen E, Lehto VP, Kontula K. Plakophilin-2 missense mutations in arrhythmogenic right ventricular cardiomyopathy. Int J Cardiol 2008;126:92–100

Lancisi GM. De Motu Cordis et Aneurysmatibus Opus Posthumum In Duas Partes Divisum. Naples, 1736

Lazaros G, Anastasakis A, Tsiachris D, Dilaveris P, Protonotarios N, Stefanadis C. Naxos disease presenting with ventricular tachycardia and troponin elevation. Heart Vessels

2009;24:63–5

Li J, Patel VV, Kostetskii I, Xiong Y, Chu AF, Jacobson JT, Yu C, Morley GE, Molkentin JD, Radice GL. Cardiac-specific loss of N-cadherin leads to alteration in connexins with conduction slowing and arrhythmogenesis. Circ Res 2005;97:474 – 481

Li J, Radice GL. A new perspective on intercalated disc organization: implications for heart disease. Dermatol Res Pract 2010;2010:207835

Li J, Swope D, Raess N, Cheng L, Muller EJ, Radice GL. Cardiac tissue-restricted deletion of plakoglobin results in progressive cardiomyopathy and activation of {beta}-catenin signaling. Mol Cell Biol. 2011;31:1134-44

Lin X, Liu N, Lu J, Zhang J, Anumonwo JM, Isom LL, Fishman GI, Delmar M. Subcellular heterogeneity of sodium current properties in adult cardiac ventricular myocytes. Heart Rhythm 2011; 8:1923–1930

Lodder EM, Rizzo S. Mouse models in arrhythmogenic right ventricular cardiomyopathy. Front Physiol. 2012;3:221

Lombardi R, da Graca Cabreira-Hansen M, Bell A, Fromm RR, Willerson JT, Marian AJ. Nuclear plakoglobin is essential for differentiation of cardiac progenitor cells to adipocytes in arrhythmogenic right ventricular cardiomyopathy. Circ Res. 2011;109:1342-53

Lowe JS, Palygin O, Bhasin N, Hund TJ, Boyden PA, Shibata E, Anderson ME, Mohler PJ. Voltage-gated Nav channel targeting in the heart requires an ankyrin-G dependent cellular pathway. J Cell Biol 2008;180:173 – 186

Ma D, Wei H, Lu J, Ho S, Zhang G, Sun X, Oh Y, Tan SH, Ng ML, Shim W, Wong P, Liew R. Generation of patient-specific induced pluripotent stem cell-derived cardiomyocytes as a cellular model of arrhythmogenic right ventricular cardiomyopathy. Eur Heart J. 2012 [Epub ahead of print]

MacRae CA, Birchmeier W, Thierfelder L. Arrhythmogenic right ventricular cardiomyopathy: moving toward mechanism. J Clin Invest 2006; 116: 1825–1828

Mallat Z, Tedjui A, Fontaliran F, Frank R, Durigon M, Fontaine G. Evidence of apoptosis in arrhythmogenic right ventricular dysplasia. N Engl J Med 1996; 335: 1190–96

Marchlinski FE, Zado E, Dixit S, Gerstenfeld E, Callans DJ, Hsia H, Lin D, Nayak H, Russo A, Pulliam W. Electroanatomic substrate and outcome of catheter ablative therapy for ventricular tachycardia in setting of right ventricular cardiomyopathy. Circulation. 2004;110:2293-2298

Marcus F, Fontaine G, Guirdaudon G, Frank R, Laurenceau JL, Malergue C, Grosgogeat Y. Right ventricular dysplasia: a report of 24 adult cases. Circulation 1982; 65:384-398

Marcus F, Nava A, Thiene G. Arrhythmogenic right ventricular cardiomyopathy/dysplasia: recent advancesSpringer Verlag, Milan (2007)

Marcus GM, Glidden DV, Polonsky B, Zareba W, Smith LM, Cannom DS, Estes NA 3rd, Marcus F, Scheinman MM. Efficacy of antiarrhythmic drugs in arrhythmogenic right ventricular cardiomyopathy: a report from the North American ARVC Registry. J Am Coll Cardiol. 2009;54:609-15

Marcus FI, McKenna WJ, Sherrill D, Basso C, Bauce B, Bluemke DA, Calkins H, Corrado D, Cox MG, Daubert JP, Fontaine G, Gear K, Hauer R, Nava A, Picard MH, Protonotarios N, Saffitz JE, Sanborn DM, Steinberg JS, Tandri H, Thiene G, Towbin JA, Tsatsopoulou A, Wichter T, Zareba W. Diagnosis of arrhythmogenic right ventricular cardiomyopathy/ dysplasia: proposed modification of the task force criteria. Circulation 2010;121:1533–1541

Marquez-Rosado L, Solan JL, Dunn CA, Norris RP, Lampe PD. Connexin43 phosphorylation in brain, cardiac, endothelial and epithelial tissues. Biochim Biophys Acta 2011

Marra MP, Leoni L, Bauce B, Corbetti F, Zorzi A, Migliore F, Silvano M, Rigato I, Tona F, Tarantini G, Cacciavillani L, Basso C, Buja G, Thiene G, Iliceto S, Corrado D. Imaging study of ventricular scar in arrhythmogenic right ventricular cardiomyopathy: comparison of 3D standard electroanatomical voltage mapping and contrast-enhanced cardiac magnetic resonance. Circ Arrhythm Electrophysiol 2012;5:91–100

Martin ED, Moriarty MA, Byrnes L, Grealy M. Plakoglobin has both structural and signalling roles in zebrafish development. Dev Biol 2009; 327:83–96

Martini B, Nava A, Thiene G, Buja GF, Canciani B, Scognamiglio R, Daliento L, and Dalla Volta S. Ventricular fibrillation without apparent heart disease: description of six cases. Am. Heart J. 1989; 118: 1203–1209

Martini B, Nazzaro GA. 1988–2003: fifteen years after the first Italian description by Nava-Martini-Thiene and colleagues of a new syndrome (different from the Brugada syndrome?) in the Giornale Italiano di Cardiologia: do we really know everything on this entity? Ital Heart J. 2004; 5: 53–60

Matsuo K, Kurita T, Inagaki M, Kakishita M, Aihara N, Shimizu W, Taguchi A, Suyama K, Kamakura S, Shimomura K. The circadian pattern of the development of ventricular fibrillation in patients with Brugada syndrome. Eur. Heart J. 1999; 20, 465–470

McKenna WJ, Thiene G, Nava A, Fontaliran F, Blomstrom-Lundqvist C, Fontaine G, Camerini F. Diagnosis of arrhythmogenic right ventricular dysplasia/cardiomyopathy. Task Force of the Working Group Myocardial and Pericardial Diseaseof the European Society of Cardiology and of the Scientific Council on Cardiomyopathies of the International Society and Federation of Cardiology. Br Heart J 1994; 71:215–218

McKoy G, Protonotarios N, Crosby A, Tsatsopoulou A, Anastasakis A, Coonar A, Norman M, Baboonian C, Jeffery S, McKenna WJ. Identification of a deletion in plakoglobin in arrhythmogenic right ventricular cardiomyopathy with palmoplantar keratoderma and woolly hair (Naxos disease). Lancet 2000, 355:2119-2124

Merner ND, Hodgkinson KA, Haywood AF, Connors S, French VM, Drenckhahn JD, Kupprion C, Ramadanova K, Thierfelder L, McKenna W, Gallagher B, Morris-Larkin L, Bassett AS, Parfrey PS, Young TL. Arrhythmogenic right ventricular cardiomyopathy type 5 is a fully penetrant, lethal arrhythmic disorder caused by a missense mutation in the TMEM43 gene. Am J Hum Genet 2008; 82:809–821

Moretti A, Bellin M, Welling A, Jung CB, Lam JT, Bott-Flugel L, Dorn T, Goedel A, Höhnke C, Hofmann F, Seyfarth M, Sinnecker D, Schömig A, Laugwitz KL. Patient-specific induced pluripotent stem-cell models for long-QT syndrome. N Engl J Med 2010;363:1397-1409

Muthappan P, Calkins H. Arrhythmogenic right ventricular dysplasia. Prog Cardiovasc Dis 2008;51:31–43

Nagar B, Overduin M, Ikura M, Rini JM. Structural basis of calcium-induced E-cadherin rigidification and dimerization. Nature 1996;380:360-364

Nava A, Thiene G, Canciani B, Scognamiglio R, Daliento L, Buja G, Martini B, Stritoni P, Fasoli G. Familial occurrence of right ventricular dysplasia: a study involving nine families. J Am Coll Cardiol 1988; 12:1222-1228

Nava A, Bauce B, Basso C, Muriago M, Rampazzo A, Villanova C, Daliento L, Buja G, Corrado D, Danieli GA, Thiene G. Clinical profile and long term follow-up of 37 families with arrhythmogenic right ventricular cardiomyopathy. J Am Coll Cardiol 2000; 36:2226-2233

Noorman M, Groeneweg JA, Asimaki A, Rizzo S, Papegaaij M, van Stuijvenberg L, de Jonge N, Dooijes D, Basso C, Saffitz J, van Veen T, Vink A, Hauer R. End-stage of arrhythmogenic cardiomyopathy due to a pathogenic plakophilin-2 mutation. Heart Rhythm 2012 [Epub ahead of print]

Noorman M, Hakim S, Kessler E, Groeneweg J, Cox MG, Asimaki A, van Rijen HV, van Stuijvenberg L, Chkourko H, van der Heyden MA, Vos MA, de Jonge N, van der Smagt JJ, Dooijes D, Vink A, de Weger RA, Varro A, de Bakker JM, Saffitz JE, Hund TJ, Mohler PJ, Delmar M, Hauer RN, van Veen TA. Remodeling of the cardiac sodium channel, Connexin43 and Plakoglobin at the intercalated disk in patients with arrhythmogenic cardiomyopathy. Heart Rhythm 2012 [Epub ahead of print]

Norgett EE, Hatsell SJ, Carvajal-Huerta L, Cabezas JC, Common J, Purkis PE, Whittock N, Leigh IM, Stevens HP, Kelsell DP. Recessive mutation in desmoplakin disrupts desmoplakin-intermediate filament interactions and causes dilated cardiomyopathy, woolly hair and keratoderma. Hum Mol Genet 2000; 9: 2761–2766

Norman MW, McKenna WJ. Arrhythmogenic right ventricular cardiomyopathy/ dysplasia: perspectives on diseases. Z Kardiol 1999, 88:550-554

Norman M, Simpson M, Mogensen J, Shaw A, Hughes S, Syrris P, Sen-Chowdhry S, Rowland E, Crosby A, McKenna WJ. Novel mutation in desmoplakin causes arrhythmogenic left ventricular cardiomyopathy. Circulation. 2005;112:636-42

Oh Y, Wei H, Ma D, Sun X, Liew R. Clinical applications of patient-specific induced pluripotent stem cells in cardiovascular medicine. Heart 2012;98:443-449

Osler WM. The principles and practice of medicine. 6th ed. New York: D Appleton, 1905:280

Oxford EM, Musa H, Maass K, Coombs W, Taffet SM, Delmar M. Connexin43 remodeling caused by inhibition of plakophilin-2 expression in cardiac cells. Circ Res 2007; 101:703 – 711

Oxford EM, Everitt M, Coombs W, Fox PR, Kraus M, Gelzer ARM, Saffitz J, Taffet SM, Moïse NS, Delmar M. Molecular composition of the intercalated disc in a spontaneous canine animal model of arrhythmogenic right ventricular dysplasia/cardiomyopathy. Heart Rhythm. 2007; 4: 1196–1205

Oxford EM, Danko CG, Kornreich BG, Maass K, Hemsley SA, Raskolnikov D, Fox PR, Delmar M, Moise NS. Ultrastructural changes in cardiac myocytes from boxer dogs with arrhythmogenic right ventricular cardiomyopathy. J Vet Cardiol. 2011;13:101-113

Paul M, Wichter T, Fabritz L, Waltenberger J, Schulze-Bahr E, Kirchhof P. Arrhythmogenic right ventricular cardiomyopathy : An update on pathophysiology, genetics, diagnosis, and risk stratification. Herzschrittmacherther Elektrophysiol. 2012;23:186-195

Peters S, Trummel M, Denecke S, Koehler B. Results of ajmaline testing in patients with arrhythmogenic right ventricular dysplasia-cardiomyopathy. Int J Cardiol. 2004; 95: 207–210

Peters S. Arrhythmogenic right ventricular dysplasia-cardiomyopathy and provocable coved-type ST-segment elevation in right precordial leads: clues from long-term follow-up. Europace 2008;10: 816–820

Philips B, Madhavan S, James C, Tichnell C, Murray B, Dalal D, Bhonsale A, Nazarian S, Judge DP, Russell SD, Abraham T, Calkins H, Tandri H. Outcomes of catheter ablation of ventricular tachycardia in arrhythmogenic right ventricular dysplasia/cardiomyopathy. Circ Arrhythm Electrophysiol. 2012;5:499-505

Pilichou K, Nava A, Basso C, Beffagna G, Bauce B, Lorenzon A, Frigo G, Vettori A, Valente M, Towbin JA, Thiene G, Danieli GA, Rampazzo A. Mutations in desmoglein-2 gene are associated with arrhythmogenic right ventricular cardiomyopathy. Circulation 2006; 113:1171-1179

Pilichou K, Remme CA, Basso C, Campian ME, Rizzo S, Barnett P, Scicluna BP, Bauce B, van den Hoff MJ, de Bakker JM, Tan HL, Valente M, Nava A, Wilde AA, Moorman AF, Thiene G, Bezzina CR. Myocyte necrosis underlies progressive myocardial dystrophy in mouse dsg2-related arrhythmogenic right ventricular cardiomyopathy. J Exp Med 2009;206:1787–802

Pilichou K, Bezzina CR, Thiene G, Basso C. Arrhythmogenic cardiomyopathy: transgenic animal models provide novel insights into disease pathobiology. Circ Cardiovasc Genet 2011; 4: 318-326

Pilichou K, Thiene G, Basso C. Assessing the significance of pathogenic mutations and autopsy findings in the light of 2010 arrhythmogenic right ventricular cardiomyopathy diagnostic criteria: a clinical challenge. Circ Cardiovasc Genet. 2012;5:384-6

Quarta G, Muir A, Pantazis A, Syrris P, Gehmlich K, Garcia-Pavia P, Ward D, Sen-Chowdhry S, Elliott PM, McKenna WJ. Familial Evaluation in Arrhythmogenic Right Ventricular Cardiomyopathy: Impact of Genetics and Revised Task Force Criteria. Circulation 2011; 123: 2701-2709

Quarta G, Syrris P, Ashworth M, Jenkins S, Zuborne Alapi K, Morgan J, Muir A, Pantazis A, McKenna WJ, Elliott PM. Mutations in the Lamin A/C gene mimic arrhythmogenic right ventricular cardiomyopathy. Eur Heart J. 2012;33:1128-36

Rampazzo A, Nava A, Danieli GA, Buja G, Daliento L, Fasoli G, Scognamiglio R, Corrado D, Thiene G. The gene for arrhythmogenic right ventricular cardiomyopathy maps to chromosome 14q23-q24. Hum Mol Genet 1994;3:959 –962

Rampazzo A, Nava A, Malacrida S, Beffagna G, Bauce B, Rossi V, Zimbello R, Simionati B, Basso C, Thiene G, Towbin JA, Danieli GA. Mutation in human desmoplakin domain binding to plakoglobin causes a dominant form of arrhythmogenic right ventricular cardiomyopathy. Am J Hum Genet 2002; 71:1200-1206

Richardson P, McKenna WJ, Bristow M, Maisch B, Mautner B, O'Connell J, Olsen E, Thiene G, Goodwin J, Gyarfas I, Martin I, Nordet P. Report of the 1995 World Health

Organization/International Society and Federation of Cardiology Task Force on the definition and classification of cardiomyopathies. Circulation 1996; 93:841–842

Rizzo S, Pilichou K, Thiene G, Basso C. The changing spectrum of arrhythmogenic right (ventricular) cardiomyopathy. Cell Tissue Res 2012; 348: 319-323

Rizzo S, Lodder EM, Verkerk AO, Wolswinkel R, Beekman L, Pilichou K, Basso C, Remme CA, Thiene G, Bezzina CR. Intercalated disc abnormalities, reduced Na(+) current density, and conduction slowing in desmoglein-2 mutant mice prior to cardiomyopathic changes. Cardiovasc Res. 2012;95:409-18

Roden DM, Balser JR, George AL Jr, Anderson ME. Cardiac ion channels. Annu Rev Physiol 2002;64:431–475

Roguin A, Bomma CS, Nasir K, Tandri H, Tichnell C, James C, Rutberg J, Crosson J, Spevak PJ, Berger RD, Halperin HR, Calkins H. Implantable cardioverter-defibrillators in patients with arrhythmogenic right ventricular dysplasia/cardiomyopathy. J Am Coll Cardiol. 2004;19;43:1843-1852.

Rohr S. Molecular crosstalk between mechanical and electrical junctions at the intercalated disc. Circ Res 2007; 101, 637–639

Ruiz P, Brinkmann V, Ledermann B, Behrend M, Grund C, Thalhammer C, Vogel F, Birchmeier C, Günthert U, Franke WW, Birchmeier W. Targeted mutation of plakoglobin in

mice reveals essential functions of desmosomes in the embryonic heart. J Cell Biol. 1996;135:215-25

Sacher F, Roberts-Thomson K, Maury P, Tedrow U, Nault I, Steven D, Hocini M, Koplan B, Leroux L, Derval N, Seiler J, Wright MJ, Epstein L, Haissaguerre M, Jais P, StevensonWG. Epicardial ventricular tachycardia ablation: A multicenter safety study. J Am Coll Cardiol 2010;55:2366-2372

Saffitz JE. Arrhythmogenic Cardiomyopathy Advances in Diagnosis and Disease Pathogenesis. Circulation. 2011;124:e390-e392

Sato PY, Musa H, Coombs W, Guerrero-Serna G, Patiño GA, Taffet SM, Isom LL, Delmar M. Loss of plakophilin-2 expression leads to decreased sodium current and slower conduction velocity in cultured cardiac myocytes. Circ Res 2009;105:523 – 526

Sato PY, Coombs W, Lin X, Nekrasova O, Green KJ, Isom LL, Taffet SM, Delmar M. Interactions between ankyrin-G, Plakophilin-2, and Connexin43 at the cardiac intercalated disc. Circ Res.2011;109:193-201

Sen-Chowdhry S, Syrris P, McKenna WJ. Genetics of right ventricular cardiomyopathy. J Cardiovasc Electrophysiol 2005;16:927–935

Sen-Chowdhry S, Syrris P, McKenna WJ. Desmoplakin disease in arrhythmogenic right ventricular cardiomyopathy: early genotype-phenotype studies. Eur Heart J. 2005;26:1582-4

Sen-Chowdhry S, Prasad SK, Syrris P, Wage R, Ward D, Merrifield R, Smith GC, Firmin DN, Pennell DJ, McKenna WJ. Cardiovascular magnetic resonance in arrhythmogenic right ventricular cardiomyopathy revisited: comparison with task force criteria and genotype. J Am Coll Cardiol 2006;48: 2132–2140

Sen-Chowdhry S, Syrris P, Ward D, Asimaki A, Sevdalis E, McKenna WJ. Clinical and genetic characterization of families with arrhythmogenic right ventricular dysplasia/cardiomyopathy provides novel insights into patterns of disease expression. Circulation 2007;115:1710-20

Sen-Chowdhry S, Syrris P, Prasad SK, Hughes SE, Merrifield R, Ward D, Pennell DJ, McKenna WJ. Left-dominant arrhythmogenic cardiomyopathy: an under-recognized clinical entity. J Am Coll Cardiol 2008; 52:2175–2187

Sen-Chowdhry S, McKenna WJ. The utility of magnetic resonance imaging in the evaluation of arrhythmogenic right ventricular cardiomyopathy. Curr Opin Cardiol. 2008;23:38-45

Sen-Chowdhry S, Morgan RD, Chambers JC, McKenna WJ. Arrhythmogenic cardiomyopathy: etiology, diagnosis, and treatment. Annu Rev Med. 2010; 61, 233-253

Sen-Chowdhry, McKenna WJ. Reconciling the protean manifestations of arrhythmogenic cardiomyopathy. Circ Arrhythm Electrophysiol. 2010;3: 566 –570

Shan W, Yagita Y, Wang Z, Koch A, Svenningsen AF, Gruzglin E, Pedraza L, Colman DR.

The minimal essential unit for cadherin-mediated intercellular adhesion comprises extracellular domains 1 and 2. J Biol Chem 2004; 279:55914-55923

Sheikh F, Ross RS, Chen J. Cell-Cell Connection to Cardiac Disease. Trends Cardiovasc Med 2009;19:182–190

Steckman DA, Schneider PM, Schuller JL, Aleong RG, Nguyen DT, Sinagra G, Vitrella G, Brun F, Cova MA, Pagnan L, Mestroni L, Varosy PD, Sauer WH. Utility of cardiac magnetic resonance imaging to differentiate cardiac sarcoidosis from arrhythmogenic right ventricular cardiomyopathy. Am J Cardiol. 2012;110:575-9

Stein M, van Veen TA, Hauer RN, de Bakker JM, van Rijen HV. A 50% reduction of excitability but not of intercellular coupling affects conduction velocity restitution and activation delay in the mouse heart. PloS one 2011;6:e20310

Stokes DL. Desmosomes from a structural perspective. Curr Opin Cell Biol 2007;19: 565–571

Syed SE, Trinnaman B, Martin S, Major S, Hutchinson J, Magee AI. Molecular interactions between desmosomal cadherins. Biochem J 2002; 362:317-327

Syrris P, Ward D, Evans A, Asimaki A, Gandjbakhch E, Sen-Chowdhry S, McKenna WJ. Arrhythmogenic right ventricular dysplasia/ cardiomyopathy associated with mutations in the desmosomal gene desmocollin-2. Am J Hum Genet 2006; 79:978-984

Syrris P, Ward D, Asimaki A, Evans A, Sen-Chowdhry S, Hughes SE, McKenna WJ. Desmoglein-2 mutations in arrhythmogenic right ventricular cardiomyopathy: a genotype-phenotype characterization of familial disease. Eur Heart J. 2007; 28: 581-588

Swope D, Cheng L, Gao E, Li J, Radice GL. Loss of cadherin-binding proteins β-catenin and plakoglobin in the heart leads to gap junction remodeling and arrhythmogenesis. Mol Cell Biol. 2012;32:1056-67

Tada H, Aihara N, Ohe T, Yutani C, Hamada S, Miyanuma H, Takamiya M, Kamakura S. Arrhythmogenic right ventricular cardiomyopathy underlies syndrome of right bundle branch block, ST-segment elevation, and sudden death. Am J Cardiol. 1998 ; 81 : 519–522

Tavora F, Zhang M, Franco M, Bosco Oliveira J, Li L, Fowler D, Zhao Z, Cresswell N, Burke A. Distribution of biventricular disease in arrhythmogenic cardiomyopathy: an autopsy study. Human Pathology 2012; 43: 592–596

Taylor M, Graw S, Sinagra G, Barnes C, Slavov D, Brun F, Pinamonti B, Salcedo EE, Sauer W, Pyxaras S, Anderson B, Simon B, Bogomolovas J, Labeit S, Granzier H, Mestroni L. Genetic variation in titin in arrhythmogenic right ventricular cardiomyopathy-overlap syndromes. Circulation. 2011;124:876-85

Tiso N, Stephan DA, Nava A, Bagattin A, Devaney JM, Stanchi F, Larderet G, Brahmbhatt B, Brown K, Bauce B, Muriago M, Basso C, Thiene G, Danieli GA, Rampazzo A. Identification of mutations in the cardiac ryanodine receptor gene in families affected with arrhythmogenic

right ventricular cardiomyopathy type 2 (ARVD2). Hum Mol Genet 2001; 10:189–194

Thiene G, Nava A, Corrado D, Rossi L, Pennelli N. Right ventricular cardiomyopathy and sudden death in young people. N Engl J Med 1988; 318:129-133

Thiene G, Nava A, Angelini A, Daliento L, Scognamiglio R, Corrado D. Anatomoclinical aspects of arrhythmogenic right ventricular cardiomyopathy. In Advances in cardiomyopathies Edited by: Baroldi G, Camerini F, Goodwin JF. Milano: Springer Verlag; 1990:397-408

Thiene G, Corrado D, Nava A, Rossi L, Poletti A, Boffa GM, Daliento L, Pennelli N. Right ventricular cardiomyopathy: is there evidence of an inflammatory aetiology? Eur Heart J 1991; 12: 22–25

Thiene G, Angelini A, Basso C, Calabrese F, Valente M. Novel heart diseases requiring transplantation. Adv Clin Path 1998; 2:65–73

Thiene G, Rigato I, Pilichou K, Corrado D, Basso C. Arrhythmogenic right ventricular cardiomyopathy. What is needed for a cure? Herz. 2012;37:657-62

Thiene G, Marcus F. Arrhythmogenic cardiomyopathy: A biventricular disease in search of a cure. Heart Rhythm. 2012 [Epub ahead of print]

Turrini P, Angelini A, Buja GF, Nava A, Thiene G. Fibrosis is the main cause of late potentials

in arrhythmogenic right ventricular cardiomyopathy. Circulation. 1994;90(suppl I):I-229

Uhl HSM. A previously undescribed congenital malformation of the heart: Almost total absence of the myocardium of the right ventricle. Bull Johns Hopkins Hosp 1952;91:197-209

Valente M, Calabrese F, Thiene G, Angelini A, Basso C, Nava A, Rossi L. In vivo evidence of apoptosis in arrhythmogenic right ventricular cardiomyopathy. Am J Pathol 1998; 152: 479–84

van der Smagt JJ, van der Zwaag PA, van Tintelen JP, Cox MG, Wilde AA, van Langen IM, Ummels A, Hennekam FA, Dooijes D, Gerbens F, Bikker H, Hauer RN, Doevendans PA. Clinical and genetic characterization of patients with arrhythmogenic right ventricular dysplasia/cardiomyopathy caused by a plakophilin-2 splice mutation. Cardiology. 2012;123:181-9

van der Zwaag P, Jongbloed J, van den Berg M, van der Smagt J, Jongbloed R, Bikker H, Hofstra R, van Tintelen J. A genetic variants database for arrhythmogenic right ventricular dysplasia/cardiomyopathy. Hum Mutat 2009;30:1278-1283

van der Zwaag PA, Cox MG, van der Werf C, Wiesfeld AC, Jongbloed JD, Dooijes D, Bikker H, Jongbloed R, Suurmeijer AJ, van den Berg MP, Hofstra RM, Hauer RN, Wilde AA, van Tintelen JP. Recurrent and founder mutations in the Netherlands : Plakophilin-2 p.Arg79X mutation causing arrhythmogenic right ventricular cardiomyopathy/dysplasia. Neth Heart J. 2010;18:583-91

van der Zwaag PA, van Rijsingen IA, Asimaki A, Jongbloed JD, van Veldhuisen DJ, Wiesfeld AC, Cox MG, van Lochem LT, de Boer RA, Hofstra RM, Christiaans I, van Spaendonck-Zwarts KY, Lekanne dit Deprez RH, Judge DP, Calkins H, Suurmeijer AJ, Hauer RN, Saffitz JE, Wilde AA, van den Berg MP, van Tintelen JP. Phospholamban R14del mutation in patients diagnosed with dilated cardiomyopathy or arrhythmogenic right ventricular cardiomyopathy: evidence supporting the concept of arrhythmogenic cardiomyopathy. Eur J Heart Fail. 2012;14:1199-207

van Hengel J, Calore M, Bauce B, Dazzo E, Mazzotti E, De Bortoli M, Lorenzon A, Li Mura IE, Beffagna G, Rigato I, Vleeschouwers M, Tyberghein K, Hulpiau P, van Hamme E, Zaglia T, Corrado D, Basso C, Thiene G, Daliento L, Nava A, van Roy F, Rampazzo A. Mutations in the area composita protein αT-catenin are associated with arrhythmogenic right ventricular cardiomyopathy. Eur Heart J. 2012 [Epub ahead of print]

van Tintelen JP, Entius MM, Bhuiyan ZA, Jongbloed R, Wiesfeld AC, Wilde AA, van der Smagt J, Boven LG, Mannens MM, van Langen IM, Hofstra RM, Otterspoor LC, Doevendans PA, Rodriguez LM, van Gelder IC, Hauer RN. Plakophilin-2 mutations are the major determinant of familial arrhythmogenic right ventricular dysplasia/cardiomyopathy. Circulation 2006;113:1650 –1658

Vasaiwala SC, Finn C, Delpriore J, Leya F, Gagermeier J, Akar JG, Santucci P, Dajani K, Bova D, Picken MM, Basso C, Marcus F, Wilber DJ. Prospective study of cardiac sarcoid mimicking arrhythmogenic right ventricular dysplasia. J Cardiovasc Electrophysiol. 2009;20:473-6

Vatta M, Marcus FI, Towbin JA. Arrhythmogenic right ventricular cardiomyopathy: a "final common pathway" that defines clinical phenotype. Eur Heart J 2007;28:529 –530

Verkerk AO, Tan HL, Ravesloot JH. Ca2+-activated Cl- current reduces transmural electrical heterogeneity within the rabbit left ventricle. Acta Physiol Scand. 2004;180:239-247

Wichter T, Borggrefe M, Haverkamp W, Chen X, Breithardt G: Efficacy of antiarrhythmic drugs in patients with arrhythmogenic right ventricular disease. Results in patients with inducible and noninducible ventricular tachicardia. Circulation. 1992; 86:29-37

Wichter T, Paul M, Eckardt L, Gerdes P, Kirchhof P, Bocker D, Breithardt G: Arrhythmogenic right ventricular cardiomyopathy. Antiarrhythmic drugs, catheter ablation, or ICD? Herz. 2005; 30:91-101

Wilders R. Arrhythmogenic right ventricular cardiomyopathy: considerations from in silico experiments. Front Physiol. 2012;3:168

Wolf CM, Berul CI. Molecular mechanisms of inherited arrhythmias. Curr Genomics 2008; 9, 160–168

Yamamoto S, Tsyplenkova VG, James TN. Morphological patterns of death by myocytes in arrhythmogenic right ventricular dysplasia. Am J Med Sci 2000; 320:310–319

Xu T, Yang Z, Vatta M, Rampazzo A, Beffagna G, Pilichou K, Scherer SE, Saffitz J, Kravitz J,

Zareba W, Danieli GA, Lorenzon A, Nava A, Bauce B, Thiene G, Basso C, Calkins H, Gear K, Marcus F, Towbin JA. Compound and Digenic Heterozygosity Contributes to Arrhythmogenic Right Ventricular Cardiomyopathy. J Am Coll Cardiol 2010; 55: 587-597

Zipes DP, Camm AJ, Borggrefe M, Buxton AE, Chaitman B, Fromer M, Gregoratos G, Klein G, Moss AJ, Myerburg RJ, Priori SG, Quinones MA, Roden DM, Silka MJ, Tracy C, Smith SC Jr, Jacobs AK, Adams CD, Antman EM, Anderson JL, Hunt SA, Halperin JL, Nishimura R, Ornato JP, Page RL, Riegel B, Blanc JJ, Budaj A, Dean V, Deckers JW, Despres C, Dickstein K, Lekakis J, McGregor K, Metra M, Morais J, Osterspey A, Tamargo JL, Zamorano JL. ACC/AHA/ESC 2006 Guidelines for Management of Patients With Ventricular Arrhythmias and the Prevention of Sudden Cardiac Death: a report of the American College of Cardiology/American Heart Association Task Force and the European Society of Cardiology Committee for Practice Guidelines (writing committee to develop Guidelines for Management of Patients With Ventricular Arrhythmias and the Prevention of Sudden Cardiac Death): developed in collaboration with the European Heart Rhythm Association and the Heart Rhythm Society. Circulation 2006; 114: e385–484